Institute of
GEOLOGICAL
& NUCLEAR
SCIENCES
Limited

The Rangipo (Desert Road) Fault: The most hazardous fault in the Taupo Volcanic Zone?

by Pilar Villamor, Russ Van Dissen, Brent Alloway, Alan Palmer, & Nicola Litchfield

Confidential

Client Report 2004/34

April 2004

The Rangipo (Desert Road) Fault: The most hazardous fault in the Taupo Volcanic Zone?

by Pilar Villamor, Russ Van Dissen, Brent Alloway, Alan Palmer & Nicola Litchfield

Prepared for

Earthquake Commission

CONFIDENTIAL

Institute of Geological & Nuclear Sciences client report 2004/34
Project Number: 430W1023

The data presented in this Report are available to GNS for other use from
April 2004

April 2004

COMMERCIAL – IN – CONFIDENCE

This report has been prepared by the Institute of Geological & Nuclear Sciences Limited exclusively for and under contract to the Earthquake Commission. Unless otherwise agreed in writing, all liability of the Institute to any other party other than the Earthquake Commission in respect of the report is expressly excluded.

CONTENTS

EXECUTIVE SUMMARY ..... **II**

1.0 INTRODUCTION **1**

1.1 Objectives 1
1.2 Background and motivation for study 1
1.3 Scope of work 2

2.0 GEOLOGIC SETTING **3**

2.1 Tectonic setting 3
2.2 Age of the landscape and stratigraphic features displaced by active faults 4

3.0 THE RANGIPO FAULT **7**

3.1 Previous studies 7
3.2 Fault geometry and displacements 7
3.2.1 Fault mapping 7
3.2.2 Displacements of geomorphic and geologic features 10
3.2.3 Age of the displaced ring plain 11
3.3 Paleoseismic studies 14
3.3.1 Selection of trench sites 14
3.3.2 Trench site geology 16
3.3.3 Tank Track trench 17
3.3.4 Zone 19 trench 22
3.3.5 Rangipo Fault earthquake history 25
3.3.6 Contribution of trench data to the age of landscape features 26
3.4 Seismic parameters of the Rangipo Fault 27
3.4.1 Fault Slip Rate 27
3.4.2 Single Event Displacement and Magnitude 27
3.4.3 Recurrence Interval and elapsed time since last event 30

4.0 THE SHAWCROFT ROAD FAULT **32**

5.0 DISCUSSION **34**

5.1 Association between tectonic faulting and volcanism 34
5.2 Earthquake hazard associated to rupture of the Rangipo Fault 35

6.0 CONCLUSIONS **37**

7.0 REFERENCES **38**

8.0 ACKNOWLEDGEMENTS **42**

APPENDIX **73**

EXECUTIVE SUMMARY

The Rangipo and Shawcroft Road faults are located at the southern end of the Taupo Volcanic Zone in the vicinity of Ruapehu Volcano. The Rangipo Fault is not the fastest slipping fault in the Taupo Volcanic Zone, as was supposed prior to this study. We have determined two well constrained estimates of slip rate of c. 1.5 mm/yr and c. 0.2 mm/yr over two different time intervals (the past c. 25.6 ka and the past c. 13.8 ka respectively) for the Rangipo Fault. This is much less than the earlier determined estimates of 3 mm/yr. The long term slip rate of 1.5 mm/yr is still comparable with other high slip rate faults in the Taupo Volcanic Zone (TVZ), but the Holocene slip rate of c. 0.2 mm/yr suggests the fault is a low slip rate fault compared with other TVZ faults.

The abrupt decrease in slip rate estimated for the Rangipo and Shawcroft Road faults coincides with an overall decrease in the eruptive activity from nearby Ruapehu Volcano from c. 15 ka to the present. We infer that there is a correlation between fast slipping periods on the Rangipo Fault and large eruptive volumes from Ruapehu Volcano. This relationship suggests that clustering of earthquakes on the Rangipo Fault is likely, but it is unclear whether the clustering of earthquakes is triggering the eruptions or vice versa. We do not favour an alternative model whereby the Rangipo Fault had increased displacement prior to c. 15 ka caused by ground surface response to emptying of the magma chamber (i.e Rangipo Fault acting as a passive structure with aseismic displacement). Further studies are needed to confirm one of these models.

Our results indicate that although rupture of the Rangipo Fault occurs less frequently than previously assessed, it is associated with large earthquakes with magnitudes between 6.3 and 7.1. Earthquake recurrence intervals of moderate M6 earthquakes are in the order of 3000 years and recurrence intervals of large M7 earthquakes are assessed to occur less frequently ($\geq$ 11,200-14,000 years). Although our new characterisation of the fault activity indicates larger recurrence intervals and lower slip rates that previously assessed, rupture of the Rangipo Fault still poses a relatively high hazard to the area due to the large earthquake magnitudes with up to M 7.1 associated with it. Rupture of the Rangipo Fault will affect the major lifelines in the region, as well as the ski fields, townships, forest processing plants and hydroelectric power schemes.

1.0 INTRODUCTION

1.1 Objectives

The aims of this research project on the Rangipo Fault are:

- To determine its earthquake generating potential (e.g. slip rate, earthquake recurrence interval) and
- To determine any relationship between its rupture history and with the eruptive activity at Ruapehu Volcano (they are only 13 km apart).

1.2 Background and motivation for study

Interest in detailed examination of the Rangipo Fault arose from preliminary results which implied that this feature could be the fastest slipping and the most hazardous fault in the Taupo Volcanic Zone, and potentially one on the most hazardous normal faults in the world.

Reconnaissance level field work conducted in June 1998 on the Rangipo Fault and previous studies (Donoghue 1991) suggested that the Rangipo Fault has a high slip rate, probably in excess of 3 mm/yr averaged over the last c. 15,000 years, and an elapsed time since last event of c. 2000 years. A slip rate of 3 mm/yr would make the Rangipo Fault the fastest slipping fault in the Taupo Volcanic Zone (TVZ). A fast slip rate and a long elapsed time since the most recent rupture could indicate that the fault has the potential to generate a large magnitude earthquake (M 6.9 to 7.5) in the near future.

Fault activity within a volcanic province, such as the TVZ, can result not only from tectonic processes (e.g. rifting) but also from processes associated with volcanic activity. For example, aseismic displacement on faults can be caused by large eruptions, as well as by low-magnitude earthquake swarms related to volcanic eruptions and movement of magma. Alternatively, regional tectonic extension can trigger large volcanic eruptions by creating the space for the magma to ascend (typically in volcanic-rift zones, e.g. Hackett et al. 1996). In the first case, the hazard posed by a fault may be overestimated because a portion of the fault displacement does not generate large earthquakes. In the second case, large earthquakes can potentially be a warning for imminent large, or sustained, eruptive periods.

In the TVZ, only recently has research into the interaction of tectonic faulting and volcanic eruptions been started (e.g. Nairn et al in press). The Rangipo Fault and the summit of Mt. Ruapehu are only c. 13 km apart. A focus of this study is to define the earthquake and movement history of the fault. We then compare this displacement history with the pre-established, well-constrained, eruptive history of Ruapehu Volcano (Hackett & Houghton 1989: Donoghue et al. 1995), over the last c. 26 ka to assess any possible relation between eruptive activity at Ruapehu Volcano and displacement on the Rangipo Fault. We also

analyse what the implications that this possible interaction between faulting and volcanic activity has on the values of fault parameters used for earthquake hazard studies.

1.3 Scope of work

The following tasks were agreed with EQC to comprise the core of the present study:

1) Conduct a detailed air photo study along the length of the Rangipo Fault.
2) Undertake detailed field studies of sites where displacement of young geological features that cross the fault (e.g. alluvial terraces, lahar surfaces, tephra) can be measured.
3) Excavate three trenches across the fault to determine the timing of recent surface rupture earthquakes on the fault, and the amount of displacement that accompanied those earthquakes.
4) Obtain ages of the displaced geological features using tephrostratigraphy, and radiocarbon dating.
5) Calculate a slip rate for the Rangipo Fault based on the displacements measured in 2) and the ages obtained in 3).
6) Estimate a maximum magnitude earthquake for the fault based on fault length and single-event displacement size, and a recurrence interval for this earthquake based the timing of the most recent large earthquakes that have ruptured the ground surface.
7) Assess the variability, if any, in fault slip rate and single event displacement in time and compare it with the already well-established chronology of major eruptions from nearby Mt. Ruapehu.
8) Report the results of the research.

We consider that we have successfully completed all eight tasks, and they are summarised in this report. In addition, this study also presents a compilation and interpretation of relevant data obtained under the FRST funded project "Impacts of Global Plate Tectonics in and around New Zealand". In particular, this involves a fourth trench on the Rangipo Fault and a fault study of the Shawcroft Road Fault (including two fault trenches). The Shawcroft Road Fault cross cuts the Rangipo Fault. The geomorphic configuration of the scarps on these faults indicate that the Shawcroft Road Fault has ruptured more recently than the Rangipo Fault. The results of the study on the Shawcroft Road Fault have contributed to an understanding of the faulting characteristics of the Rangipo Fault.

2.0 GEOLOGIC SETTING

2.1 Tectonic setting

Our study area is located at the southeastern end of the Taupo Volcanic Zone (TVZ; Fig. 2.1). The TVZ is the late Pliocene to Quaternary volcanic arc, associated with the Hikurangi Margin, i.e. with the subduction of the Pacific plate beneath the North Island of New Zealand (Wilson et al. 1995). The TVZ is also regarded as the southern onshore, continuation of the Havre Trough, a region north of New Zealand charaterised by normal faulting and calk-alkaline volcanism (Wright 1993). While in most of the Havre Trough a clear backarc basin to the Kermadec subduction zone exists (with the active volcanic arc located to the east of the tectonic basin; Gamble & Wright 1995), extension onshore occurs within the volcanic arc itself. The TVZ is also characterised by high crustal heat flow (up to 700 mW/m^2), and numerous shallow focus earthquakes (Bibby et al. 1995 and 1998).

Within the TVZ, extension is accommodated by movement on normal faults which form a rift structure that we will refer hereafter to as the Taupo Rift (a.k.a. the Taupo Fault Belt, Berryman & Villamor, 1999). At the southern end of the Taupo Rift active faulting was initiated < 400 ka ago (Villamor & Berryman, 2004a submitted) coinciding with the initiation of extensive volcanism in the southern TVZ at c. ≤ 300 ka (Hobden et al. 1996; Hackett & Houghton 1989; Gamble et al 2003).

Several prominent active faults in the southern end of the Taupo Rift were identified as early as the 1930's, such as the Raurimu, Rangipo and Ohakune faults (e.g. Grange and Williamson 1933; Ongley 1943; Schofield 1954; Gregg 1960; Hay 1967). Recent detailed mapping of active fault traces in the southern Taupo Rift reveals that the late Quaternary (post c. 80 ka) discrete deformation comprises three fault sets (Villamor & Berryman 2004a submitted): the NNE trending Mt Ruapehu Graben, the with E-W trending Ohakune-Raetihi fault set and the NE-SW trending Karioi Fault set (Fig. 2.2). Villamor & Berryman (2004b submitted) infer pure dip-slip motion on most of the faults at the southern termination of the Taupo Rift.

The 40-km-wide Mt Ruapehu Graben is bounded by the Raurimu and Rangipo faults to the west and east respectively (Fig. 2.2). These marginal, bounding, faults have a more northerly trend and form a wider graben than Taupo Rift faults further north of Ruapehu Volcano. The extension rate for the Mt Ruapehu Graben, calculated from active fault offsets and in a direction perpendicular to the structures, is 0.75 ± 0.29 mm/year (Villamor & Berryman, 2004a submitted). Results from the present study will further constrain this extension rate.

The Mt Ruapehu Graben is terminated abruptly at its southern end by active normal faults, that strike at high angles to the marginal faults of the Taupo Rift (Villamor & Berryman,

2004a submitted). The western half of Mt Ruapehu Graben is truncated at its southern end by the E-W to WNW-ESE trending Ohakune-Raetihi fault set, defined from north to south by the Ohakune, Raetihi North, Raetihi South, Waipuna and Ourakukuru faults (Fig. 2.2). Faulting is purely normal in style with a dip to the south. The fault set has a total width of 15 km and an summed extension rate of 4.97 ± 0.85 mm/year.

The NE-SW trending Kariori fault set cuts across the southeastern margin of Mt Ruapehu Graben. This fault set is defined, from north to south by the Wahianoa, Karioi, Shawcroft Road, and Snowgrass faults (Fig. 2.2; Villamor & Berryman, 2004a submitted). This fault set has a dip to the southeast (except for the Snowgrass Fault whose sense of dip is uncertain). The fault set has a width of 24 km and has a total extension rate of 1.91 ± 0.40 mm/year. The intersection of Mt Ruapehu Graben with the Karioi Fault is expressed by a cross-cutting relation between the Rangipo Fault and the Shawcroft Road Fault creating a complicated scallop-like pattern of fault scarps (Fig. 2.3). The Shawcroft Road Fault seems to displace the Rangipo Fault, implying that the most recent event of the former is younger than the most recent event in the latter. Paleoseismic studies on the Shawcroft Road Fault were undertaken to help constrain the age of the last event on the Rangipo Fault.

2.2 Age of the landscape and stratigraphic features displaced by active faults

Volcanic and volcanic-derived deposits in the area (Fig. 2.1) provide very good age control of the stratigraphic sequence, and an opportunity to bracket the timing of faulting. Once a recognisable tephra deposit is dated it provides a time-horizon wherever it is located. Such tephra marker beds are useful in correlating eruptive deposits of similar age around and beyond a volcano and also for constraining the ages of faulted cover-bed successions and the geomorphic surfaces on which they occur. Aside from the prominent composite volcanic edifice of Ruapehu Volcano with its summit crater-lake, the other significant geomorphic landscape element that occurs in the region is the ring plain surrounding the volcano on its lower topographic flanks. The ring plain, is volumetrically larger than the volcanic edifice itself and has been constructed over the last c. 100 ka by the growth of an extensive apron of coalesced fans comprising laharic, pyroclastic and alluvial volcaniclastic detritus (Neall et al. 1995).

The occurrence of recognisable andesitic and rhyolitic tephra beds has also facilitated the stratigraphic subdivision of five lahar formations on the Ruapehu Volcano ring plain. These lahar formations are (oldest to youngest): the >50-m-thick Te Heuheu Formation (c. >25.6-17.6 cal ka) and less voluminous younger formations such as Tangatu (c.17.6- 6.2 cal ka), Manutahi (c. 6.2-1.7 cal ka), Mangaio (5.2 cal ka) and Onetapu (c. 1.7 cal ka to present) (Donoghue et al. 1995; Donoghue and Neall 2001; Fig. 2.4).

The stratigraphy and chronology of volcaniclastic cover-beds of the Ruapehu Volcano ring plain has been previously documented (Purves 1990; Donoghue 1991; Donoghue et al. 1995;

Cronin & Neall 1997; Donoghue & Neall 2001). Late Quaternary andesitic tephra layers from the Tongariro Volcanic Centre (TgVC) are found interbedded with local fluvio-laharic deposits, and with distal rhyolitic tephra layers from the Taupo (TVC) and Okataina (OVC) Volcanic Centres. Andesitic tephra layers are primarily identified from their field characteristics and their stratigraphic positions with respect to dated rhyolitic tephra marker beds. Recognisable andesitic tephra marker beds close to the Rangipo Fault include: Tufa-Trig, Mangatawai, Black Ash, Orange lapilli, Poutu, Ohinepango, Ngamatea-1 & -2, Porohau, L17 and Shawcroft tephra beds (Fig. 2.4). Similarly, recognisable silicic tephra marker beds include: Taupo, Waimihia, Waiohau, Rerewhakaaitu and Kawakawa tephra beds.

Donoghue & Neall (2001) recognised four main periods of fluvio-laharic aggradation on the southeastern Ruapehu Volcano ring plain post-dating the deposition of Kawakawa Tephra at c. 26.5 cal ka. These aggradation periods broadly coincide with the last two cone-building eruptive phases represented by the Mangawhero (c. 60-17.6 cal ka) and Whakapapa (c. 17.6 cal ka to present-day) Formations (Hackett and Houghton 1989). The first period of ring plain aggradation occurred between 26.5 to 17.4 cal ka and is mainly characterised by a thick (>50 m) sequence of syn-eruptive lahar deposits (Te Heuheu Formation) that forms an extensive surface over the eastern to south-eastern sectors of the ring plain and possibly south in the vicinity of Hautapu Stream. It is generally considered that uplift along the eastern block of the Rangipo Fault beheaded the Hautapu Stream and consequently, diverted the river away from the Waiouru area. Uplift also appears to have caused a cessation of fluvio-laharic deposition on the upthrown side of the fault, with Te Heuheu lahar deposits emplaced on the downthrown side then subsequently buried by younger lahar deposits. The large volume of laharic sediments deposited during this period can be broadly related to a episode of intense but sporadic sub-plinian activity occurring at Ruapehu Volcano and as well as elevated sediment flux occurring during the cold climate conditions of the Last Glacial Maximum (LGM; Oxygen Isotope Stage 2) where the landscape was largely devoid of vegetation (Donoghue & Neall 2001).

In comparison to Te Heuheu lahar deposits, post-17.6 cal ka lahar deposits are not as extensive on the south-eastern portions of ring plain. From 17.6 to 6.2 cal ka deposition on the ring plain is dominated by syn- and inter-eruptive laharic events (Tangatu Formation; Donoghue and Neall 2001). Syn-eruptive lahar events were generated up to c. 10 ka while Ruapehu Volcano was undergoing an episode of intense eruptive activity (climactic eruption formed the Tauwera Formation at c. 10 ka ago, Donoghue et al. 1999). Inter-eruptive Tangatu laharic deposits were more common after c. 10 ka and intermittently extended up to c. 6.2 cal ka. From 6.2 to 1.7 cal ka during the third period of fluvio-laharic deposition, lahar events were composed of dilute inter-eruptive sediments (the Manutahi Fm) that were locally deposited in ring plain channels. Also at this time larger, less dilute laharic events formed a fan-like surface (Mangaio Fm) in the northernmost section of Whangaehu River. The fourth and last period of fluvio-laharic aggradation which occurred from 1.7 cal ka to the present day

is represented dominantly by syn-eruptive laharic events and subordinate inter-eruptive lahar events that appear to relate to Crater Lake overflow. From c. 17.6 cal ka to the present day, a reduction in sediment flux to the southeastern ring-plain occurred resulting in stream downcutting and dissection. This interval is coincident with the onset of post-glacial climatic conditions and corresponding expansion of podocarp-hardwood forests (Donoghue & Neall 2001).

3.0 THE RANGIPO FAULT

3.1 Previous studies

The Rangipo Fault was first defined by Ongley (1943) as the Whangaehu River Fault or Whangaehu Fault, but its Quaternary activity was described earlier by Grange & Williamson (1933). Donoghue (1991) and Donoghue & Neall (2001) have reported a 3 mm/yr slip rate for the Rangipo Fault (Whangaehu Fault or Desert Road Fault; Figs. 2.3 & 3.1). This value is based on the interpretation that the 50 m difference in elevation of the main constructional ring plain surface (c. 15,000 yr old based on the presence of the Rerewhakaaitu tephra which immediately overlies the lahar surface) at the Whangaehu River escarpment represents the fault offset. Reconnaissance level field work conducted on the Rangipo Fault by Van Dissen and Villamor in June 1998, strongly suggested that this fault has a high vertical slip rate, probably in excess of 3 mm/yr averaged over the last 15,000 years and that fault had probably not ruptured in the last 1800 years.

More recent Late Quaternary slip rates on the Rangipo Fault estimated from geologic cross-sections and published geophysical data achieved a lower net slip rate of 1.52±0.9 mm/yr (Villamor & Berryman, 2004b submitted). This result was limited by assumptions such as:

- the offset of the base of the lahar and lava deposits is based on just one geophysical study on the ring plain (Sissons & Dibble 1981) which has not been corroborated with other techniques.
- the c. 230 ka age of the base of the volcanic derived sediments of is based on the onset of volcanism but not on a specific known reference marker.

This is a very preliminary result that has been improved substantially in the present study.

3.2 Fault geometry and displacements

3.2.1 Fault mapping

We define the Rangipo Fault (Fig. 3.1) as a system of N-S striking normal faults, 1-4 km wide, that are predominantly west side down, and that are at least 32 km in total length. The fault extents from T21/415837 (grid references hereafter will be presented in truncated way as per the NZMS 260 Topomap series) (location 1 on Fig 3.1) to at least T20/446060 where the Whangaehu scarp terminates (location 2 of Fig. 3.1). Several short fault traces occur 2 km NE from this point (some traces are downthrown to the east) and may represent the continuation of the Rangipo Fault. It may even extend further north to intercept the Kaimanawa Fault, 3 km south of the intersection between SH1 and Lake Rotoaira Road (T19/530295, Location 3 on Figure 3.1). This would extend the length of the fault to 43 km. The northern extent of the fault, north of T20/446060 (Location 2 of Fig. 3.1) remains unclear.

Along its length, the fault has both right and left stepovers (for example at locations T20/427919 and T20/402960), and in some cases linked by NE trending traces (T20/425962).

The characteristics of single traces that together constitute the Rangipo Fault are described separately. The division of the fault into 4 traces is to facilitate the description of the fault geometry and its location. These traces should not be construed as fault rupture segments. They may be described as (Fig. 3.1):

- Trace A: the southernmost trace of the Rangipo Fault extends for 14 km from just north of the Snowgrass Fault (location 1 on Fig. 3.1) to 800 m to the west of Pimple Peak (T20/434948; Location 4 on Fig. 3.1). The fault strike varies from N20°W to N20°E along this trace. The fault scarp disappears when it crosses very recent terraces. At its southern end, at its intersection with Hautapu stream (Location 5 on Fig. 3.1) there are good exposures on the stream banks of the c. 1,7 cal ka old Taupo pumice alluvium up to 2 m thick, that indicate the fault scarp may be buried by thick post-Taupo alluvium deposits. North of Waiouru Stream (Waiouru Military Camp, Location 6 on Fig. 3.1) the trace steps to the west and further north it steps back to the east. These stepovers appear to be linked by small less pronounced fault scarps with a N60°E trend.
- Trace B: the southern-middle portion of the Rangipo Fault, steps 3 to 4 km to the west, relative to Trace A (Fig. 3.1). It extends for 4 km from Shawcroft Road (T20/402921; Location 7 on Fig. 3.1) to the Whangaehu River where the fault crops out in the river bank (Figs. 3.2 & 3.3; Location 8 on Fig. 3.1). It varies in strike from N170°E to N10°E along a continuous, but complex, scarp that splays in several locations into two scallop-shaped strands (Fig. 3.2). Another fault exposure further NE along the river bank shows a main fault plane with a N50°E trend (Location 9 on Fig. 3.1; Fig. 3.4). The northern extension of the N10°W to N10°E trending scarp has been eroded by the river and its northern extension is therefore uncertain. However, deformation is most probably transferred to Trace C by the N50°E trending scarp (Location 9 on Fig. 3.1) and by the southern end of the Trace C which has a N40°E trend. The N50°E trending scarp of Trace B is eroded in part by the Whangaehu River and has currently the appearance of a river terrace riser.
- Trace C: the northern-middle portion of the Rangipo Fault, is parallel to both Trace A and B but lies about 2 km to the east of Trace B (Fig. 3.1). It extends for 12 km generally parallel to the Desert Road and the Whangaehu River from T20/419952 (Location 10 on Figure 3.1) to the end of the large topographic/geomorphologic scarp at T20/445060 (Location 2 on Fig. 3.1), which coincides with the gentle drainage divide between the south flowing Whangaehu River and the north flowing Tongariro River. It is a continuous N-S striking trace, except at the southern end where the fault strikes N40°E. At the southern end of Trace C, weak shattered rock associated with normal faults was found during Mangaio Tunnel excavation (Paterson, 1980). Tertiary sediments to the east were juxtaposed, across the Rangipo Fault, against laharic deposits and alluvium to the west at the Whangaehu escarpment, on the western end of the Tunnel (Paterson, 1980). A major tunnel collapse occurred at this location (T20/435986, Location 11 on Fig. 3.1), which

eventually led to the development of a chimney that day-lighted at the ground surface above the tunnel, along the line of the prominent Rangipo Fault scarp just east of SH 1. At this location a small scarp can be traced at the surface that lies parallel to the main large one located 200 m to the east. Small scarps can also be traced to the north of this point about 200 m to the east of the main scarp (e.g. at T20/445055, Location 12 on Fig. 3.1). Similar small scarps were identified and trenched just 200 m SW of location 11 on the downthrown side of the fault but proved instead to be sand dunes (see chapter on Fault History for details on trench results). It is difficult to confirm whether the small scarps close to locations 11 and 12 are fault strands or sand dunes without excavating exploratory trenches. Along Trace C the Rangipo Fault plane is exposed in two locations: (1) the SH1 roadcut at S20/433985 (Fig.3.5) where it strikes NNE and dips 80°W (close to Location 11 on Fig. 3.1); and (2) further north along the Whangaehu River escarpment where it strikes N05°E and dips 60°W (Location 13 on Fig 3.1; Fig.3.6).

- Trace D: the northernmost trace identified in this study has a length of 2 to 4 km and extends from Mangaio Stream northeast from the northern end of Trace C to Waipahihi Stream (T20/479107, Location 14 on Figure 3.1). The fault trend is c. N20°E and it downthrown to SE. It is unclear whether this fault strand belongs to the Rangipo Fault or is part of a different fault that extends further into Kaimanawa Mountains.

The northern extent of the Rangipo Fault, north of Trace D, remains unclear. Recent fault scarps have not been recognised from aerial photo review. Further north, the Kaimanawa Fault (Fig. 2.1) has been identified as the main boundary between the greywacke basement rocks of the Kaimanawa Mountains and the volcanic and volcanic derived rocks of the TVZ (Gregg 1960). From their structural position as the boundary between volcanic and basement rocks, the Kaimanawa and Rangipo faults could be regarded as having similar roles with respect to the modern Taupo Rift and could be physically connected. Nevertheless, it is not clear that the Kaimanawa Fault is an active structure. If it is not an active structure then the extension of the Rangipo Fault does not necessarily need to join with the Kaimanawa Fault and might have migrated further towards the west on to the Poutu Fault (Fig. 3.1) in a similar fashion to the marginal faults that migrated towards the centre of the Rift in the central Taupo Rift (south of Rotorua, Berryman & Villamor 1999).

A major fault zone was intersected in the Moawhango-Tongariro Tunnel (100 m wide crush zone) in the No-name Creek area (T20/511158, Location 15 on Figure 3.1), 2300 m from the Tongariro Outfall (Hegan, 1980), about 17 km north of the northern extent of Trace D shown in Figure 3.1. A strand of the fault may intersect the Rangipo Tailrace tunnel about 1150 m from the outfall, where an extensive (550 m wide) zone of crushed and sheared greywacke was encountered during tunnel excavation (Beetham 1979) (c. T19/546259). Further investigations could discriminate if these fault zones belong to the Rangipo Fault or to another structure, and whether they are active or not. Resolution of this question is beyond the scope of this study.

3.2.2 Displacements of geomorphic and geologic features

Fault displacements have been measured at several localities along each of the fault traces. We have measured three types of fault offset: (1) net displacement of strata as measured along the fault plane where exposed; (2) vertical offset of geomorphic surfaces in the field (with altimeter or detailed topo maps); and (3) vertical offset of geomorphic surfaces from the 1:50,000 scale digital topo maps developed from LINZ data (digital data of the MZMS 260 map series). Vertical offsets are expressed by the fault scarp heights and represents vertical displacement as opposed to net displacement. Most of our measurements are scarp heights because there are very few exposures of the fault plane. We will present the data grouped according to the different fault traces that comprise the Rangipo Fault (Fig. 3.1). Ages of displaced features are explained in section 3.1.3.

- Trace A: The scarp height along Trace A is c. 13 m high at its southern end, south of Waiouru (between the Ngamatea swamp and the southern termination of the fault, Figure 3.1), but the age of the offset terrace surface is unknown. Scarp heights are smaller (2-3 m) at locations where it crosses streams that flow into the swamp from the east, indicating cumulative displacements. These scarps are developed on a relatively younger surface, but still of unknown age. There is no scarp at the intersection of the fault with the Hautapu Stream. At this point there is a thick sequence of alluvial deposits that are attributed to the Taupo Pumice (eruption from Lake Taupo at c. 1.7 cal ka) suggesting no fault rupture since some time less than 1.7 cal ka years ago.

  Along the northern part of Trace A, the fault scarp crosses Waitangi Stream terraces and nearby the fault plane is exposed in a road cutting (T20/438940, Location 5 on Figure 3.1). Fault scarp heights on these stream terraces of unknown age are 2.7, 3.7 and 5.1 m. The road cutting exposes a N03°W striking fault plane with a 66°W dip. Taupo, Mangatawai, Papakai and Bullot Formations can be recognised on the upthrown side of the fault but they cannot be matched on the downthrown side, so no fault displacement could be measured. It is unclear whether Taupo pumice (c. 1.7 cal ka) and younger tephra are displaced in this exposure but it is certain that Bullot Formation is faulted so there has been displacement on the fault within the last 10,000 years. The morphology of the scarp seems to be very fresh since the steep stream slopes are displaced by the fault suggesting fault movement much younger than 10,000 years ago.
- Trace B: Scarp heights along Trace B extend up to 35 m in height on the ring plain surface when measured from the 1:50,000 scale digital topographic map (Profiles 4 and 5 of Fig. 3.7). At site T20/405935 (area labelled as Shawcroft Road trench site in Fig 2.3; see also Fig. 3.2) we constructed a local digital topographic model using a Real Time Kinematic GPS system which has better constrained the scarp height of Trace B to c. 27 ± 0.25 m (Fig. 3.8). The ring plain surface at this location is c. 26.5 to 17.6 cal ka in age (see section 3.1.3).

The fault plane is exposed on the south bank of the Whangaehu River (Fig. 3.3; Location 8 on Figure 3.1) where sedimentary and volcanic units on both sides of the fault are recognised. It has not been possible to match stratigraphic markers across this fault plane. There is also minor faulting (decimeter to meter scale displacements) to the west of the main fault plane, distributed across a 200 m wide exposure with displacements of Kawakawa Tephra (Figs. 2.4 & 3.3 & 3.9).

- Trace C: Along the southern part of Trace C the scarp has a strike of N40-45 °E (T20/425963) and displaces the ring plain (with a possible age of 25.6 to 17.6 cal ka) by c. 30 m (Profile 6 of Fig. 3.7). At the northern end of this scarp the height diminishes to only 2-2.6 m (T20/435972, close to Moawhango Access Road). This is the site of one of the exploratory trenches (Zone 19 trench; see section 3.3). The fault steps northwest to a strand with a scarp height of 17 m based on digital topograhic model constructed with a Real Time Kinematic GPS system (Fig. 3.11). At this location the fault plane was exposed and studied in the Tank Track exploratory trench (see section 3.2.3). The surface displaced by the fault it possibly somewhat younger (17.6 to 13.8 cal ka) than the main ring plain surface (see section 3.1.3). The same fault strand is also exposed at SH1 (T20/443985, Fig. 3.5) where there is a 3.3 m displacement of the 17.6 cal ka old Rerewhakaaitu tephra.

  North of the Moawhango Dam access road the scarp is 40+ m high (Profiles 1, 2 & 3 of Fig. 3.7). However, we regard this scarp height to be the combined results of both tectonic and erosional processes based on the arguments presented below, and therefore the scarp heights are not representative of the true fault offset of the ring plain.

3.2.3 Age of the displaced ring plain

Knowing the age of the ring plain surface and associated cover-beds is crucial for characterising the earthquake hazard of the Rangipo Fault. Although the ring plain in the area is very extensive there are locally some geomorphic features that indicate that a period of incision of the plain occurred prior to the present incision of active river courses. In this case some parts of the ring plain could be younger than the highest, extensive surface. This is especially important as the age of the displaced surface might therefore be different on both sides of the fault due to erosion or aggradation. For example, Trace C seems to display the largest offset, up to 70 m (Fig. 3.7), of the extensive ring plain surface. Because the Whangaehu River flows at the base of this escarpment it is possible that erosion has downcut into the downthrown side of the fault scarp and enhanced the fault scarp height. In this case, a value of 70 m is an overestimate of tectonic faulting. It is also possible that sediments from the streams flowing from Ruapehu Volcano were buttressed against the fault scarp, filling part of the space created by faulting, reducing the scarp height (Donoghue & Neall 2001). In this later case a value of 70 m would represent a minimum value for tectonic faulting. In this section of the report, we present evidence that attempts to establish the age of the ring plain on both sides of the Rangipo Fault for those locations where we have been able to measure fault scarps.

In exposures along the edge of the Whangaehu River where Trace B is exposed (location 8 Fig. 3.1) tephrostratigraphy enables the age of the main lahar surface at c. 26.5 to 17.4 cal ka to be well-constrained on both sides of the fault. The cover-bed stratigraphy exposed on the upthrown side of the fault at this site comprises a c. 8-m-thick succession of lapilli, ash and medial beds overlying indurated laharic deposits. This sequence is equivalent in composition to that described by Donoghue et al. (1995) in a section 1 km to the north, also on the upthrown side of the Whangaehu River escarpment (T20/411966; Whangaehu River Section 9; Donoghue 1991; Fig 3.8). Donoghue's stratigraphy indicates c. 1 m of the upper part of Bullot Formation (with 13.8 cal ka old Waiohau Tephra at 0.15 m depth from ground surface) and c. 3 m of the Te Heuheu laharic deposits interbedded within older Bullot tephras. At T20/409965 (a few meters north of Donoghue's Section 9; Location '98 sample on Fig 3.10) a 0.1 m thick rhyolitic tephra bed was sampled a few centimeters above the laharic sequence and was tentatively identified as the 17.6 cal ka old Rerewhakaaitu Tephra based on its ferromagnesian mineralogy (Nairn pers. comm. 1998). At this same location, another rhyolitic tephra bed was sampled from c. 30 m below the upper lahar surface. Based on its lower stratigraphic position, this tephra bed was regarded as being considerably older than Rerewhakaaitu Tephra. The mineralogy of this tephra bed appeared inconsistent with both Okareka Tephra (biotite is absent) or Kawakawa Tephra (crystal content is too high compared with a Kawakawa Tephra correlative located 100 m further downstream) which are both known to occur in the area. Therefore, the observed rhyolitic tephra bed is considered to be older than 26.5 ka and may be Okaia, Omatoaroa, Hauparu or Rotoehu Tephras – all of which have been described on the north-eastern Ruapehu ring plain in the vicinity of Waikato Stream (Cronin & Neall 1997).

The cover-bed stratigraphy on the downthrown side of the fault appears similar to that described by Donoghue (1991) c. 700 m to the SSW (T20/399954; Whangaehu River sections 1 & 2 of Donoghue 1991; Fig 3.10). Here, c. 5 m of andesitic tephra beds interbedded with thinner rhyolitic tephra beds (Waiohau and Rerewhakaaitu Tephras) mantle laharic deposits of Te Heuheu Formation. At the base of the river bank exposure Kawakawa Tephra was identified (Nairn pers comm. 1998; Fig 3.9) interbedded with laharic deposits c. 20 m below the uppermost laharic deposits occurring near ground surface.

The occurrence of Kawakawa and Rerewhakaaitu Tephras enveloping the lower laharic succession appears to constrain the age of laharic deposition on both sides of Trace B between 26.5 to 17.6 ka. This age range refines previous age estimates of >c. 20 ka (Donoghue and Neall 2001) for the cessation of laharic deposition on their surfaces B and C where Trace B is located.

The age of the ring plain of both sides of the Whangaehu River escarpment along Trace C appears different on both sides of the fault, which was first noted by Donoghue (1991) and Donoghue and Neall (2001). Nevertheless, our analysis of their data and newly acquired field

data differs from their interpretation in that the main ring plain surface on the downthrown side of the escarpment has been eroded rather that buried by younger laharic deposits. Our interpretation argues for younger laharic deposits being emplaced west of the Whangaehu escarpment after erosion has removed at least part of the c. 26.5-17.6 cal ka surface.

Along the eastern (upthrown) side of Whangaehu escarpment the cover bed stratigraphy appears to indicate that the main surface was constructed by Te Heuheu laharic deposits and has not been an active depositional surface between c. 26.5- 17.6 cal ka (Donoghue's 1991 stratigraphic sections along the Wahianoa Aqueduct and Whangaehu River 5, Fig. 3.10, show Rerewhakaaitu Tephra covering very coarse lahar deposits).

On the western side of the Whangaehu escarpment (downthrown) the cover bed stratigraphy indicates that after the Te Heuheu related (i.e. c. 26.5-17.6 ka) ring plain surface was abandoned, deposition of post-Te Heuheu laharic deposits only occurred where river channels had incised into the surface. North-west of the intersection between the fault and SH1, the surface of the ring plain close to the fault is formed by young laharic deposits belonging to the Onetapu, Manutahi and Tangatu Formations (Fig. 2.4). These young laharic deposits have been described at least as far as 2 km west from the Whangaehu escarpment (Donoghue & Neall 2001; stratigraphic sections: Rangipo Section 2, Aqueduct 1, 2 & 3 and Whangaehu Ford of Donoghue 1991; Fig 3.10). In the same general vicinity, c. 5 km west of the escarpment, Te Heuheu deposits are exposed at the surface (Wahianoa Rd Section 1 and Aqueduct Rd section of Donoghue 1991; Fig 3.10). These stratigraphic sections reveal that Te Heuheu laharic deposits in the vicinity of the fault are always overlain by ash, lapilli and ashy-medial beds, and are never buried by younger laharic deposits on the downthrown side of the fault.

Topographic differences between the stratigraphic sections also point to the fact that post-Te Heuheu laharic deposits are primarily deposited in and adjacent to surface channels. Profiles 1 to 4 of Fig 3.10 show that Te Heuheu laharic deposits are more elevated that those surfaces associated with younger Onetapu, Manutahi and Tangatu laharic deposits. Only data from two of Donoghue's 1991 sections could contradict our statement that Tangatu and younger lahars are always deposited in localised channels which are incised into the extensive Te Heuheu lahar surface. These two sections have Tangatu laharic deposits overlying older Te Heuheu deposits (see Fig 3.10): (1) Whangaehu River Section 8 has up to c. 1 m of Tangatu laharic deposits overlying Te Heuheu Formation; (2) Aqueduct Rd section has a 11-cm-thick layer of possible Tangatu Fm above Waiohau Tephra. Profile 4 of Fig. 3.10 shows that Whangaehu River Section 8 is topographically lower than the Te Heuheu extensive surface indicating that the Te Heuheu deposits of the section represent older depositional events implying erosion has removed younger Te Heuheu laharic deposits. Regarding Aqueduct Rd section, it is possible that some small Tangatu age deposits can cover Te Heuheu lahars in the steep slopes of the ring plain where incision is not very pronounced and lahars can spill over the edge of the stream course. We consider that these two sections do not contradict our interpretations.

In addition to the topographic relation between stratigraphic columns, also stratigraphic and topographic relations from the trenches excavated across the Rangipo Fault, at the southern end of Whangaehu escarpment, have revealed that major erosion occurred at least prior to deposition of Waiohau Tephra and possibly prior Rerewhakaaitu on the fault scarp itself and to the W (see section 3.2.2). The implication of these topographic relations is that the edge of the Whangaehu River escarpment has been fluvially modified and incised on its downthrown side prior to deposition of younger laharic deposits. The Whangaehu escarpment height has been exaggerated by erosion at its downthrown edge and does not accurately represent the fault offset. We therefore disregard previous estimates of fault offset based purely on the elevation difference either side of the Whangaehu escarpment.

Based on combined stratigraphic and geomorphic evidence we interpret that there was a short period of intense erosion occurred just after deposition of Te Heuheu laharic deposits and prior to deposition of Rerewhakaaitu Tephra (Rerewhakaaitu Tephra is found at the basal part of Tangatu laharic deposits). This erosion was essentially confined to an area bounded to the east by the fault scarp and to the west by "a distinct topographic divide", which delimits the eastward extent of the Tangatu Formation of Donoghue & Neall (2001). Erosion due to incision of the Whangaehu River (and probably Whangaehu-Hautapu River, see Donoghue & Neall 2001) was probably not greater than 20 to 30 m at the western side of the channel and probably larger in dimension at the Whangaehu escarpment. The low resolution of the existing topographic maps (1:50,000 scale series) makes it extremely difficult to assess subtle topographic variations for c. 20 m differences in elevation. It is not surprising then that previous interpretations of the ring plain evolution did not include a phase of river incision prior to post 17.6 ka laharic sedimentation.

3.3 Paleoseismic studies

3.3.1 Selection of trench sites

Field reconnaissance of the central and southern part of the Rangipo Fault was undertaken in December 2001 and seven potential trench sites were selected (Figs. 2.3, 3.2 & 3.5 for locations). Only six sites were excavated. We next state the selection criteria for all seven sites. Results from those sites that were trenched are represented in sections :

- **Sites 1, 2 & 3 (Figs. 3.5 & 3.10):** If the whole height of the Whangaehu River escarpment (up to 70 m) is produced by faulting then displacement at the SH1 roadcut (Fig. 3.5) can only account for part of the deformation across the fault. There is only c. 3 m of displacement on the 17.6 cal. ka old Rerewhakaaitu Tephra at the road exposure, therefore, to account for c. 70 m of proposed displacement on the c. 26.5 to 17.6 cal. ka lahar surface there would have to be more fault strands W of the main scarp. Just a few meters south of the exposure of the Rangipo Fault at SH 1 (on the main c. 17 m high scarp, Fig. 3.11), the fault seems to splays into several 2 to 4 m high scarps. Excavation of two trenches across the lower scarps could prove if they are fault features or other

geomorphic features such as sand dunes (sites 1 & 2; Zone 3 Lower and Upper trenches). Cleaning of the tank tracks adjacent to the access road to Moawhango dam (14 m scarp; Tank Track trench; site 3) could help establish the faulting history over the last c. 17.6 cal ka BP. This scarp is very big and it is possible that clear displacement on young units might not be shown in trenches (due to scarp erosion) and some strata might not be matched across the fault plane (if the offset is too large then any excavation might not be deep enough).

- **Site 4 (Zone 19 trench; Figs. Fig 3.5 & 3.10)**: One trench at the northern end of the N70°E striking scarp just SE of Moawhango dam access where the scarp dies out could: (1) help establish that N70°E trending traces rupture together with N10°E trending ones and (2) contribute to the faulting history since single event displacement is smaller at the tip of faults and it might be easier to observe strata offsets. The only inconvenient aspect of this site is that not all earthquakes are recorded at the tip of faults and may not record all or be representative.
- **Site 5:** One trench at the southern end of Ngamatea Swamp. This site offers good potential for identifying the most recent events. Volcanic ash is generally well preserved in low energy environments such as swamps and we might obtain a very good record of the very recent strata in the upper layers of the swamp.
- **Sites 6 & 7 (Harding #1 and #2 trenches; Fig 3.2 & 3.8)**: Two trenches on Shawcroft Road Fault. The Shawcroft Road Fault (see section 4) and the Rangipo Fault crosscut each other. Aerial photographs show clearly that the most recent movement on the Shawcroft Road Fault is younger than the most recent movement, at this site, of the Rangipo Fault. Timing of the last event on Shawcroft Road Fault would constrain the most recent Rangipo Fault event.

Six of the seven potential trench sites have been excavated. In January 2002 we undertook excavation and study of exploratory trenches across the Rangipo Fault at the sites 1, 2, 3, & 4 (trenches: Zone 3 North; Zone 3 South; Tank Track and Zone 19 respectively; Fig 3.5). In February-March 2003 we excavated and analysed two trenches on the Shawcroft Road Fault (Harding 1 and Harding 2 trenches at sites 6 & 7 respectively). Site 5 (Ngamatea Swamp) was not excavated. Further exploration of the Ngamatea swamp site included literature review of previous stratigraphy studies in the area (mainly Donoghue 1991) and undertaking an auger hole at the possible trench site to gain knowledge on the stratigraphy of the site. Donoghue (1991) studied the soil layers exposed in drainage ditches in the swamp which exposed a few tephra layers among peat layers. We decided not to excavate a trench across the Rangipo Fault in the Ngamatea swamp area because the groundwater table was too high to excavate a safe trench.

The earthquake history of the Rangipo Fault was studied from two trenches: Tank Track and Zone 19 trenches (Fig 3.5a for location). The fault plane was exposed and a detailed analysis of the deformation of volcanoclastic beds was undertaken at the Tank Track trench. Although

minor faulting was observed in Zone 3 North trench, Zone 3 North and South trenches did not show any major fault plane that could be of use to analyse the earthquake history of the fault. However, the stratigraphic and geomorphic relations found in these two latter trenches contributed greatly to the understanding of the age of the landscape, the lack of major faulting to the west of the Tank Track scarp; and the processes forming the up to 70-m-high Whangaehu escarpment.

3.3.2 Trench site geology

The trenches across the Rangipo Fault are located near the eastern margin of the south-eastern Ruapehu ring plain. In this vicinity, a thick succession of bouldery diamicton deposits of fluvio-laharic origin are extensively distributed, and form a broad undulatory surface on the upthrown side of the Rangipo Fault. We correlate this laharic succession with Te Heuheu Formation (c. >25.6-17.6 cal ka; see section 3.1.3). In this area, the oldest rhyolitic tephra bed overlying the laharic succession has been previously identified as Rerewhakaaitu Tephra (Donoghue 1991; Fig. 2.4; at SH1 road-cut at location 10 of Fig. 3.1 and Fig 3.5). At the road cut the lahars are mantled by an alternating sequence of tephra (lapilli and ash beds) and andesitic tephric layers.

The main geomorphic features of the site are two high fault scarps, which trend N-S and N50-30°E (Figs. 3.5a and 3.11). Minor subparallel small scarps to the west of the large N-S trending scarp could also be related to faulting. A major fault plane with faulted tephric cover-beds is well exposed on the west-facing road-cut on SH1 (Fig. 3.5) on the edge of a topographically prominent N-S scarp feature. This high scarp can be continuously traced southward to the vicinity of the Tank Track site (Fig 3.5a) where trenching has revealed two major fault planes (Fig. 3.12). Tank Track trench is located in a wind gap along the fault scarp (Fig 3.11). The scarp is a few metres lower than immediately to the north and to the south, indicating that a stream cut into the extensive Te Heuheu surface and crossed the fault scarp at this point. This stream course was consequently abandoned and is not active at present.

The stratigraphy of the trenches is similar to that exposed at the road cut. It comprises an alternating sequence of andestic tephra (ash and lapilli beds) and ashy-medial layers overlying fluvio-laharic deposits (Figs. 3.12. 3.13 & 3.14). Although twelve rhyolitic tephra marker beds are known to occur in the area (Donoghue et al. 1995), only three beds are observed at the Rangipo Fault trench sites and include (from youngest to oldest): Taupo Tephra, Waimihia Tephra and Waiohau Tephra. These silicic tephra beds have been identified by a combination of major element glass shard chemistry and stratigraphic position (Appendix).

Several subtle scarp features occur further west which were considered to be minor splays of the main scarp. Excavation of two trenches (Zone 3 upper and lower) across these possible fault splays revealed only minor secondary faulting. Minor fault planes were identified in the lower Zone 3 trench offsetting tephra and ashy-medial beds by 9 to 22 cm. In contrast to this,

the upper Zone 3 trench showed no fault planes and revealed that the scarp was in fact a linear-shaped sand dune feature. The lack of major faulting in Zone 3 trenches was the reason why we did not produce detailed trench logs, but a detailed stratigraphy study was undertaken (Fig 3.13). A <0.20-m-thick debris flow deposit is observed at the western end of the Zone 3 lower trench (Fig 3.11). This debris flow deposit occurs above a prominent lapilli bed correlated with Porohau Tephra (c.10-11.8 ka; Donoghue et al. 1995) and is directly overlain by a centimetre-thick aeolian sand bed. Eastward along the trench (profiles 10 to 19), the debris flow deposit wedges out completely and the aeolian sand bed correspondingly thickens to over c. 2 m thick (Fig 3.13).

The last of the trenches excavated at this site is Zone 19 trench, which is located on a fault trace with N50 to 30°E (Fig. 3.5a). This fault trace steps over to the southeast from the main fault scarp and increases in fault throw to the southwest. Zone 19 trench was excavated in the northernmost part of the trace where the low scarp height allowed excavation. Logs of trench walls are presented in Figs. 3.14 a & 3.14 b

3.3.3 Tank Track trench

The Tank Track trench was excavated in an existing cutting where the scarp was c. 14 m in height. The c. 2 m cut in the tank track showed that at least the upper layers were not deposited horizontally but mantling pre-existing sloping topography. This increased the likelihood of matching layers across the fault itself (even for a high scarp). We only logged the north wall of the trench, because exposures on the south wall were poor because of extensive modification of the original ground surface.

At the Tank Track trench (Fig. 3.12), Taupo Tephra (1.7 cal ka) comprise c. 0.2-m-thick fine-grained, massive structured, poorly sorted, pumiceous coarse sandy ignimbrite deposit containing charcoal fragments directly overlying a prominent (<0.24-m-thick) buried soil horizon (Fig. 3.12). The upper contact of this ignimbrite deposit is usually erosional and overlain by variably-thick (<0.3 m), planar to cross-bedded pumiceous coarse sands. Waimihia Tephra (3.4 cal ka) comprises distinct c.0.02-m-thick pods (or cream cakes) of pale brown to white fine vitric ash occurring in andesitic soil material between 1 to 1.3 m depth below the ground surface. In the Tank Track trench site, Waimihia tephra underlies a bedded dark grey coarse to fine ash correlated with Mangatawai Tephra (Donoghue et al. 1995). Waiohau Tephra (13.8 cal ka) comprises c. <0.05-m-thick, white vitric fine ash occurring in andesitic soil material between 3 to 4 m depth below the ground surface. Waiohau Tephra directly overlies an unnamed cm-thick dark grey lithic coarse ash and in turn overlain by a prominent c. 0.20-m-thick strong brown to brownish yellow fine pumiceous lapilli bed with subordinate very dark grey fine lithic lapilli. This prominent lapilli bed is correlated with Shawcroft Tephra (Donoghue et al. 1995). Fluvio-laharic deposits typically occur c. < 1 m below Waiohau Tephra at the trench site (Fig. 3.12). The strata in the trench exposure have a

clear general dip to the west. The strata have an almost horizontal dip at the eastern end of the trench (5°W), while they dip west at the centre (20 to 30°W) and at the western end (5 to 10°W).

The excavation exposed two main fault zones (c. 6 m apart) comprising 1 and 3 major fault planes each (Fig. 3.12). Each major fault plane splays upwards into two or more strands. Fault F1 is located at vertical line 16 (Fig. 3.12) and splays upwards into three fault strands. F1 ruptures through most of the stratigraphic section except for reworked Taupo (reTp) that lies on the top of the fault. F1 has metre scale offsets. Fault F2, located at vertical line 20 (Fig. 3.12), splays into two strands and stops at about middle depth of the trench wall (at about the bench position) displacing Porahu Tephra (Prh) but not Ngamatea 1 Tephra (Nga1). Displacements on F2 are only decimetre scale. Fault F3 (Fig. 3.12) is located at vertical 21 and splays into three strands, one joins with F2 and another is a short splay in the upper part of that fault. F3 displaces a layer containing reworked Taupo Tephra (Tp) by a few cms, but has metre scale offsets of older strata. Fault F4 is the easternmost fault in the trench and displaces all the stratigraphic section up to at least Ngamatea 2 (Nga2) Tephra by a few cms. The stratigraphic section between Mangamate (Mnt) and reworked Taupo (reTp) has been eroded at this location. Reworked Taupo unit is not displaced by F4.

Other important features of the strata exposed in the Tank Track trench are the unconformities. Unconformities are sometimes related to erosion/deposition process and sometimes to tectonic deformation. The geometry of the layers and the presence of unconformities together with the topographic relations shown in Fig. 3.11 (see section 3.2.2.) indicate periods of deposition of volcanic ash and periods of erosion. Erosion can be enhanced on the upthrown side of the fault as a result of footwall uplift related to faulting. We will use these relations to analyse the timing and amount of displacement. For example, the most clear unconformity in Fig. 3.12 is the base of Taupo Tephra (Tp) and reworked Taupo Tephra (reTp) which lie over eroded Mangamate Formation (Mnt), Papakai Formation (Pp) and Ngamatea 2 Tephra (Nga2). Assumptions on the original shape of the scarp before deposition of the different layers introduce some uncertainties in the faulting interpretations.

We have analysed the number of prehistoric earthquakes on the Rangipo Fault in two different ways. Firstly we have analysed the amount of offset of each of the main stratigraphic units exposed in the trenches. Layers present offset values that are larger in older strata (the increase in offset is called progressive displacement). Large differences in offset values between closely spaced stratigraphic horizons are interpreted as representing an earthquake event, constraining the timing of rupture and defining the single event displacement (SED). Secondly we have restored the offset of the different layers. In this second exercise we "un-fault" the layers to the position they had prior to the occurrence of each earthquake (Fig. 3.15 a-f). The amount of movement that is needed to restore the layers is assumed to represent the amount of displacement that occurred during that specific earthquake (i.e. the single event

displacement caused by that earthquake). We can also bracket that timing of an event by analysing which layers are brought into juxtaposition in each restoration. We will also take into account other fault related features such as: local unconformities; colluvial wedges derived from the fault scarp after the earthquake occurs; presence of fissures; and termination of the fault into the different layers, to confirm and/or contribute to the analysis of the timing of faulting and its magnitude.

Table 3.1 Rangipo Fault earthquake history obtained by progressive displacement analysis of Tank Track trench

RANGIPO FAULT - Tank Track trench						
	Total offset (m)					
	Fault 1	Fault 2	Fault 3	Fault 4	Total	Displacement Group, DG (m)
Tufa Trig	0	0	0	0	0	
Taupo & and base of reTp	0	0	0.16	0	0.16	DG 1 (0.16m)
Orange Lapilli	0.94	0	0.41	0	1.35	DG 2 (1.20 m)
Mangamate	0.74	0	0.41	0.20	1.36	
Ohinepango	1.92	0	0.61	0.10	2.63	DG 3 (1.30 m)
Ngamatea 2	1.92	0	0.51	0.10	2.53	
Ngamatea 1	1.81	0	0.70	0.08	2.59	
BUN 2	1.83	0	0.86	0.08	2.77	
Porahu	1.92	0.04	1.21	0.10	3.26	DG 4 (0.50m)
Shawcroft	1.83	0.10	1.10	0.12	3.16	
Waiohau	1.81	0.06	1.02	0.06	2.95	
Diamicton	1.92	0.08	1.08	0.08	3.16	

Table 3.1 summarises the progressive displacement results. To assess displacement we have accounted for drag folding geometries, therefore, some offset measurements are not simply represented by the distance between piercing points along the fault. When drag folds are clear (see for example, Bun2 Tephra just west of F1 in Fig 3.12) we have projected the marker horizon onto the fault following the general geometry of the horizon. For the upper layers, we have also projected the horizons onto the fault plane when the horizon has been eroded away. For this exercise we have assumed that the projected horizon followed the general geometry of the preserved horizon. When preservation is poor we have used the shape of the current scarp as a proxy to shape of the marker horizon (since air fall deposits tend to acquire the shape of existing topography). We have estimated at least four different displacement value groups: (a) layers from the basal lahars (e.g. diamicton) up to Porohau Tephra are displaced by c. 3.10 m; (b) layers Bun2 Tephra to Ohinepango Tephra are displaced by c. 2.6 m; (c) layers Mangamate Tephra to Orange lapilli Member are displaced by c. 1.2 m; and (d) layers Taupo Tephra to Tuffa Trig Formation are displaced by c. 0.15 m. In summary the steps from older to younger are: 0.5, 1.30, 1.20 and 0.15 m. The simplest interpretation of this result is that 4 earthquake events have occurred since deposition of the diamicton and the step values

represent the SED associated to each event. The results of the restoration of the events can help confirming one of this hypothesis.

Figs. 3.15a to 3.15f show possible restorations of the different offsets of the layers exposed in Tank Track trench. We will refer to the different earthquakes obtained as TT_*x* (for example, TT_1 is the youngest event in Tank Track trench) to differentiate them from the events obtained later on in Zone 19 trench (which will be labelled Z19_*x*). Each figure represents the geometry of the layers immediately prior to the event. For example, Fig. 3.15a represents the trench wall before TT_1 occurred, Fig 3.15b represents the trench wall before TT_2 occurred, etc. There are intermediate stages in between the figures which are the subsequent erosion and deposition of new layers. For simplicity we will not show these intermediate stages. In this fashion the ground surface of each figure represents an event horizon.

We first restore the displacement of the base of reworked Taupo Tephra (reTp in Fig 3.15a) which is the youngest unit affected by faulting (by F3). Reworked Taupo Tephra is preserved in the whole trench wall and it only affected by faulting across F3. Restoration of the offset on F3 is achieved by **10 cm**. Restoration of the base of reworked Taupo Tephra brings Taupo Tephra into its original "un-faulted" configuration across F3. The event occurred after deposition of the basal part of reworked Tp (only part of it is displaced on Fig. 3.12) and before deposition of Tuffa Trig Formation (non dated). Timing of this event, TT_1 is younger than 1.7 cal ka.

The next youngest layer that is still displaced after the first restoration is the paleosol on the Mangatawai Tephra (Mng in Fig 3.15a). Because this layer is eroded on the upthrown side of the scarp (between vertical lines 18 and 26) we are not sure if erosion has removed evidence of faulting in faults F3 and F4. The geometry of a remnant of the Mangatawi Tephra (Mng) at vertical line 24 which lies unconformably over older sediments indicates that the Mangatawai Tephra was probably deposited on a steep eroded scarp (Fig. 3.15b) and that if it was displaced by F1 and F2, the amount of displacement might not have been large. We therefore assume that there was no displacement on Mng on F3 and F4. Restoration of the Mangatawai Tephra in F1 (Fig. 3.15b) implies only **0.14 m** of displacement. Restoration of the Mangatawai Tephra does not restore any other layer. Event **TT_2** happened between the Mangatawai and Taupo Tephras (Taupo Tephra was fully restored in Fig. 3.15a), that is between 2.5 and 1.7 cal ka.

Fig 3.15 b shows that next highest layer that is displaced is Papakai Tephra (Pp in Fig. 3.15b and c). Pp is clearly displaced by F1 and F3 but it has been eroded from the east side of faults F1 and F3 and both sides of F4 (Fig 3.15b). The geometry of the small remnant of Pp at vertical 21 implies that Pp was most likely deposited conformably over Orange lapilli Member (Olap) and Mangamate Tephra (Mnt). To restore the base of Pp we have to assume (Fig. 3.15 c):

- Across F1 the top of the Mnt is used as the base of Pp (Pp on the eastern side of F1 has been eroded). If we assume that Mnt was not eroded before faulting and that Pp lay conformably over Mnt, we can then extend the top of Mnt (from vertical line 18) westwards following the slope of the top of Mnt that is assumed to be not eroded (Fig. 3.15 c). If we restore the base of Pp from this position, Ngamatea 1 Tephra (Nga1) would end up at a higher elevation on the downthrown side (west) of F1 than on the upthrown side (east). Therefore Mnt had to be eroded at F1 before deposition of Pp. If we use the current shape of the top of Mnt as the base of Pp (with the erosional geometry shown between vertical 18 and F1), we can now restore the base of Pp on F1 by 65 cm. This now brings Ngamatea 1 into an unfaulted position on the eastern strand of F1 (Fig. 3.15 c).
- Across F3 we assume that the base of Pp east of F3 is the top of Mnt. We restore 0.15 m on F3. This is a minimum value because erosion of Mnt implies that the base of Pp is even higher.
- It is difficult to assess whether there was displacement of Pp across F4 because it is absent on both sides of F4. For simplicity and because the total offset on F4 is small we will assume no displacement on F4.

Therefore a total of **0.8** m of offset occurred for **TT_3** (Fig 3.15 c). This restoration does not bring back in alignment the base of Mnt which shows small offsets on faults F1 and F2 (Fig. 3.15 c). Event TT_3 happened after deposition of Pp and before Mng, i.e. between 3.4 and 2.5 cal ka.

Restoration of the base of Mnt (Fig. 3.15 d) implies only **0.35** m offset and does not bring any other layer into juxtapositon. This event, **TT_4**, is very small, similarly to event TT_1. Restoration of Mnt does not make any other unit match across the fault. Event **TT_4** happened after deposition of Mnt and before deposition of Pp, i.e. between 11.2 (we can not constrain the age of Mnt better, see Fig. 2.4) and 6.2 cal ka.

The youngest displaced layer on Fig. 3.15d is the Ohinepango Tephra, Oh, or possibly the Poutu Tephra (Pt) but Pt is not preserved on the eastern side of the trench. We use Oh to restore event **TT_5**. Oh is preserved in several parts of the trench and always lies conformably with the Ngamatea 2 Tephra (Nga 2) indicating that not much erosion happened in the time bracketed by Nga 2 and Oh. We assume that Oh was deposited comformably on Nga 2 along the entire trench wall to extrapolate the parts of Oh that have been eroded. The restoration is achieved by (Fig. 3.15 e):

- 0.9 m displacement on F1. All the layers are restored in F1.
- 0.2 m displacement on F3. There is no Oh at F3 but we have assumed that restoration of Oh will bring Nga_1 into juxtaposition.
- 0.1 m displacement on F4. The situation is similar to F1. All the layers are restored across F4.

A total displacement of **1.2 m** occurred during **TT_5.** Along F3 all the layers down to Bullot unnamed tephra 2 (Bun 2) have been restored in Fig. 3.15e. Event **TT_5** happened after deposition of Oh or possibly Pt and before Mnt, i.e. between 11.2 and 6.2 cal ka and before event TT_4. Also, two units interpreted to be colluvial wedges, located between the Ohinepango/Poutu and Mangamate Tephras close to faults F1 and F3, seem to have formed after rupture of the fault in TT_5.

The earliest event, **TT_6**, is restored by bringing Poarehu Tephra (Prh) in juxtaposition across F2 (Fig 3.15 f). A displacement of **0.4 m** of is required to do this. All the exposed layer contacts are now restored. Event TT_6 happened after deposition of Poarehu and before deposition of Bullot unmaned tephra 2 (Bun 2) just below Ngamatea 1 Tephra, i.e. between 13.8 and 11.8 cal ka.

In Fig 3.15 f, after restoration of all the exposed contacts there is still a c. 5 m high topographic scarp. This scarp can be interpreted in two ways. It can be an erosional scarp not related to faulting or it can represent the amount of faulting that occurred just before deposition of volcanic cover beds. The scarp is possibly a mixture of both. The presence of a tectonic scarp may have focused the location of the river course along it and led to subsequent erosion.

A summary of the results of the restoration analysis is presented in Table 3.2. In comparison with Table 3.1, Table 3.2 shows two more events, events TT_2 and TT_4. These have small offsets and were difficult to distinguish with the progressive displacement analysis. Events TT_2 and TT_4 are secondary and do not add to the primary rupture history of the fault. However it is important to detect these events because their displacements would otherwise be added to a primary rupture and the single event displacement would then be slightly overestimated. The presence of these events resulted in the single event displacement obtained by progressive displacement analysis to be somewhat larger.

Table 3.2 Rangipo Fault Earthquake history obtained by offset restoration analysis on the Tank Track trench

Event	After	Before	Offset per event (m)
TT_1	Tp	TT	0.10
TT_2	Mng	Tp	0.14
TT_3	Pp	Mng	0.8
TT_4	Mnt	Pp	0.35
TT_5	Oh/Pt	Mnt	1.2
TT_6	Prh	Nga 2	0.4

See Fig 3.12 for meaning of acronyms.

3.3.4 Zone 19 trench

The Zone 19 and Tank Track trenches were excavated across two strands of the Rangipo Fault which have different trends. Only with exploratory trenches on each strand can we establish if both traces have the same rupture history. Zone 19 trench is excavated at the northern tip of a

fault trace across a small scarp. The small height of the scarp is attributed to the fault trace dying out to the north and deformation being transferred to the Tank Track scarp.

Deformation at the tip of a normal fault has several characteristics that obscure the earthquake history of the fault. Firstly, single event displacement is very small and, therefore, hard to distinguish form secondary faulting. Secondly, not every primary rupture will necessarily reach the very end of the fault trace due to the natural variability of the rupture length of a fault. Nevertheless, we logged both trench walls (Figs. 3.14a & 3.14b) and present the results below.

The stratigraphy found in Zone 19 trench (Figs. 3.14a & 3.14b) was similar to that exposed in the Tank Track trench (Fig. 3.12) which implies that the topographic surface displaced by the fault at this location is similar in age to the surface displaced by the Rangipo Fault at the Tank Track site. On the north wall of Zone 19 trench we identified an additional paleosol and a rhyolitic tephra within Papakai Tephra above the Orange Lapilli Member. We have not identified this tephra in the laboratory but we have correlated it to Hinemaiaia Tephra because of its stratigraphic position in comparison with other reference sections (Donoghue 1991). We could also identify an additional unit between Orange Lapilli Member and Mangamate Tephra which we have correlated to the lower part of Papakai Tephra. We have distinguished three subunits within Papakai Tephra: Papakai a (containing the 3.4 cal ka old Waikiki Tephra); Papakai b (containing the 5.2 cal ka old Hinemaiaia Tephra) and Papakai c (below Orange lapilli, which in other areas contains the 6.2 cal ka Moturere Tephra).

The Zone 19 trench is located on a fault trace with N30-50°E trend. The excavation revealed one major fault plane that offsets most of the layers (except the top few dcms; Fig 3.14a & 3.14b). The fault geometry on opposite walls is somewhat different. The northern wall (Fig. 3.14b) shows a wide central fault zone below the bench with fault slivers and fissure fills and several small strands branching upwards towards the ground surface on both sides. The fault becomes a single plane with a big fissure on the wall above the bench. The southern wall presents simpler geometry with a major plane and a small splay to the west.

Table 3.3 shows the results from the progressive displacement analysis of Zone 19 trench. Because of the uncertainties associated with the tip of a normal fault mentioned above, we have not attempted to undertake a full restoration of the displacement on the Zone 19 trench. We present the interpretation of displacement groups from each wall and an interpretation of earthquake events through a combination of data from both walls. We have measured offsets in those layers which are well-known in the area and can therefore provide with an age frame. It is clear from the obtained measurements that it is difficult to distinguish between events when the SED value is in the range of 10 to 20 cm. We have tried to group the layers with the allowing for a c. 0.10 m variability.

Table 3.3 Rangipo Fault earthquake history obtained by progressive displacement analysis of Zone 19 trench.

RANGIPO FAULT - Zone 19 trench					
	North		South		Combined events
	Total offset (m)	Displacement group, DG . (SED in m)	Total offset (m)	Displacement group, DG . (SED in m)	
Taupo (Tp)	0	unfaulted	0	unfaulted	
Mangatawai (Mng)	c. 0.25	DG 1 (0.25)	c.0.10 (< 0.3)	DG 1 (0.10)	Z19_1
Papakai a (Ppa)	c. 0.50	DG 2 (0.25)	c.0.20 (<0.38)	DG 2 (0.10)	Z19_2
Papakai b (Ppb)	c. 0.59	DG 3 (0.10)			
Orange Lapilli (Olap)	-		c.0.20 (<0.36)		
Mangamate (Mnt)	-		c.0.36 (<0.44)	DG 3 (0.16)	Z19_3
Ohinepango (Oh)	-		c.0.36 (<0.44)		
Ngamatea 2 (Nga 2)	0.32-0.59		-	DG 4 (0.12)	Z19_4
Ngamatea 1 (Nga1)	0.39-0.56		c. 0.48		
Bullot unnamed 2 (Bun2)	-		c. 0.48		
Poarehu (Prh)	0.62-0.78	DG 4 (0.20)	c.0.68 (>0.48)	DG5 (0.20)	Z19_5
Bun3	0.64-0.94		-		
Shawcroft (SC)	0.48?-0.82		c. 0.68		
Waiohau (Waih)	c. 0.8		0.58-0.68		
Bun 7	0.8-0.9		-		
Diamicton	c. 0.6		-		

- offset has not been measured because layer is missing or can not be correlate because of the bench (see text)

Although soil layers in the Zone 19 trench have not undergone as much erosion as in Tank Track trench we encountered difficulties matching some of the layers across the fault. For example Mangamate Tephra and Orange lapilli are present on both sides of the fault but they are on different levels separated by the middle bench in the trench. Matching layers across different bench levels is not recommended because of tridimensional problems with tephra mantling an existing topography (the same layers can have a difference in height of more than 0.2 m in to different vertical planes that are 1.5 m apart). This was not a problem in Tank Track trench because layers crossed through the bench because it was on a steeper slope.

We obtained a total of 5 events using results from both sides of the trench. We tried to find evidence to confirm these events using the geometry of the offset layers. We found slightly overthickened sequences on the downthrown side which may indicate that a small scarp existed prior to deposition of the overthickened layer. Also, tephras mantle a strand of the fault and could indicate layers that represent event horizons. This is not compelling evidence, but there are no other earthquake related geological features (such as scarp derived colluvial wedges) typical of normal faults that help us confirm our interpretation. These features are not present because the small SED will not produce large topographic scarps.

The timing of these events is constrained by the stratigraphy (Table 3.3 and Fig 2.4). Event Z19_1 occurred after deposition of Mangatawai Tephra (2.5 cal ka) and before deposition of Taupo Tephra (1.7 cal ka). Taupo Tephra is clearly not displaced on both walls (Fig 3.14). Event Z19_2 occurred after deposition of Papakai Tephra (3.4 cal ka) and before deposition of Mangatawai Tephra (2.5 cal ka). Mangatawai Tephra seems to be slightly over-thickened on the downthrown side of the fault implying that it was deposited on a existing scarp. Event Z19_3 occurred between Orange Lapilli (Olp in Fig 3.14; 6.2-5.5 cal ka) and Papakai (it is not clear which subunit within Papakai; Ppa, 3.4 cal ka or Ppb 5.2 cal ka). Papakai a and b also show an overthickened sequence on the downthrown side on the south wall of the trench (Ppa and Ppb in Fig 3.14a). Event _4 occurred after deposition of Ngamatea 2 Tephra (13.8-11.2 cal ka) and before Ohinepango Tephra (11.2-6.2 cal ka) was deposited. Finally, event Z19_5 occurred after deposition of Pourahu Tephra (13.8-11.2 cal ka) and before deposition of Shawcroft Tephra (13.8-11.2 cal ka).

3.3.5 Rangipo Fault earthquake history

We present our final interpretation of the Rangipo Fault history in Fig 3.16. Fig 3.16 shows that chronological position of the different tephra and alluvial units, which are represented by a line when their age is known and as a rectangle when their age is inferred (bracketed between Tephras of known age). We have assigned three different colours to the lines and rectangles based on the presence of the unit in the trench wall:

- Blue indicates that the unit is present on both sides of the fault. In this case the offset can be measured with low uncertainty.
- Red indicates that the unit is missing on one side of the fault. Estimates of offset and the geometry of the unit for restoration purposes have been inferred from other geological evidence. In this case the uncertainties are higher.
- Green indicates that the layer is not present in the wall and we cannot assess if faulting occurred after or before deposition of that particular layer. This is taken into account when comparing events on two walls or two trenches.

We interpret that 7 events occurred on the Rangipo Fault in the last c. 14 ka (Fig. 3.16). Events 1 & 2 are secondary events. **Event 1** (TT_1) occurred between 1.7 ka and before deposition of Tufa Trig formation (non dated) and ruptured the Tank Track strand of the Rangipo Fault but not Zone 19 strand. **Event 2** (TT-2 & Z19_1) occurred between 2.5 and 1.7 ka and ruptured both strands. **Event 3** (TT_3 and Z19_2) has a large offset (0.8 m) and is recorded in both trenches. Timing for this event is between 3.43 and 2.5 ka. **Event 4** (TT-4 & Z19_3) has a 0.35 m offset and occurred between 5.2 and 3.43 ka. We use the timing of the event in Zone 19 trench because the preservation of the layers in the trench is better (blue colour in fig. 3.16). **Event 5** (TT_5) has the largest offset of all (1.2 m) and can be bracketed between 11.2 and 6.2 ka. It is unclear why such a large offset is not recorded in Z19 trench but, as mentioned in section 3.2.4, surface rupture might not always reach the very end of a fault strand. **Event 6** (Z19_4) is only recorded in Zone 19 strand and occurred between 11.2

and 6.2 ka but before Event 5. The earliest event that is recorded since 13.8 ka is **Event 7** (TT_6 & Z19_5) which has a similar offset to event 4 and occurred between 13.48 and 11.2 ka.

3.3.6 Contribution of trench data to the age of landscape features

Stratigraphic analysis of the Rangipo Fault trenches (Tank Track, Zone 3 upper and Zone 3 lower) and the position of the trenches with respect to the present-day topography (Fig 3.11) appears to indicate that fluvial incision occurred on the western (downthrown) side of the fault prior the deposition of the Waiohau Tephra (c. 13.8 cal ka) and eroded part of the extensive ring plain dominated by Te Heuheu laharic cover-bed deposits. The wind gap surface where Tank Track trench is located seems to be the same age as the sloping surface where Zone 3 trenches are located based on the cover beds overlying the fluvio-laharic deposits. Fluvio-laharic deposits in the trenches were mostly deposited prior to deposition of the Waiohau Tephra. These fluvio-laharic deposits can be correlated to the Tangatu Formation of Donoghue (1991). Fig 3.11 shows the topographic relation between the different trenches indicating the landscape configuration c. 13.8 cal ka ago was very similar to the present day topography at the site and also illustrates the extent of fluvial incision.

From trench data the incision period after formation of the Te Heuheu extensive surface predates deposition of Waiohau Tephra (c. 13.8 cal ka) but it is unclear if it also predates deposition of Rerewhakaaitu Tephra (c. 17.6 cal ka) because Rerewhakaaitu Tephra was not found in the trenches. To the west of the trench site, Rerewhakaaitu Tephra has been identified covering Tangatu lahar deposits (Donoghue 1991; see section 3.1.3). It is possible that the erosional period started somewhat earlier than is shown by trench data.

The westward dipping geometry of the andic and tephric layers in the Tank Track trench and the geometry of the restored offsets in Fig 3.15f show that the topographically prominent scarp which they mantle existed prior to the deposition of Waiohau Tephra. The tilt of these layers does not appear to be tectonic The dip of the strata is due to deposition of airfall volcanic deposits in an existing topographic surface. All of the sediments in the trench except for the lowermost laharic units are airfall beds which acquire the shape of the topography that they fall onto. A west dip is not explained by normal faults dipping to the west as tectonic tilting of such layers would be to the east.

Fluvio-laharic deposits typically occur c. < 1 m below Waiohau Tephra at all trench sites (Figs. 3.12, 3.13 & 3.14). This indicates increased depositional frequency towards the termination of the Last Glacial Maximum (LGM; Oxygen Isotope Stage 2) and is in contrast with the dominance of tephra accretion occurring in this sector of the ring plain during post-glacial times (post-Waiohau). A <0.20-m-thick debris flow deposit is observed at the western end of the Zone 3 lower trench (Fig. 3.13). This debris flow deposit occurs above a prominent lapilli bed correlated with Pourahu Tephra (c. 13.8 -11.2 cal ka) and is directly overlain by a

centimetre-thick aeolian sand bed. Eastward along the trench (profiles 10 to 19 of Fig. 3.13), the debris flow deposit wedges out completely and the aeolian sand bed correspondingly thickens to over c. 2 m. This suggests that laharic inundation of the south-eastern Ruapehu ring plain during early post-glacial times had a significant destabilising effect and locally promoted the formation of aeolian dunes.

3.4 Seismic parameters of the Rangipo Fault

In order to characterise the earthquake generating potential of a fault, the following parameters need to be defined: fault rupture length, single-event surface displacement, earthquake timing (previous section) and recurrence interval of surface rupture. Fault length and single-event surface displacement are directly related to the earthquake magnitude expected to be generated by the fault. Earthquake timing and recurrence interval will indicate how often the fault ruptures and when the last earthquake occurred.

3.4.1 Fault Slip Rate

Fault slip rate of the Rangipo Fault is variable in time (Fig. 3.17). Slip rates over three different periods are available for the Rangipo Fault. The long term slip rate value calculated by Villamor & Berryman (2004b submitted) is 1.5±0.9 mm/yr from the beginning of the construction of the ring plain, at c. 230 ka (oldest known lava flows of Ruapehu; Hobden et al. 1996; Gamble et al. 2003) to 65 ka (minimum Porewan age that has been assigned at the western side of Ruapehu ring plain: Waimarino Formation, Lecointre et al., 1998) .

Two short term slip rate values have been obtained in the present study. An average vertical slip rate of 1.2± 0.5 mm/yr since laharic and alluvial sedimentation ceased (17.6 to 26.5 ka) is calculated from a total vertical displacement of the ring plain surface is 27 ± 7.3 m (mean value from our best estimate of displacement at T20/405935; Fig. 3.8; uncertainty value takes into account the offsets measured with 1;50,000 topo data; Fig 3.7). This vertical slip rate converts to a dip-slip rate of 1.5 ± 0.2 mm/yr if we assume a fault plane dip within a range to 50 to 70° (dip-slip offset of 32 ± 10 m).

A value 0.2±0.2 mm/yr is obtained from the offset of Waiohau Tephra (13.8 ± 0.3 ca. ka BP) in Tank Track trench (3.1± 0.2 m of displacement). Fig 3.17 shows the variability of slip rate in time. The two longer term values are similar and differ substantially form the short term one. This pattern of slip rate change implies a high incremental slip rate of 2.6 to 5.8 mm/yr for the time period pre 13.8 ka and post 17.6-26.5 cal ka.

3.4.2 Single Event Displacement and Magnitude

Single event displacement (SED) of the Rangipo Fault has been obtained for the Tank Track trench. Results from Zone 19 trench have not been used because they are not representative

(the trench is at the tip of a fault trace). There are four main SED values on the fault: 0.1-0.2; 0.4; 0.8; 1.2. We regard the smallest value as secondary faulting and recommend not using it for hazards studies. Values up to 0.3 m have been reported for secondary and antithetic faulting for the Edgecumbe earthquake (Beanland et al 1989). The other three values could be interpreted in two different ways:

- First, these values can represent multiples of 0.4 m. This has two interpretations: (a) the fault has three different types of fault rupture, and then three earthquake magnitudes associated with the fault (i.e. the fault ruptures sometimes as a whole and sometimes as segments); or (b) the SED displacement is 0.4 m and values larger than this represent multiple earthquakes. We disregard this last option because we did not find evidence for multiple events of the larger SED (i.e. 1.2 m) such as fault derived colluvial wedges of different erosional periods within the time interval when the earthquake event happened.
- Second, the different values are caused by natural variability of the rupture parameters. We then have three options: (a) there are two types of SED , 0.4-0.8 and 1.2 m; (b) there are two different characteristic SED, 0.4 and 0.8-1.2 m; (c) there is only one SED, 0.8 m, with a variability of ± 0.4 m.

In order to assess which of the three options may be most viable, we look at worldwide information which relates SED (and maximum magnitudes) and rupture length. For this we will use the SED/ rupture length regressions of Wells & Coppersmith (1994) and Webb et al (in prep). Wells & Coppersmith (1994) compiled statistics on a large number of historical fault ruptures and formulate regressions between fault length and SED (single event displacement) and fault length and earthquake magnitude. The relationships they deduced for normal faults are:

$$\log (MD) = -1.98 + 1.51 \times \log (SRL),$$

$$\log (AD) = -1.99 + 1.24 \times \log (SRL),$$

and

$$M_w = 4.86 + 1.32 \times \log (SRL)$$

where MD = maximum surface displacement (m); AD = average surface displacement (m); SRL = Surface rupture length (km); and M_w is earthquake moment magnitude.

We will also look at the relationship developed by Webb et al (in prep) which has been specifically developed for the Taupo Volcanic Zone. This relationship is based on magnitude duration of large earthquakes in the TVZ including Edgecumbe 1987 and assumes that moderate and large events might rupture the whole crust. This relationship is:

$$\log M_o = 23.25 + 2.0 \log SSRL$$

and

$M_w = 4.80 + 1.33 \log SSRL,$

were where M_o is seismic moment (in dyne-cm); SSRL is subsurface rupture length in km. We have used a ratio of subsurface/surface rupture of 1.164 based on international data (Webb et al in prep) and M_w is earthquake moment magnitude. To obtain SED from this equation we have used Aki and Richards (1980)

$M_o = \mu \times A \times SED$

M_o is seismic moment, μ is the rigidity modulus (3E+10 Nm^2) of the crust and A is fault area.

The different fault rupture segments that we can define for the Rangipo Fault based on its surface geometry (we lack paleoseismic data along the fault to confirm segmentation) are:

- Rupture of each of the traces defined in Fig. 3.1 (Trace A, B and C)
- A combination of adjacent traces (Traces A+B and Traces B+C)
- The whole fault (with a known length of 32 km possibly up to 43 km).

The different lengths associated to this segments and the SED and Magnitudes obtained for them with the two scaling relationships are presented in Table 3.4. Analysis of Table 3.4 points to possibly two SED values associated with rupture of the Rangipo Fault. Despite the difference between the two scaling relationships, Table 3.4 shows that the SED values from paleoseismic studies are in agreement with the possible ruptures (segmented or whole length). We consider the Webb et al (in prep) relationship more appropriate for this area because the seismogenic crust is thin (c. 12 to 14 km) and it is possible that short faults can rupture the whole crust, at least those faults with length that are c. $\geq$ 12 km. We assign values from 0.4 to 0.8 m to a segmented rupture of the fault (either as an 11 km or a 15 km long rupture) and the larger value of c. 1.2 m to a whole fault rupture. This implies that earthquakes generated by the Rangipo Fault can have magnitudes ranging from 6.3 to 7.1.

We can now classify the individual earthquakes exposed in the Tank Track trench (Table 3.2) as either primary or secondary, and the primary ones as either segmented rupture or whole-fault rupture (Fig. 3.16). Events 1 and 2 of Table 3.2 (with SED up to c. 20 cm) are regarded as secondary ruptures. The rest of the events are interpreted as primary ruptures. From the primary ruptures we define events 3, 4 and 7 as associated with segmented rupture and event 5 as associated with whole–fault rupture. Events exposed in the Zone 19 trench which coincide in time with Tank track trench have been correlated (Fig. 3.16). Event Z19_4 (Fig. 3.16) occurs only at the Zone 19 trench and could be either secondary or single segment primary event (Table 3.5).

Table 3.4 Single Event displacement obtained from trench data and derived from scaling relationships.

Segment name	Segment Length (km)	Wells & Coppersmith			Webb et al	
		AD_N (m)	MD_N (m)	Mw	AD (m)	Mw
Trace B	5	0.07	0.1	5.78	0.3	5.86
-	8.5				0.4	6.15
Trace A or Trace C	11	0.2	0.4	6.23	0.6	6.32
Trace A +Trace B Or Trace B + Trace C	15	0.3	0.6	6.41	0.8	6.70
Whole Fault	32	0.75	1.5	6.84	1.7	6.90
Whole Fault Max	43	0.99	2.74	7.01	2.3	7.10

3.4.3 Recurrence Interval and elapsed time since last event

The recurrence interval (RI) for large earthquakes on the Rangipo Fault is estimated to be of the order of 3000 years for the last c. 14 ka from trench data, but it is shorter is we use the longer term (since c. 26.5 ka) slip rate values (Table 3.5). Table 3.5 shows the possible range of RI for all large earthquakes, separated into segmented ruptures and whole fault ruptures. From trench data we have simply divided the number of events by the time. We consider two options: (a) 4 primary surface rupture earthquakes occurred in the last 13.8 ka (those clearly represented in the Tank Track trench); and (b) up to 5 earthquakes have occurred in the last 13.8 ka (assuming event Z19_4 is primary). We found evidence for only one whole fault rupture in the trenches so we are unable to accurately constrain the RI for whole fault rupture. Table 3.5 also shows the possibility that if 0.8 m represent a lower bound for whole fault rupture SED (as suggested by Wells & Coppersmith 1994, see Table 3.4) then the RI for whole fault rupture could be as small as c. 6900 years.

The RI using the long term (c. 26 ka) slip rate has been calculated using the shorter term (c. 1 4 ka) SED displacement values. We split the total value of 1.5 mm/yr into the amount that will be assigned to whole fault and segmented rupture. In the last c. 14 ka a total of c. 3 m of displacement occurred of which: 1.2 m is assigned to whole rupture events (one event in the last 14 cal ka with an SED of 1.2 m); 1.6 m is assigned to segmented rupture (3 events with SED of 0.8, 0.35 and 0.4 m); and c. 0.2 m to secondary rupture. In other words, the percentage of segmented versus non segmented versus secondary slip rate on the Rangipo Fault is 40:53:7. This results in a slip rate of 0.8 mm/yr associated with to segmented rupture and 0.6 mm/yr associated with whole-fault rupture, and RI of 750 and 2000 years for segmented and non-segmented respectively.

Table 3.5 Earthquake recurrence interval of the Rangipo Fault (years)

		Number of primary events (whole: segmented)	RI (all: segmented and whole rupture)	RI (for individual segments)	RI (for whole fault rupture)
Short term (c. 14 ka present)	Tank Track trench data (a)	4 (1:3)	3450	4600	≥11,200-13,800*
	Tank Track & Zone 19 trench data (b)	5 (1:4)	2760	3450	≥11,200-13,800*
Long term (26 ka to present)	surface offset	-	-	750	2000

* could be 6900 years if a SED of 0.8 m represents a whole rupture (i.e 2 events in 13.8 ka)

The last large earthquake on the Rangipo Fault occurred between 3.43 and 2.5 ka ago. Therefore the elapsed time since last event is in the same range as the post 14 ka RI for primary surface rupture (Table 3.5), but longer than the RI derived from the post 26 ka slip rate.

4.0 THE SHAWCROFT ROAD FAULT

The Shawcroft Road Fault cross cuts the Rangipo Fault. The geomorphic configuration of the scarps on these faults indicate that the Shawcroft Road Fault has ruptured more recently than the Rangipo Fault. We excavated trenches across the Shawcroft Rd with the aim of better constraining the timing of the last event on the Rangipo Fault. This purpose was not achieved (as it is explained below) but data from the Shawcroft Road Fault suggested that this fault displays a similar change in slip rate with time to that of the Rangipo Fault. We present evidence for a change in slip rate in this section.

The Shawcroft Road Fault has a NE-SW trend, and is downthrown to the SE (Fig. 2.3), and has a short active trace (7 km) that displaces the extensive c. 26.5-17.6 ka surface. Vertical offset of this surface has a mean value of 10.5 ± 1.5 m (obtained from a high resolution DTM; average scarp height of several profiles, one of them is represented in Fig. 3.8). Using this displacement value we obtain a dip slip rate of 0.6 ± 0.2 mm/yr, after conversion of vertical offset to total offset (accounting for a dip range from 50 to 70°).

We excavated two trenches across the Shawcroft Road Fault (Figs. 4.1a & b) close to where it cross-cuts the Rangipo Fault at Waiouru Station (T20/404928). One of the trenches, Harding 2 (Fig. 4.1b) is located across a c. 8 m scarp, displacing the c. 26.5-17.6 ka surface, and the second trench, Harding 1 (Fig. 4.1a) is located across a c. 1 m high scarp in a gully floor cut into the extensive lahar surface. This lower surface was inferred to be of a younger age. The stratigraphic record found on these trenches is similar to that of the Rangipo Fault and it is presented on Figs. 4.1 a & b.

Trenching revealed that the age of the lower surface (where Harding 1 is excavated) was similar to the age of the surface where Harding 2 trench was excavated. We did not find young deposits that could help us constrain the age of the last event on the Shawcroft Road Fault and consequently on the Rangipo Fault. From the Shawcroft Road trenches we infer that the last event on the fault occurred after the formation of the paleosol on Papakai (b2Bw is clearly faulted in both trenches by c. 0.4 m; Figs. 4.1 a & b) and before Taupo Tephra (Tp). Taupo Tephra is displaced by < 0.20 m in Harding 2 (where it is preserved) but we do not consider this displacement as primary. The last primary rupture of the Shawcroft Road Fault occurred between 3.4 and 1.7 cal ka, a time interval that is less accurately constrained than the last primary event on the Rangipo Fault (between 3.4 and 2.5 cal ka; Fig. 3.16).

However, data from the Shawcroft Road trenches has reinforced our interpretation that a phase of erosion occurred after deposition of the Te Heuheu lahars and before deposition of most of the cover beds in the ring plain of Ruapehu Volcano. The age of the deposits found on Harding 1, and subsequently the age of the small gully where the trench is excavated, had

to be formed at least before deposition of Waiohau Tephra (c. 13.8 ca ka ago), which is found a few cm above the top of the lahar deposits.

From the trenches across the Shawcroft Road Fault we estimate a short term slip rate for the Shawcroft Road Fault (13.8 ka to present) of 0.07 ± 0.01mm/yr derived from the total offset of 1 ± 0.2 m of Waiohau Tephra. If we compare this value with the long term (c. 25.6 ka to present) value (c. 0.6 mm/yr), we note a similar drastic reduction in slip rate, over the same time period, as on the Rangipo Fault.

5.0 DISCUSSION

5.1 Association between tectonic faulting and volcanism

Our study indicates a clear correlation between a high slip rate period on the Rangipo and Shawcroft Road faults with increased eruptive volumes from Ruapehu Volcano. The change from a high fault slip rate to a low slip rate on both the Rangipo and Shawcroft Road faults (from 2.6-5.8 mm/yr to 0.2 mm/yr and from 0.8-2 mm/yr to 0.07 mm/yr respectively) at around c.13.8 ka years ago could be explained by either a complex association of faulting and eruptive activity at nearby Ruapehu Volcano, or simply by independent tectonic processes such as earthquake clustering in time. In this section we discuss the validation of the possible models in our study area.

Distinct pulses of enhanced magma production from Ruapehu Volcano have been described by Gamble et al (2003) at <15, 15-30, 45-55, 115-160 and 180-250 ka (the Whakapapa, Mangawhero, Waihianoa and Te Herenga Formations of Hackett & Houghton, 1989). Donoghue et al. (1995) define the Bullot Formation (c. 26.5 cal yr to c. 10 ka) as the period of greatest volcanic production from Ruapehu Volcano in the last c. 26 ka. This is revealed by the > c. 11-m thick Ruapehu Volcano-devired airfall sequence on the southeastern ring plain, compared to the 0.5 m thick Tufa Trig Members derived for Ruapehu Volcano in the period from 1.7 ka to the present. The c. 10 to 2.5 ka time interval represents a period of less significant activity of Ruapehu Volcano (small eruptive volmune compare with previous periods). The chronology of post c. 26 ka volcanic activity from different studies indicates that Ruapehu Volcano was very active up to c. 10 ka with the largest volumes of eruptives happening before c. 15 ka.

The change in slip rate over time can be associated with volcanic activity of Ruapehu Volcano can be achieved by two different phenomena. Fault displacement can be driven by adjustment of the ground surface to the emptying of the magma chamber, e.g. in dyke intrusion events. This is a similar process to caldera collapse but of a smaller order (usually short faults <14 km long and offsets <2 m; Hackett et al. 1997). Fault displacement can also be enhanced by the clustering of earthquakes that are triggered by the eruptions (Hackett et al. 1997) or, vice versa, earthquakes on tectonic faults can trigger volcanic eruptions (Marzocchi et al. 1993; Nostro et al. 1998). Movement and extrusion of magma changes the stress state of the crust around it and can alter the stress on a fault plane bringing it closer to failure. Similarly the change of stress produced by fault rupture can compress the magma chamber and accelerate the eruption process. Earthquake triggering is a common process in purely tectonic environments where tectonic faulting can trigger rupture of nearby faults (e.g. Robinson & Benites, 1996).

We consider it less likely that displacements on the Rangipo and Shawcroft Road faults are related to adjustment of the ground surface resulting from emptying of the Ruapehu Volcano magma chamber. In order to be able to analyse this phenomena, it would be necessary to define about the shape and location of the magma chamber of Ruapehu Volcano, and its distance to the faults. However there is evidence which suggests that adjustment of the ground surface to the emptying of a magma chamber is not a very likely model to explain the relation between Rangipo and Shawcroft Road faults and Raupehu Volcano. The throw of the Shawcroft Road fault, and of other faults surrounding the volcano such as the Wahiaona, Karioi, Ohakune faults, is to the southeast which will not be expected is the fault movement is caused by collapse/dyke-intrusion processes from Ruapehu Volcano. In the case of the mentioned faults responding to an adjustment of the ground related to emptying of the Ruapehu Volcano magma chamber, these fault should have throws to the north and northeast.

The most probable cause for the change in the slip rate of the Rangipo Fault is earthquake clustering. Earthquake and eruption triggering can occur beyond 13 km of distance between volcanoes and faults (Robinson & Benites 1996; Nostro et al 1998). With the current data and without any numerical modelling it is difficult to establish the interacting relation between Ruapehu Volcano and the surrounding faults. Clustering can just be a natural tectonic phenomena and if it coincide with a time when the magma chamber is full, eruptions can be triggered. Alternatively, eruptions can trigger rupture of surrounding faults and therefore a period of voluminous eruptions can cause clustering of earthquakes on surrounding faults. Within the scope of this project, it is difficult to conclude if fault ruptures are triggering volcanic eruptions or vice versa. Numerical modelling could be applied to try unravel this question.

On a broader scale, it is possible that rifting in the TVZ is achieved by pulses of relatively fast tectonic activity accompanied by large eruptions separated by phases of relative quiescence. Nairn et al. (1998), for example, suggest a model of volcanic rifting in the Tongariro Volcanic Centre (TVC). Sequenced eruption episodes at ~10 ka, that involved eruptions from different vents of Mt. Ruapehu and Mt. Tongariro during a 200-400 year period, were related to a major NNE regional extension event. This model needs validating with paleoseismic data on faults. Our results indicate that at least the Rangipo and Shawcroft Road faults do not seem to have been involved in that particular phase of rifting at c. 10 ka, but could have been involved in a previous one, pre 13.8 ka and possibly pre c. 15 ka.

5.2 Earthquake hazard associated to rupture of the Rangipo Fault

The results of this study indicate that rupture of Rangipo Fault is associated with earthquakes of magnitudes between 6.3 and 7.1 that have recurrence intervals between at least 2700 and possibly $\geq$ 11,200-14,000 respectively (if we assume the short term slip rate of the fault).

Several geologic hazards exist as a consequence of large earthquakes on the Rangipo Fault. Rupture of the fault will cut access along SH 1. Secondary effects can also have a significant impact on the economy of the area around Ruapehu Volcano. Landslides, lahars and an increase in river sediment load will affect a large area around Mt. Ruapehu. Landsliding is potentially a major hazard because of the instability of volcanic cones, such as Mt. Ruapehu. For example, a collapse of the NW flank of Mt. Tongariro 55-65 thousand years ago could have been earthquake triggered (Lecointre, 2002 pers. com.). Lahars and a rapid increase in river sediment load can be caused by shaking and landsliding. These effects will affect the major lifelines around the volcano, as well as the ski fields, tourist industry, townships, forest processing plants and hydroelectric power schemes.

We recommend to use the shorter term slip rate value of c. 0.2 mm/yr and recurrence intervals of at least 2700 years obtained in this paleoseismic study for seismic hazard assessment purposes.

6.0 CONCLUSIONS

The Rangipo Fault is not the fastest slipping fault in the Taupo Volcanic Zone. We have obtained two well constrained slip rate values of c. 1.5 and c. 0.2 mm/yr for two different time intervals (the last 25.6 ka and the last 13.8 ka respectively) for the Rangipo Fault. Both these rates are much slower than the preliminary values of 3 mm/yr. A slip rate of 1.5 mm/yr is comparable with other high slip rate faults in the Taupo Volcanic Zone (TVZ), such as the Paeroa Fault south of Rotorua (Villamor & Berryman, 2001). However, a slip rate of c. 0.2 will classify the fault as a low slip rate fault in comparison with other TVZ faults.

The abrupt decrease in slip rate at c. 14 ka estimated for the Rangipo and Shawcroft Road faults coincides with a decrease in the eruptive volume from Ruapehu Volcano from c. 15 ka to the present. We suggest there is a relationship between fast slip rate periods on Rangipo Fault and large eruptive episodes of Ruapehu Volcano. This relationship is most likely associated with the clustering of earthquake events on the Rangipo Fault, but it is unclear whether the clustering of earthquakes are triggering the eruptions or vice versa.

Our results indicate that rupture of the Rangipo Fault can be associated with earthquakes with magnitudes between 6.3 and 7.1 that have recurrence intervals between 2700 and $\geq$ 11,200-14,000 years respectively (if we assume the short term slip rate of the fault is representative of the near future activity of the fault). Although our new characterisation of the fault's activity indicates longer recurrence intervals and lower slip rates than previously assessed, rupture of the Rangipo Fault still poses a significant hazard to the area. Rupture of the Rangipo Fault will affect the major lifelines around the volcano, as well as the ski fields, townships, forest processing plants and hydroelectric power schemes.

7.0 REFERENCES

Aki, K. y Richards, P.G. (1980). *Quantitative Seismology: Theory and Methods, vol 1 and 2.* San Francisco, California, W.H.Freeman (ed.) p.932

Beetham, R.D. 1979: Anticipated tunnelling conditions in the Rangipo Tailrace Tunnel, Tongariro Power Development. *New Zealand Geological Survey EG Report 327*, DSIR, Turangi.

Beanland, S.; Berryman, K.R.; Blick, G.H. 1989: Geological investigations of the 1987 Edgecumbe earthquake, New Zealand. *New Zealand Journal of Geology and Geophysics 32:* 73-91.

Berryman, K.; Villamor, P. 1999: Spatial and temporal zoning of faulting in the Taupo Volcanic Zone, New Zealand. *Geological Society of New Zealand Miscellaneous Publication 107A*: 15.

Bibby, H.M.; Caldwell, T.G.; Davey, F.J.; Webb, T.H. 1995. Geophysical evidence on the structure of the Taupo Volcanic Zone and its hydrothermal circulations. *Journal of Volcanology and Geothermal Research 68*: 29-58.

Bibby, H.M.; Caldwell, T.G.; Risk, G.F. 1998: Electrical resistivity image of the upper crust within the Taupo Volcanic Zone, New Zealand. *Journal of Geophysical Research 103*: 9665-9680.

Cronin, S. J.; Neall, V.E.; 1997: A late Quaternary stratigraphic framework for the northeastern Ruapehu and eastern Tongariro ring plains, New Zealand. *New Zealand Journal of Geology and Geophysics 40:* 185-197.

Donoghue, S.L. 1991: Late Quaternary volcanic stratigraphy of the southeastern sector of the Mount Ruapehu ring plain, New Zealand. Unpublished PhD. thesis, lodged in the Library, Massey University.

Donoghue, S.L.; Neall, V.E.; Palmer, A.S. 1995: Stratigraphy and chronology of late Quaternary andesitic tephra deposits, Tongariro Volcanic Centre, New Zealand. *Journal of the Royal Society of New Zealand 25*: 115-206.

Donoghue, S.L.; Palmer, A.S.; Mc Clelland, E.; Hobson, K.; Stewart, R.B.; Neall, V. E.; Lecointre, J.; Price, R. 1999: The Taurewa Eruptive Episode: evidence for climactic eruptions at Ruapehu Volcano. *Bulletin of Volcanology, 60:*223-240.

Donoghue, S.L.; Neall, V. E. 2001: Late Quaternary constructional history of the southeastern Ruapehu ring plain, New Zealand. *New Zealand Journal of Geology and Geophysics 44:* 439-458.

Froggatt, P.C.; Lowe, D.J. 1990: A review of late Quaternary silicic and some other tephra formations from New Zealand: their stratigraphy, nomenclature, distribution, volume and

age. *New Zealand Journal of Geology and Geophysics* 33: 89-109.

Gamble, J.A.; Wright, I.C. 1995. The Southern Havre Trough geological structure and magma petrogenesis of an active backarc rift complex. In: Taylor B ed. *Backarc basins: tectonics and magmatism*. Plenum Press, New York: 29-62.

Gamble, J.A.; Price, R.C.; Smith, I.E.M.; McIntosh, W.C.; Dunbar, N.W. 2003; $^{40}Ar/^{39}Ar$ geochronology of magmatic activity, magma flux and hazards at Ruapehu volcano, Taupo Volcanic Zone, New Zealand. *Journal of Volcanology and Geothermal Research 120*: 271-287.

Grange, L.I.; Williamson, J.H. 1933: Tongariro District. *New Zealand Geological Survey* 27th Annual Report, pp 18-21.

Gregg, D.R. 1960: The Geology of Tongariro Subdivision. New Zealand Geological Survey Bulletin 40. 152 p.

Hackett, W.R.; Houghton, B.F. 1989: A facies model for a Quaternary andesitic composite volcano: Ruapehu, New Zealand. *Bulletin of Volcanology 51*: 51-68.

Hackett W.R.; Jackson S.M.; Houghton, B.F. 1996: Paleoseismology of Volcanic Environments. In *Paleoseismology*. McCalpin, J. (ed). International Geophysics Series, 62. Academic Press: 439-494.

Hay, R.F. 1967: Sheet 7 -Taranaki. Geological Map of New Zealand 1:250000. Wellington, New Zealand. *Department of Industrial and Scientific Research.*

Hegan, B.D. 1980: Engineering Geology of the Moawhango-Tongariro Tunnel, Tongariro Power Development. *N Z Geological Survey EG Report 343, DSIR*, Turangi.

Hobden, B.J.; Houghton, B.F.; Lanphere, M.A.; Nairn, I.A. 1996: Growth of the Tongariro volcanic complex: new evidence from K-Ar age determinations. *New Zealand Journal of Geology and Geophysics 39*: 151-154.

Lecointre, J.A.; Neall, V.E.; Palmer, A.S. 1998: Quaternary lahar stratigraphy of the western Ruapehu ring plain, New Zealand. *New Zealand Journal of Geology and Geophysics 41*: 225-245.

Marzocchi, W.; Scandone, R., Mulargia, F. 1993. The tectonic setting of Mount Vesuvius and the correlation between its eruptions and earthquakes in the Southern Apennines. *Journal of Geothermal Research* 58: 27-41

Nairn, I.A.; Kobayashi, T.; Kakagawa, M. 1998: The ~ 10 ka multiple vent pyroclastics eruption sequence at Tongariro Volcanic Centre, Taupo Volcanic Zone, New Zealand: Part 1. Eruptive processes during regional extension. *Journal of Volcanology and Geothermal Research 86*: 19-44.

Nairn, I. A.; Hedenquist, J.W.; Villamor, P.; Berryman, K. R.; Shane, P. A. 2004 in press. The ~AD1310 Tarawera and Waiotapu eruptions, New Zealand: contemporaneous rhyolite and

hydrothermal eruptions driven by a CO2-rich arrested basalt dike system? *Journal of Volcanology.*

Neall, V.E.; Cronin, S.J; Donoghue, S.L.; Hodgson, K.A.; Lecointre, J.A.; Palmer, A.S.; Purves, A.M.; Stewart, R.B. 1995: New lahar risk map for Ruapehu, New Zealand. *Geological Society of New Zealand Miscellaneous Publication 81A*: 155.

Nostro, C.; Stein, R.S.; Cocco, M.; Belardinelli, M.E.; Marzocchi, W. 1998. Two-way coupling between Vesuvius eruptions and southern Apennine earthquakes, Italy, by elastic stress transfer. *Journal of Geophysical Research 103:* 24,487-24,504.

Ongley, M. 1943: Wairarapa earthquake of 24th June, 1942, together with map showing surface traces of faults recently active. *New Zealand Journal of Science and Technology B25*: 67-78.

Paterson, B.R. 1980: Summary geological log of the Mangaio Tunnel, Tongariro Power Development. *Unpublished NZ Geological Drawing NZGS 100/M/75* (TPD 8190/5/246).

Purves, A.M. 1990: Landscape ecology of the Rangipo Desert. Unpublished M.Sc. Thesis, Massey University.

Robinson, R.; Benites, R. 1996. Synthetic seismicity models for the Wellington region , New Zealand: implications for the temporal distribution of large earthquakes. *Journal of Geophysical Research* 101*:* 27,833-27,844.

Schofield, J.C. 1954: Geological reconnaissance of the Retaruke coalfield, west of National Park. *New Zealand Journal of Science and Technology* B36(3): 268-276.

Sissons, B.A.; Dibble, R.R. 1981: A seismic refraction experiment southeast of Ruapehu volcano. *New Zealand Journal of Geology and Geophysics* 24: 31-38.

Stuiver, M.; and Reimer, P.J. 1993: Extended (super 14) C data base and revised CALIB 3.0 (super 14) C age calibration program. *Radiocarbon* 35: 215-230.

Villamor, P.; Berryman, K.R. 2001. A late Quaternary extension rate in the Taupo Volcanic Zone, New Zealand, derived from fault slip data. *New Zealand Journal of Geology and Geophysics* 44: 243-269

Villamor, P.; Berryman, K. 2004a submitted. Late Quaternary geometry and kinematics of faults at the southern termination of the Taupo Volcanic Zone, New Zealand. *Submitted to New Zealand Journal of Geology and Geophysics.*

Villamor, P.; Berryman, K. 2004b submitted. Evolution of the southern termination of the Taupo Volcanic Zone, New Zealand. *Submitted to New Zealand Journal of Geology and Geophysics.*

Webb, T.; Berryman, K; Sommerville, P.; Villamor, P.; Stirling, M. in prep. Width-limited fault rupture scaling relations for use in normal faulting and low slip rate regions. *Bulletin of Seismological Society of America.*

Wells, D.L.; Coppersmith, K.J. 1994. New empirical relationships among magnitude, rupture length, rupture area, and surface displacement. *Bulletin Seismological Society of America* 84: 974-1002.

Wilson C.J.N.; Switsur, V.R.; Ward, A.P. 1988. A new ^{14}C age for the Oruanui (Wairakei) eruption, New Zealand. *Geological Magazine* 125: 297-300.

Wilson C.J.N.; Houghton, B.F.; McWilliams, M.O.; Lanphere, M.A.; Weaver, S.D.; Briggs, R.M. 1995: Volcanic and structural evolution of Taupo Volcanic Zone, New Zealand: a review. *Journal of Volcanology and Geothermal Research 68*: 1-28.

Wright, I.C. 1993: Southern Havre Trough-Bay of Plenty (New Zealand); structure and seismic stratigraphy of an active back-arc basin complex. *In*: Ballance, P.F. *ed.*: South Pacific sedimentary basins, Sedimentary Basins of the World 2: 195-211.

8.0 ACKNOWLEDGEMENTS

We thank the NZ Army and Mr. and Mrs Harding of Waiouru Station for access to study sites; Maurice True for assistance with the trench excavation logistics; Ian Frame for superb trench excavation; Peter McGrath, Kate Wilson, Robert Langridge, Vasso Mouslopoulus, Nigel Hill, Gwendolin Peters and Thies Buchman for assistance with logging of fault trench exposures. Carolyn Hume and Philip Carthew draughted the figures. Grant Dellow and Kelvin Berryman provided helpful review comments.

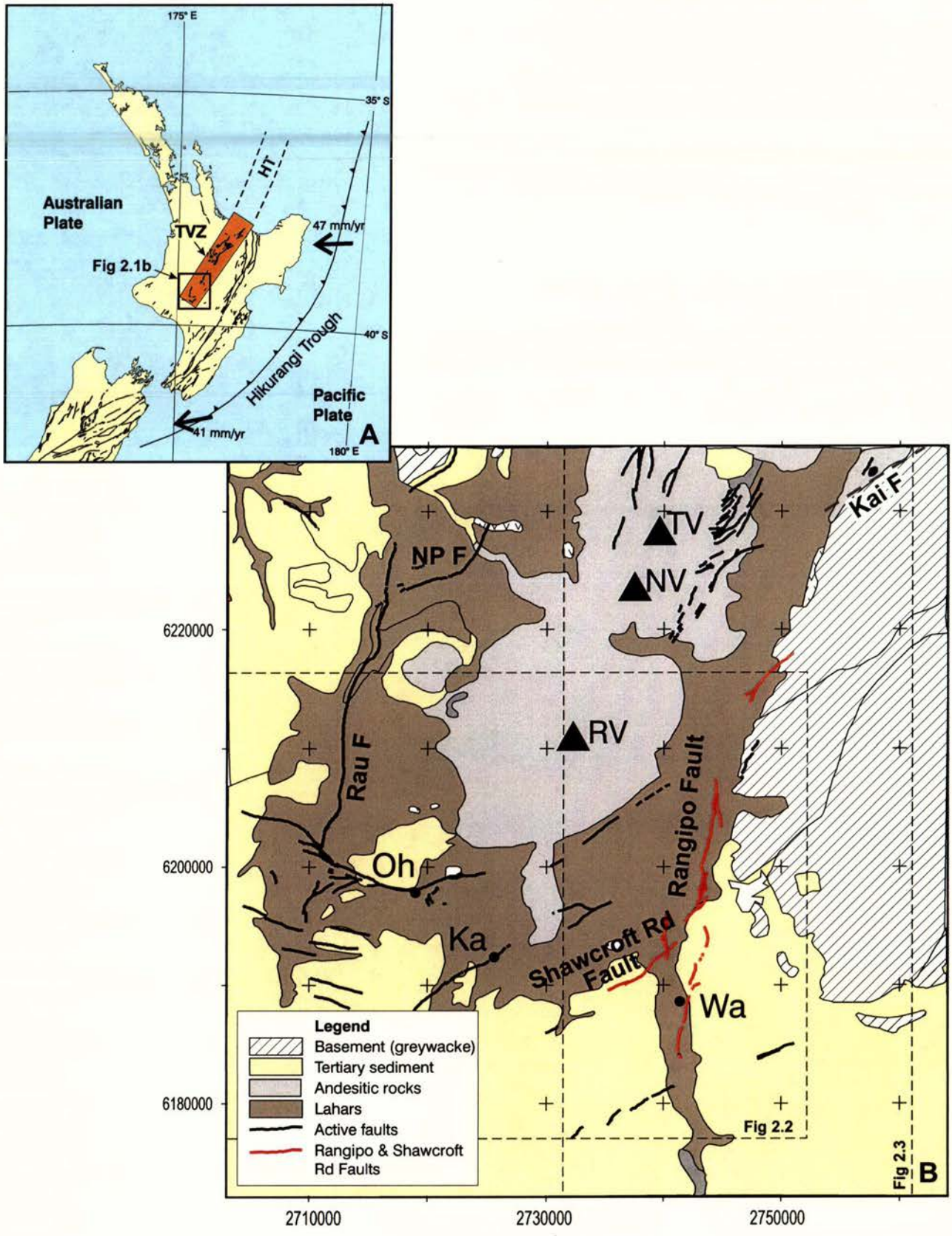

Figure 2.1: **A)** Tectonic setting of the study area at the southern end of the Taupo Volcanic Zone (TVZ). HT = Havre Trough. Bold arrows show azimuth of motion of Pacific Plate relative to Australian Plate. **B)** Geology map of the southern end of the Taupo Rift. NP F = National Park Fault, Rau F = Raurimu Fault Kai F = Kaimanawa Fault, TV = Tongariro Volcano, NV = Ngauruhoe Volcano, RV = Ruapehu Volcano, Oh = Ohakune, Ka = Karioi, Wa = Waiouru. See Fig. 2.2 for a more detailed map of the southern end of the Taupo Rift, including fault names.

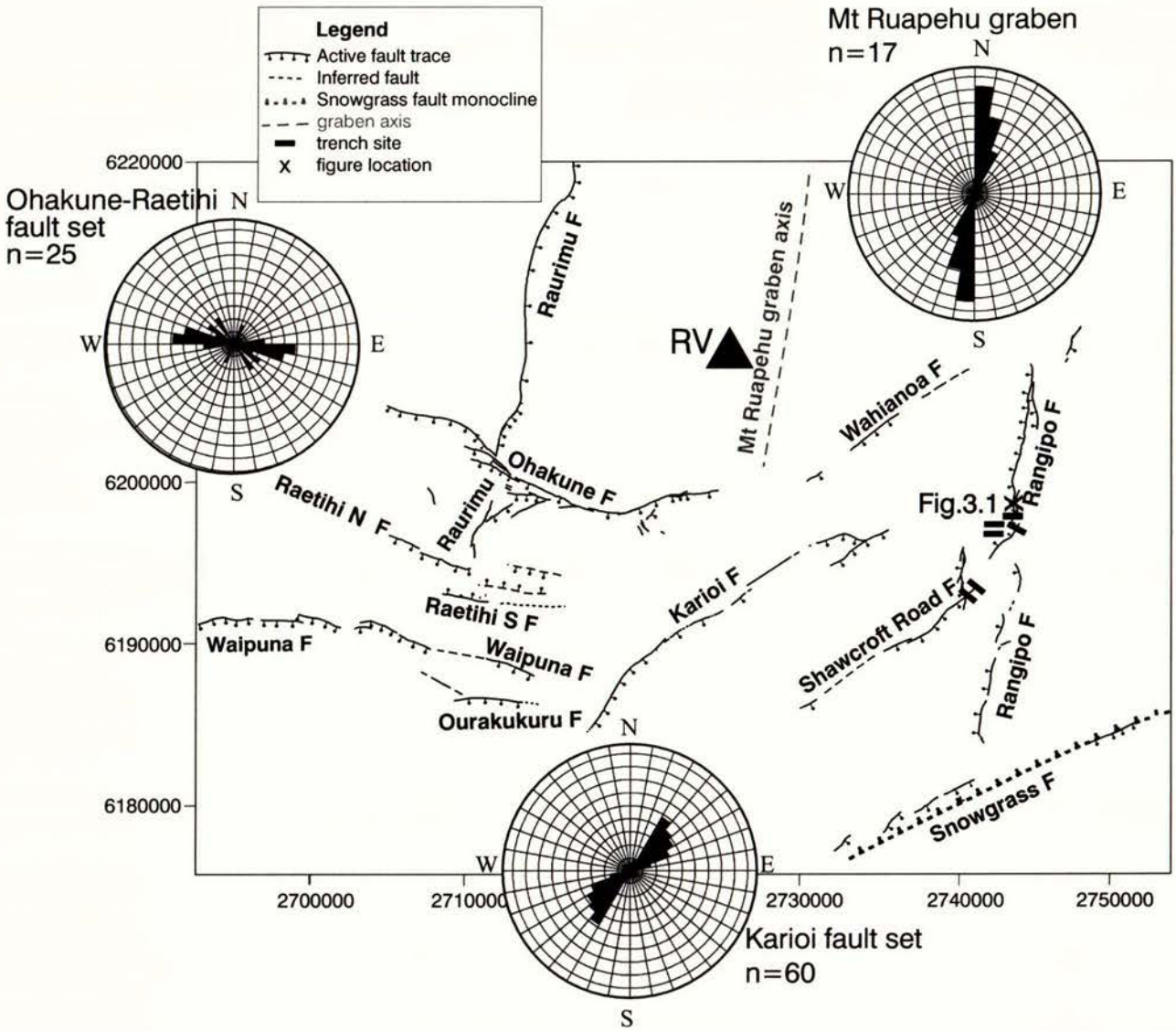

Figure 2.2: Fault map of the southern end of the Taupo Rift. Three major fault sets have been identified, with strike orientations as shown in the rose diagrams. Mt Ruapehu Graben includes Raurimu and Rangipo faults. Karioi fault set includes Wahianoa, Karioi, Shawcroft Road and Snowgrass faults. Ohakune-Raetihi fault set includes Ohakune, Raetihi North, Raetihi South, Waipuna and Ourakukuru faults. Tick marks on faults indicate downthrown side. RV = Ruapehu Volcano

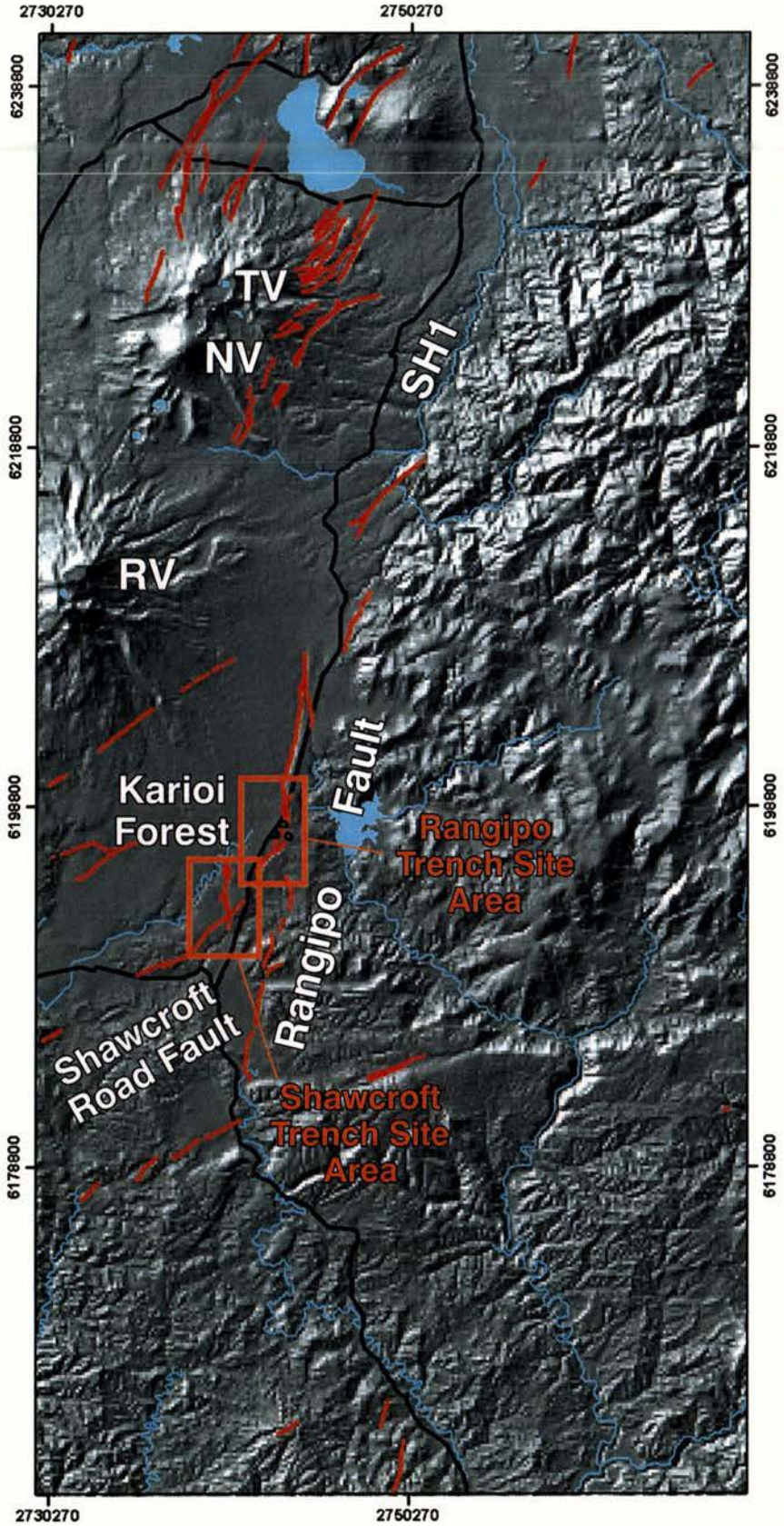

Figure 2.3: Enlargement of the complex cross-cutting relationship between the Rangipo and Shawcroft Road Faults (see also figures 3.1 & 3.2). Location of Rangipo and Shawcroft Road trench sites and study areas also shown.

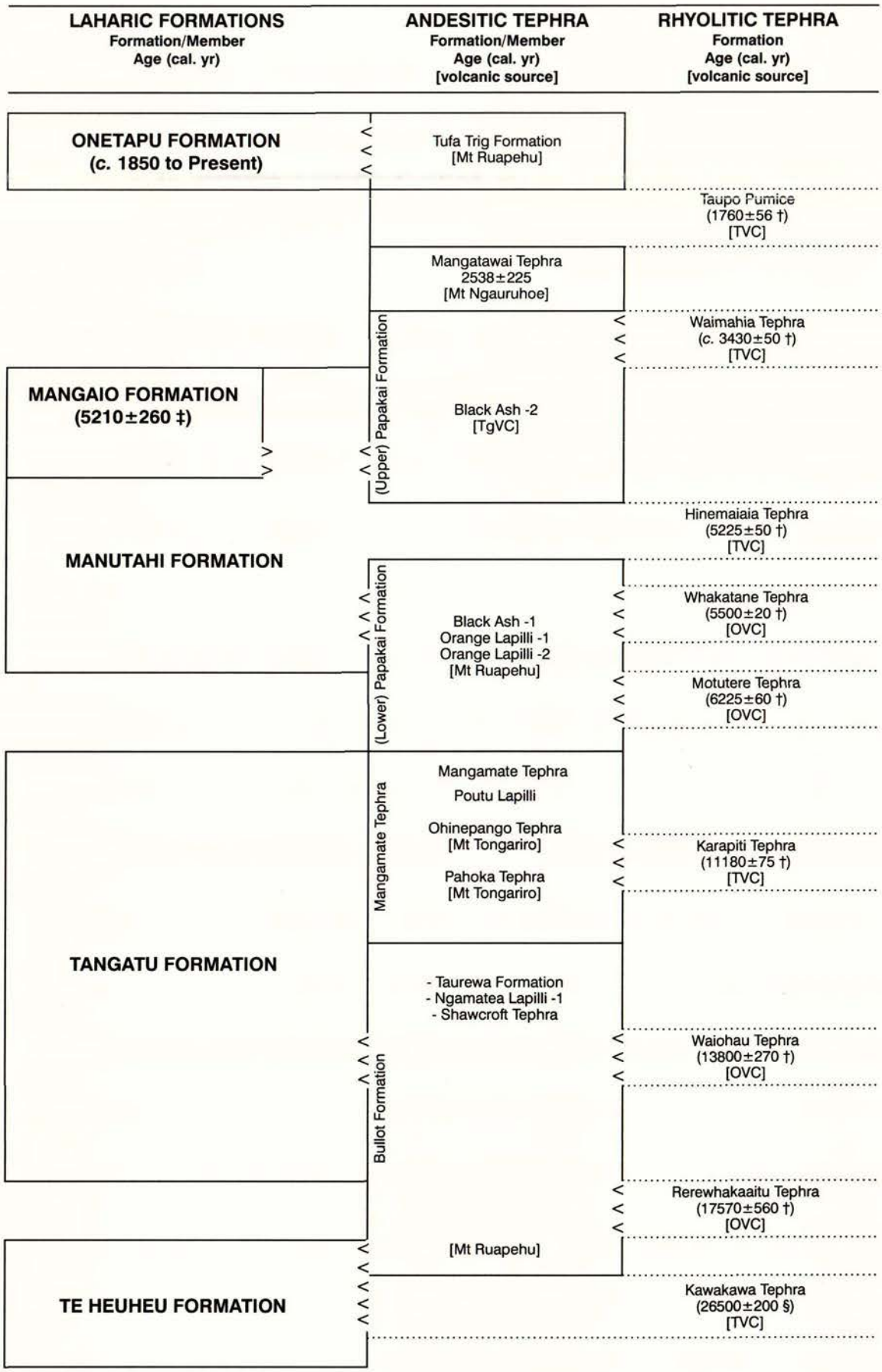

Figure 2.4: Chronosequence of the lahars and tephras that provide age constraints for evaluating the timing for specific faulting events on the Rangipo and Shawcroft Road faults. Radiocarbon ages are from † Froggatt & Lowe (1990), § Wilson et al. (1988), and ‡ Donoghue et al. (1995), and have been calibrated using the calibration of Stuiver and Reimer (1993). Adapted from Donoghue & Neall (2001).

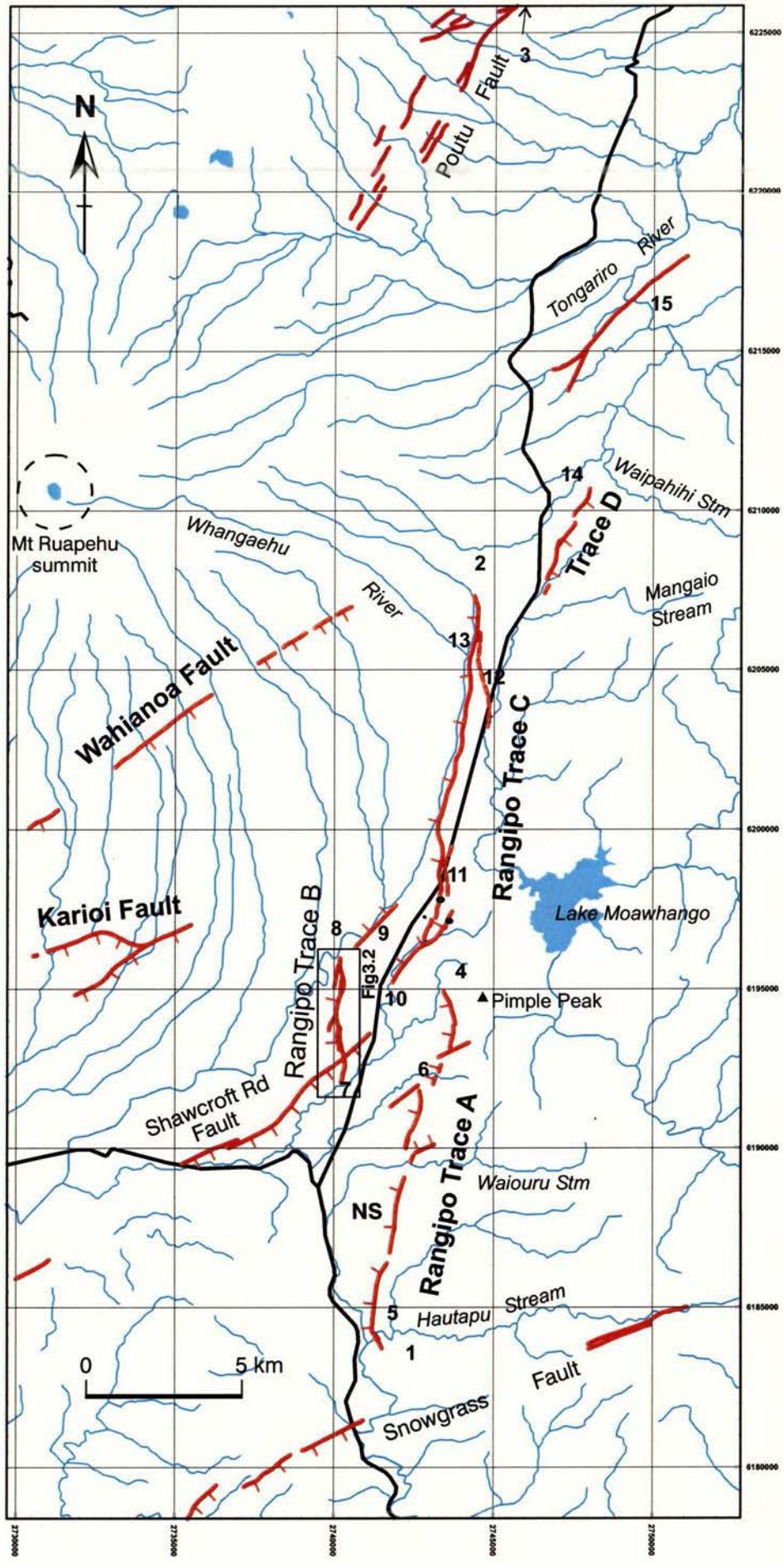

Figure 3.1: Fault trace map of the Rangipo Fault, Shawcroft Road Fault and nearby faults (see Figures 2.2 & 2.3 for additional fault names). Numbers denote locations referred to in the text. NS = Ngamatea Swamp. Tick marks on downthrown side of faults.

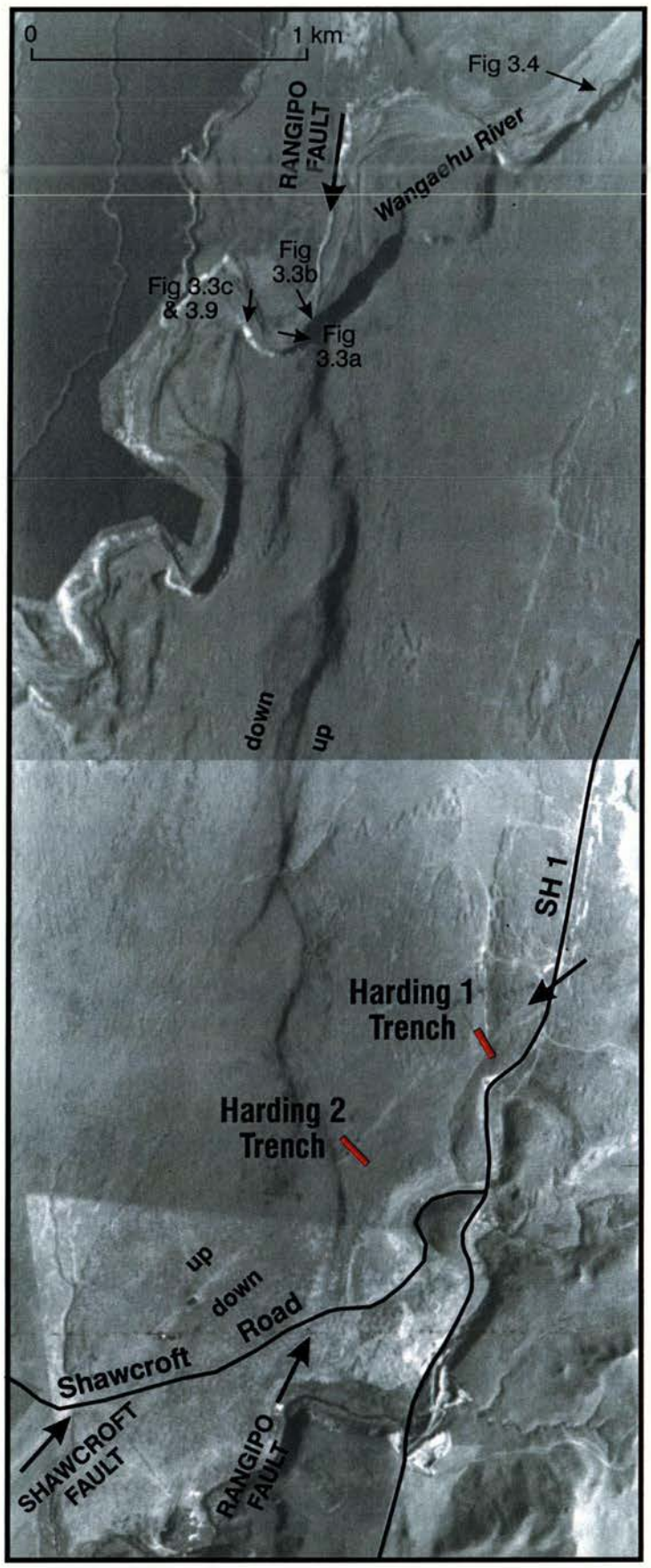

Figure 3.2: Vertical aerial photograph of the intersection area between Rangipo Fault Trace B and the Shawcroft Road Fault. NZ Aerial mapping photograph number 1745/17 dated 1950. Location 8 of Figure 3.1.

A

RANGIPO FAULT SCARP

B

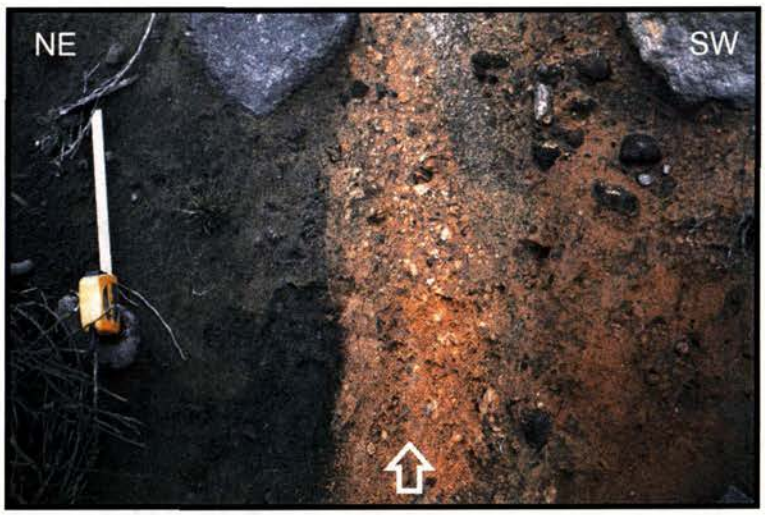

FAULT GOUGE

C

SMALL SCALE FAULTING

Figure 3.3 A) Looking east across 27 m high scarp of the Rangipo Fault (Trace B) where it meets the Whangaehu River. T20/402960, location shown on Figure 3.2.

B) Rangipo Fault (Trace B) fault gouge exposed in the Whangaehu Riverbank (see Figure 3.2 for location).

C) Small scale faulting 100m west of the Rangipo Fault in the Whangaehu Riverbank (see Figure 3.2 for location).

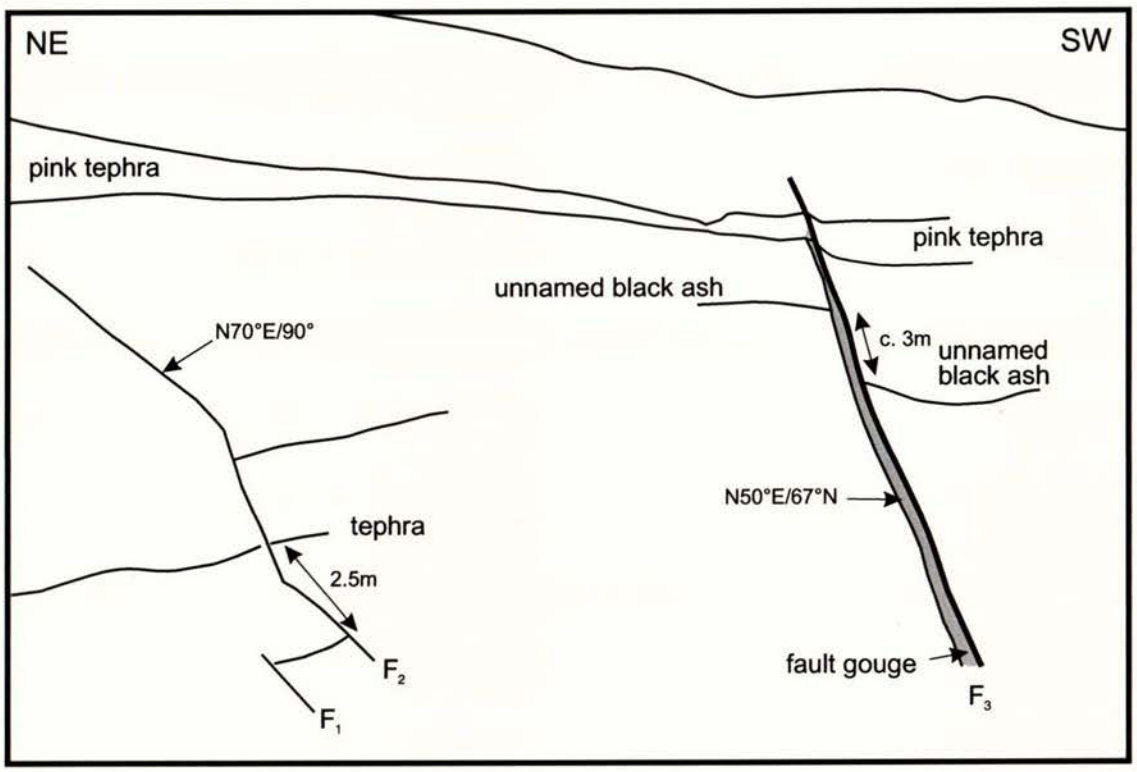

Figure 3.4 : Rangipo Fault (Trace B) exposure in the Whangaehu Riverbank (location 9 in Figure 3.1; see also Figure 3.2 for location).

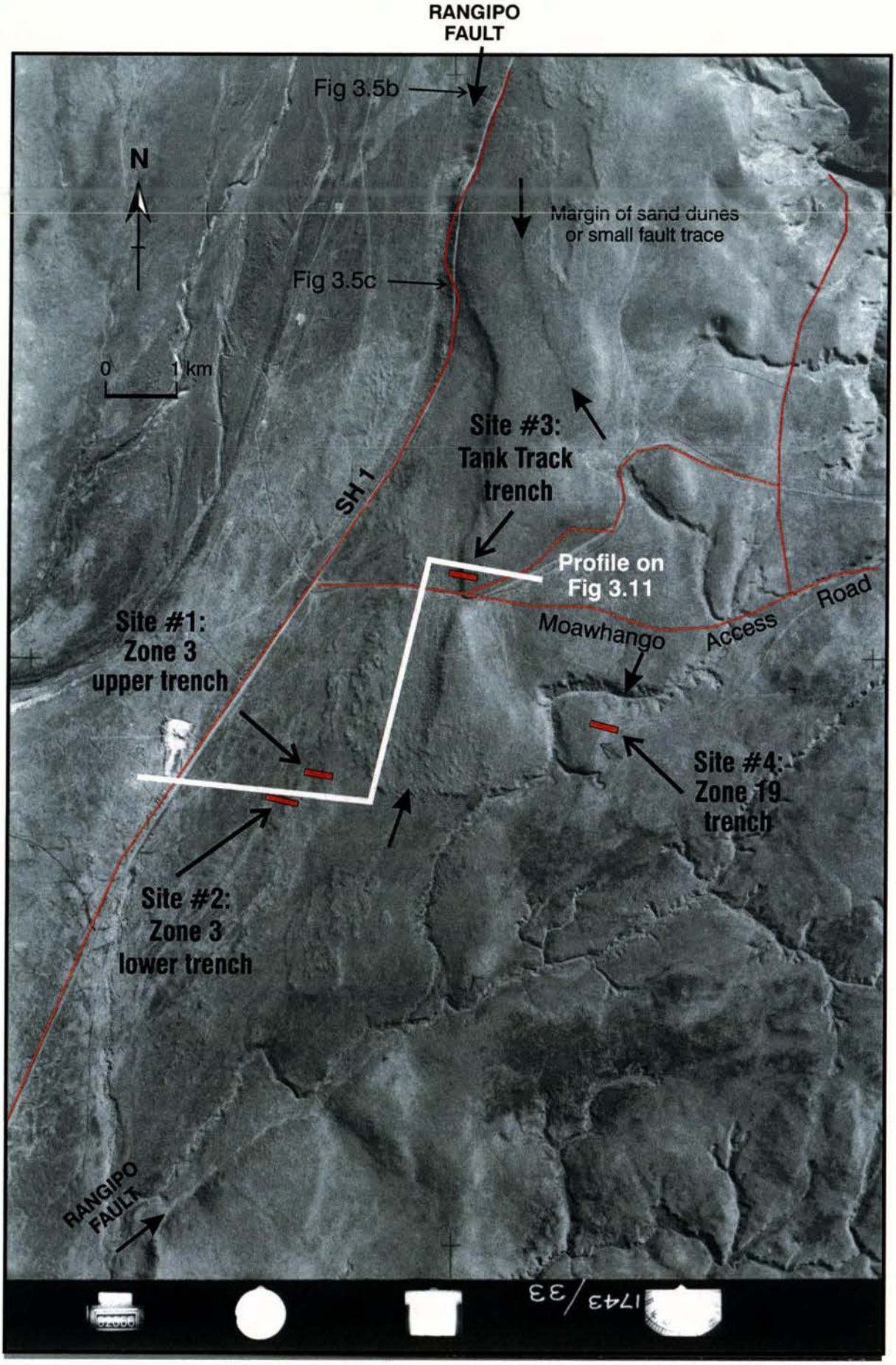

Figure 3.5 A) Southern end of Rangipo Fault Trace C.

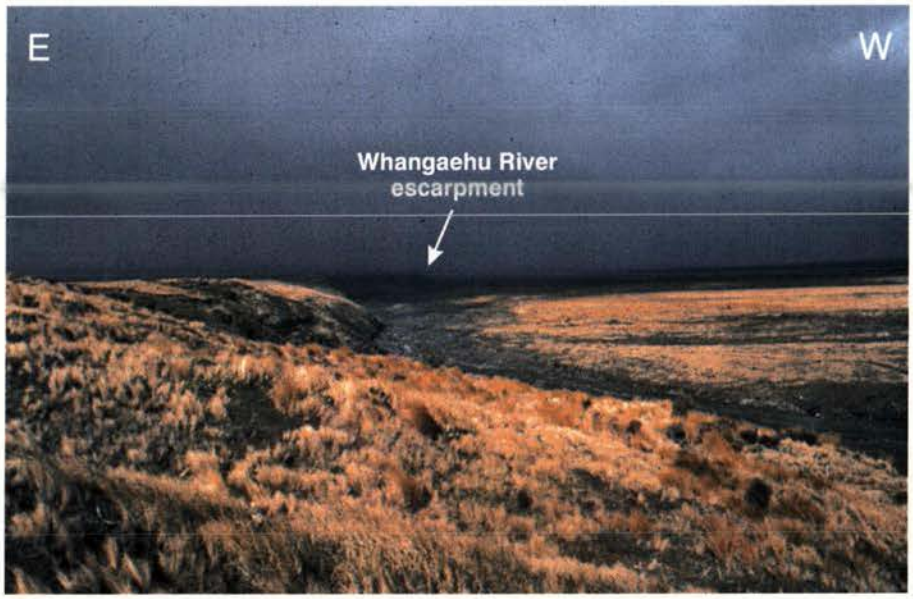

Figure 3.5B) Rangipo Fault Trace C scarp west of State Highway 1 (Desert Road), view to the south. (See Figure 3.5A for location).

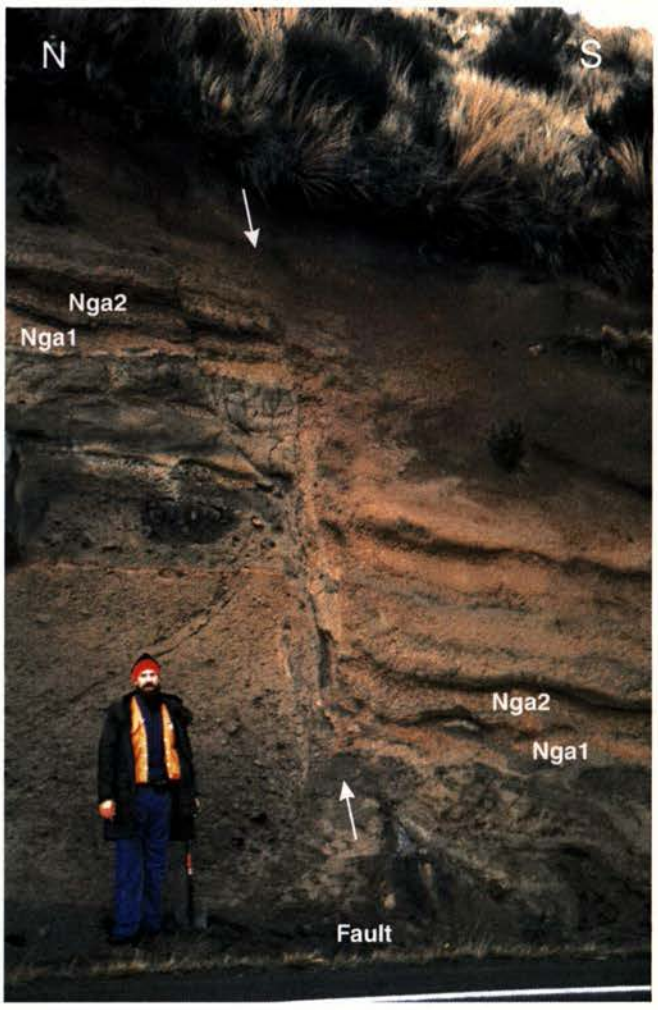

Figure 3.5C) Rangipo Fault (Trace C) exposure in State Highway 1 (Desert Road) roadcut. (NZMS 260 T20/433985, see Figure 3.5A for location). Nga2 = Ngamatea 2 Tephra, Nga1 = Ngamatea 1 Tephra.

Figure 3.6: Exposure of the Rangipo Fault, northern end of Trace C. (NZMS 260 T20/444057, location 13 in Figure 3.1).

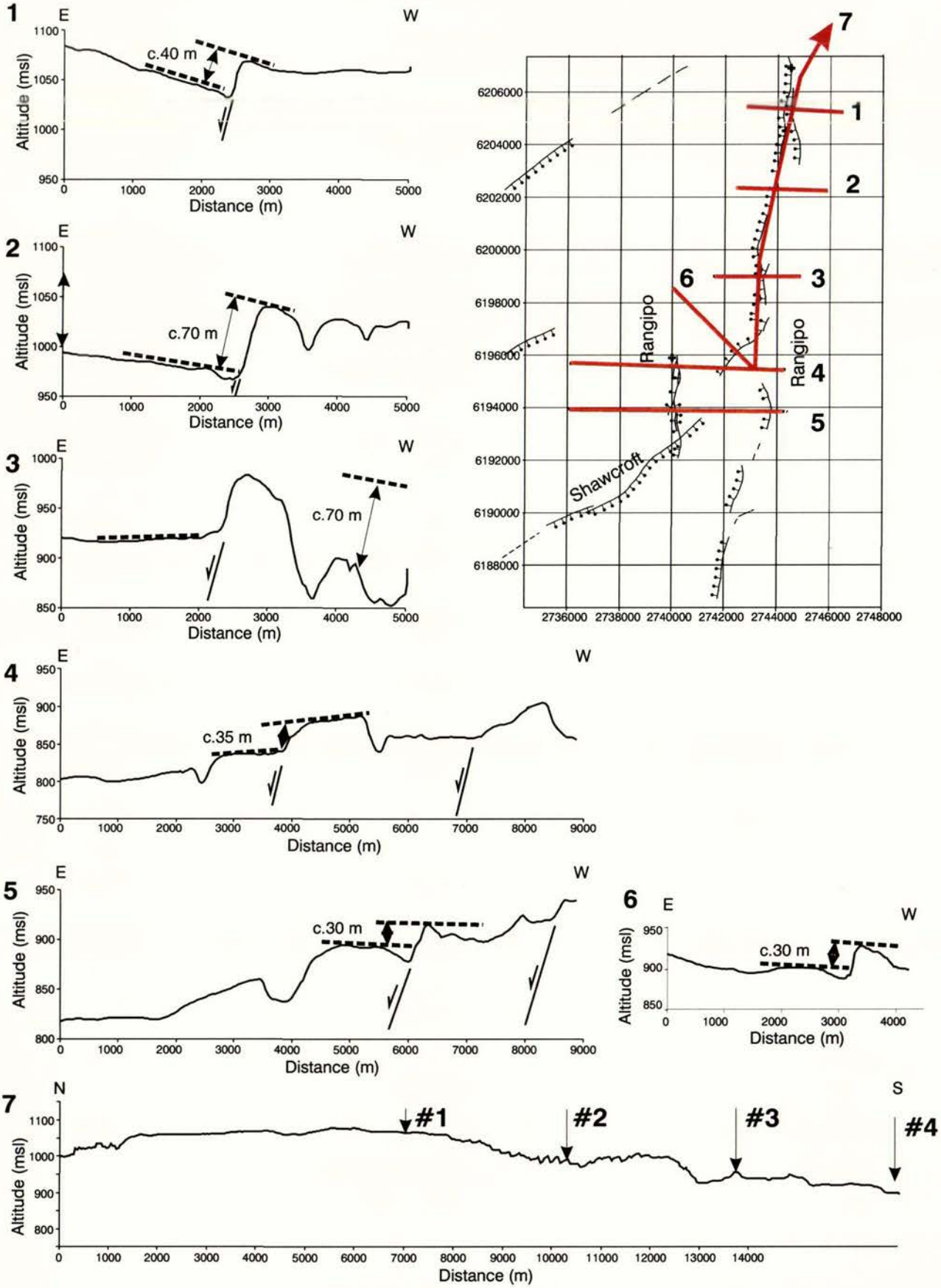

Figure 3.7: Fault scarp profiles across the Rangipo Fault Trace B, estimated using NZMS 260 1:50,000 topographic data. Surfaces across the Rangipo Fault on profiles 1, 2, 3 are not correlative, therefore, fault scarps heights are not representative of the fault offset. See text for explanation.

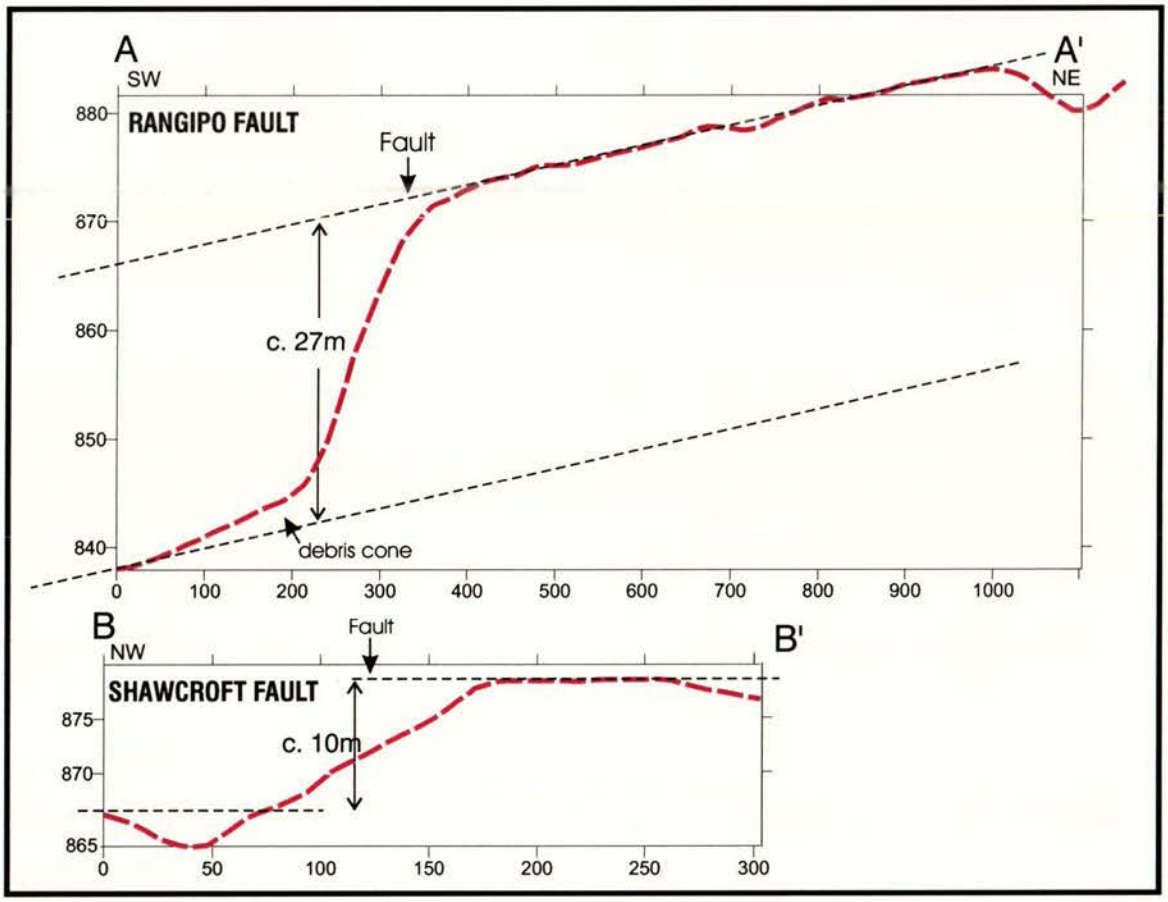

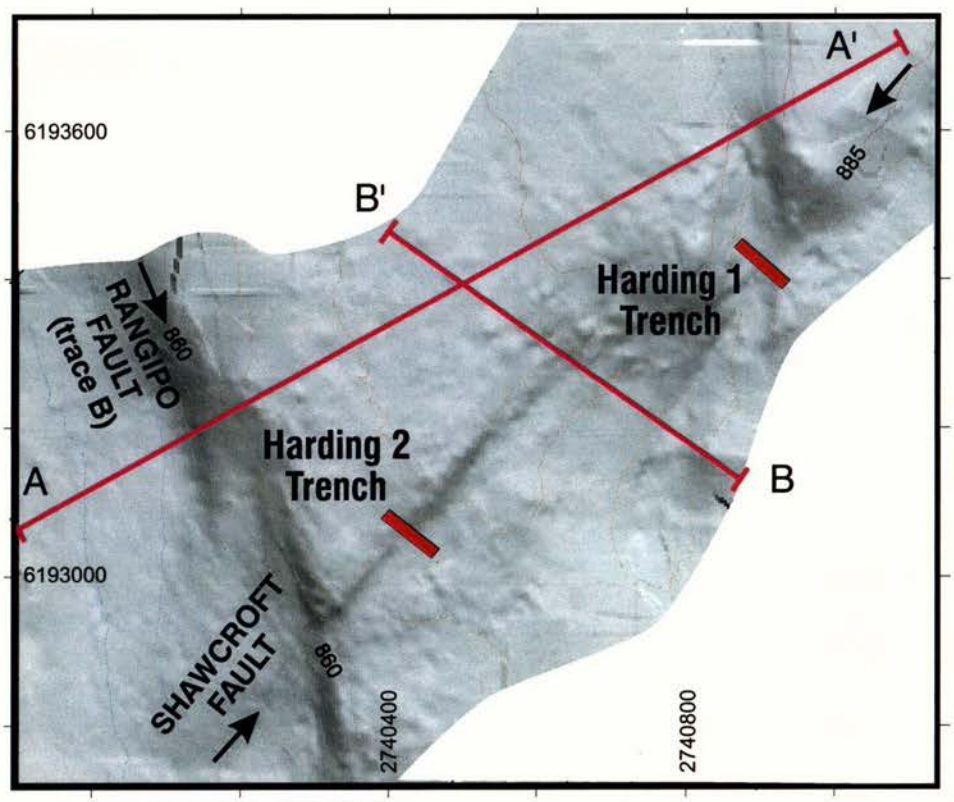

Figure 3.8: Fault scarp profiles across the Rangipo Fault (Trace B) and Shawcroft Road Fault measured from a digital topographic model constructed from a RTK GPS field survey.

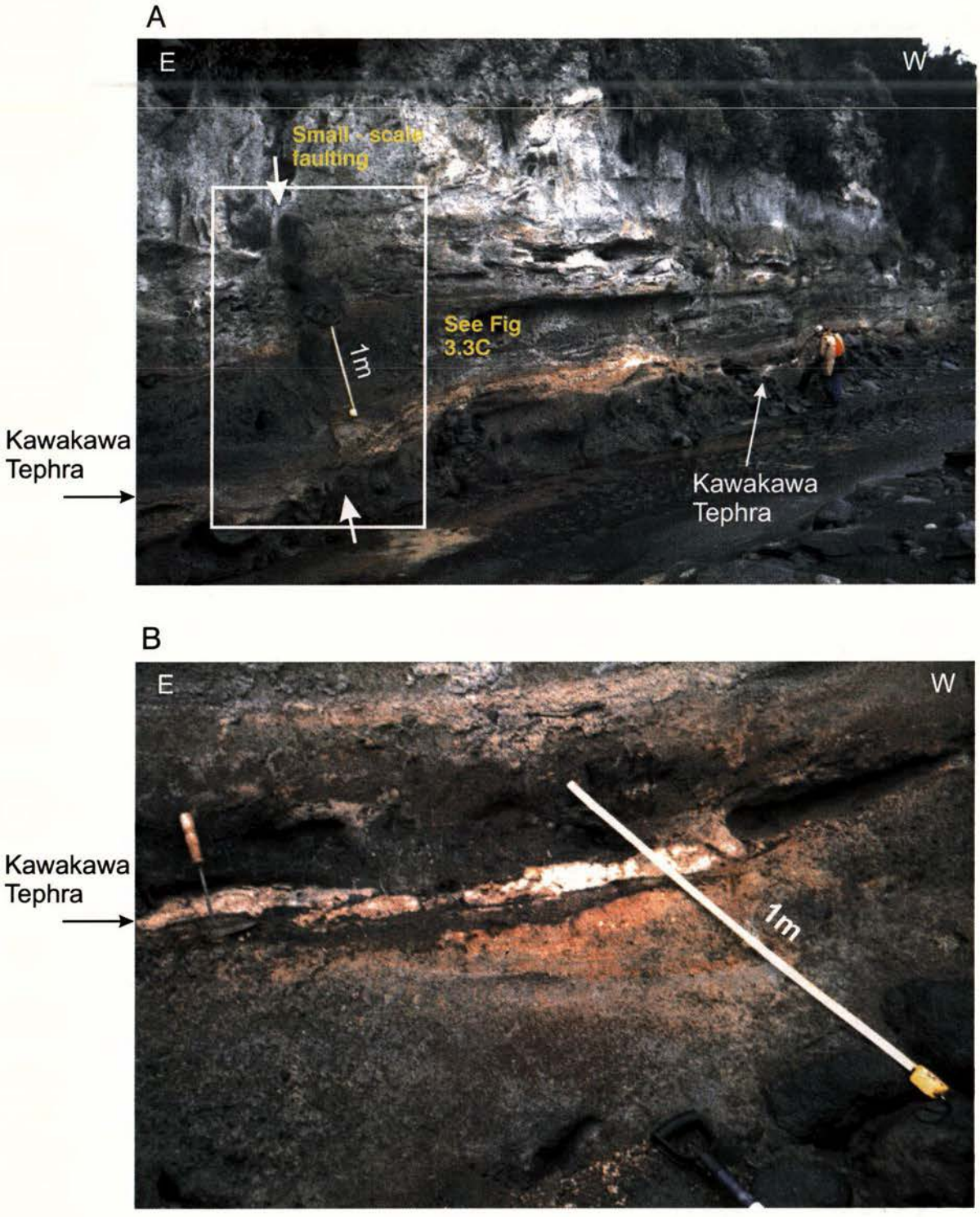

Figure 3.9A) Small scale faulting within Kawakawa Tephra in the riverbank of the Whangaehu River (see Figure 3.2 for location). B) Detail of Kawakawa Tephra exposure.

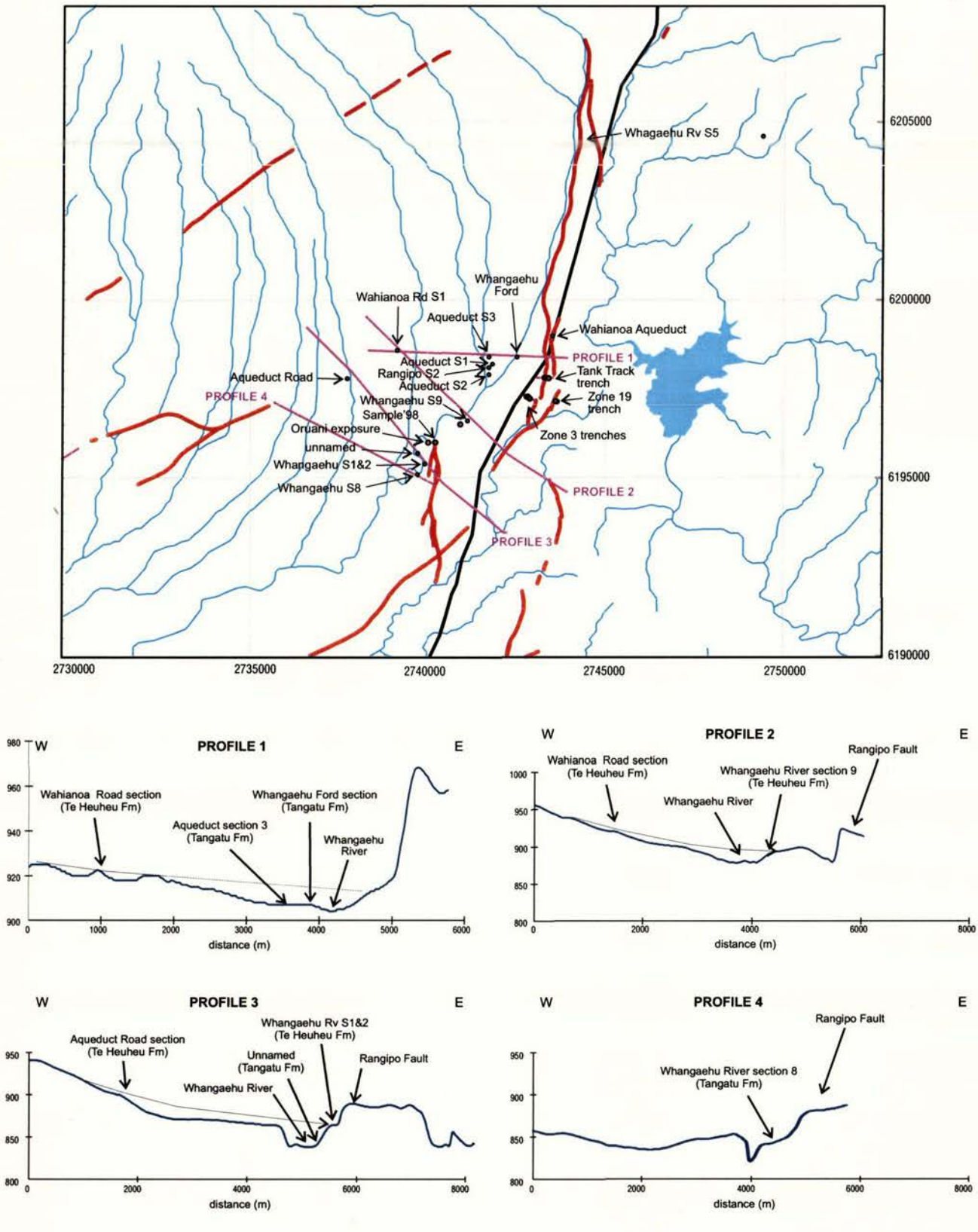

Figure 3.10: Fault scarp profiles across the southern end of the Rangipo Fault (trace B) measured using NZMS 260 1:50,000 topographic data. The lahar surface on the downthrown side of the fault is interpreted to be eroded and the original surface is shown as the thin line on the profiles.

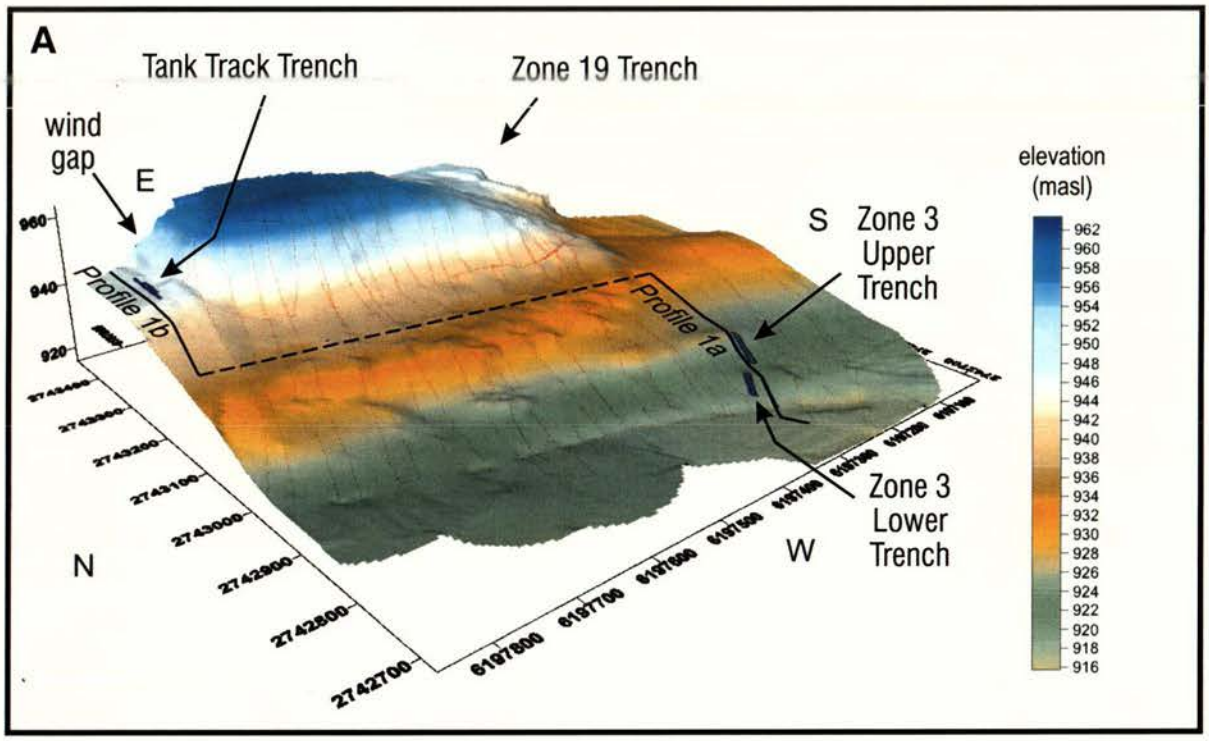

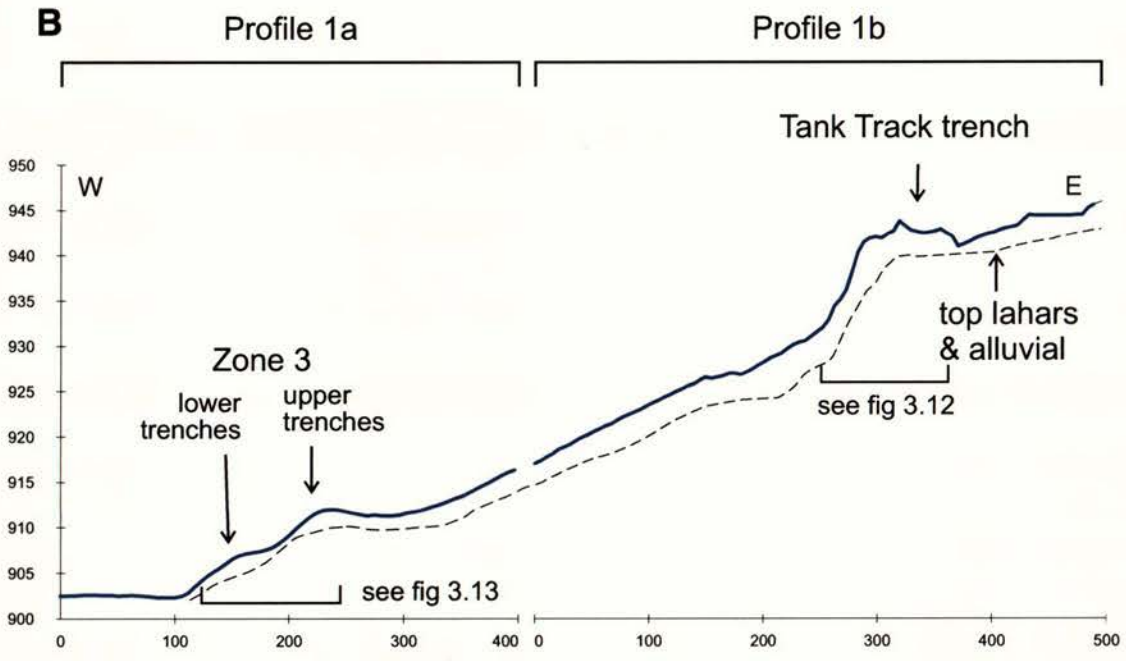

Figure 3.11A) Digital topographic model constructed from a RTK GPS field survey across two scarps of the southern end of Rangipo Fault trace C.

B) Composite profile constructed from the digital topographic model in A.

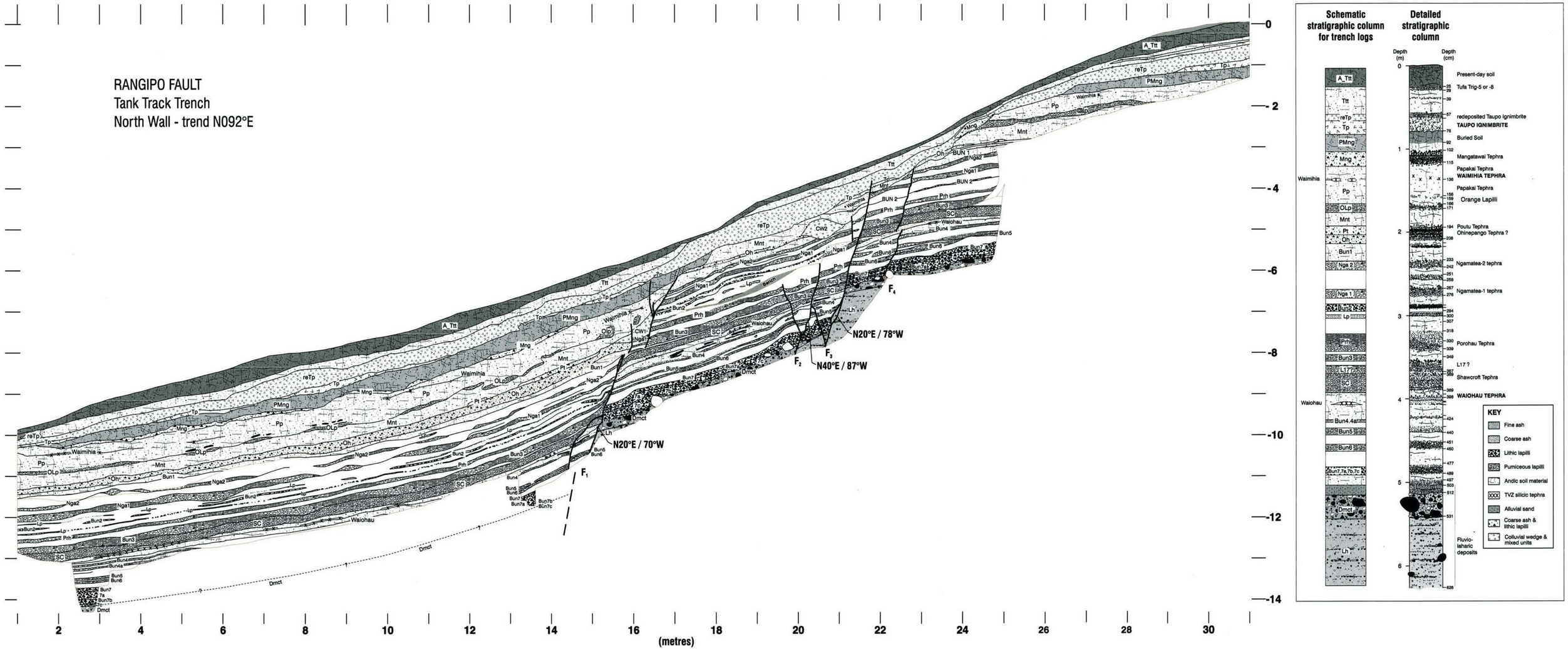

Figure 3.12: Tank Track trench log (north wall). NZMS 260 (T20) 2743320E, 6197810N. Composite stratigraphic log was compiled at trench grid verticals 5-6 (0-4 m depth), 18-19 (4-5 m depth), and 20-21 (5-6.25 m depth).

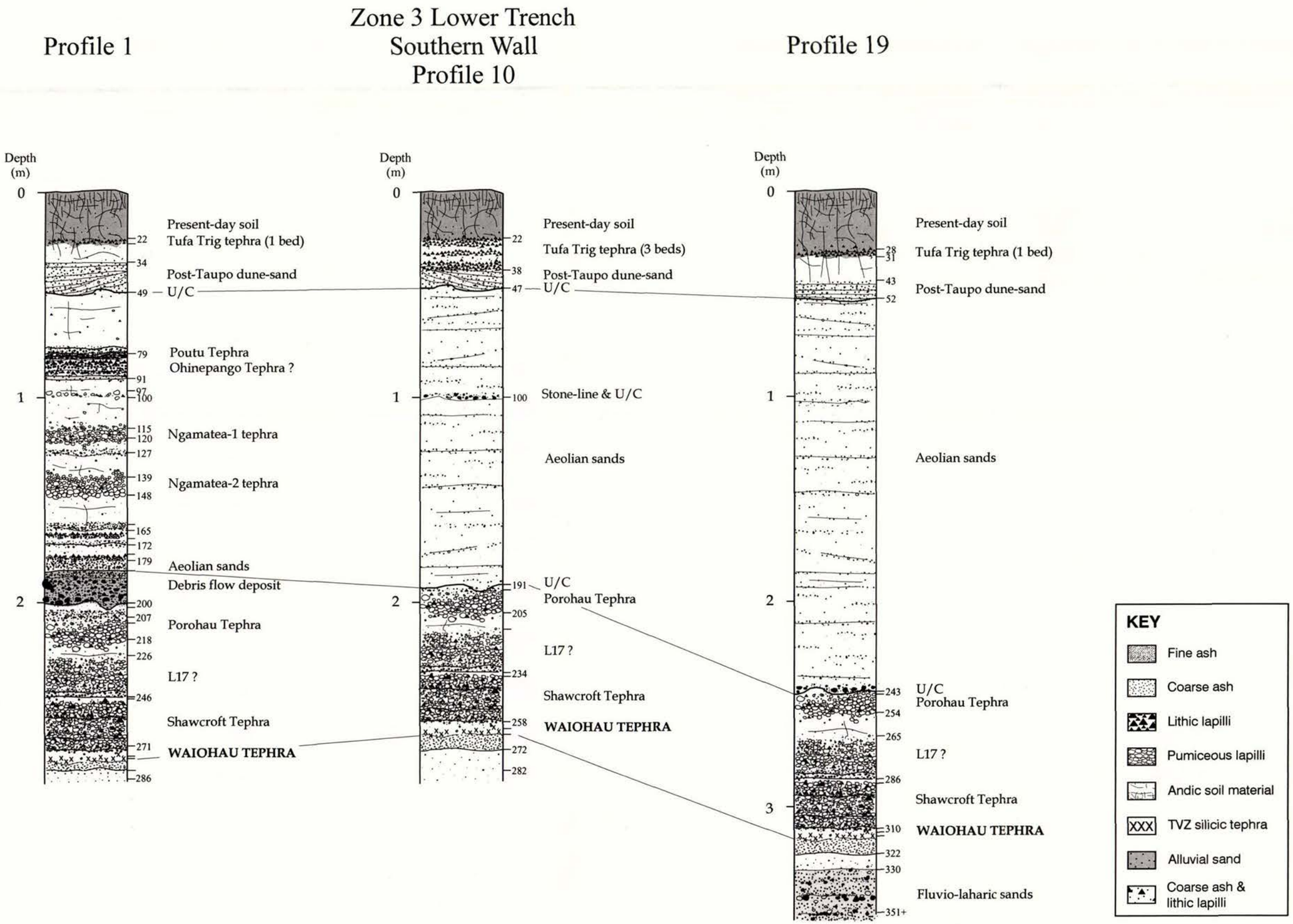

Figure 3.13: Stratigraphic logs at trench grid verticals 1, 10, and 19 of the north wall of the Zone 3 Lower trenches. Zone 3 Lower NZMS 260 (T20) 2742831, 6197275. Zone 3 Upper NZMS 260 (T20) 2742882, 6197228.

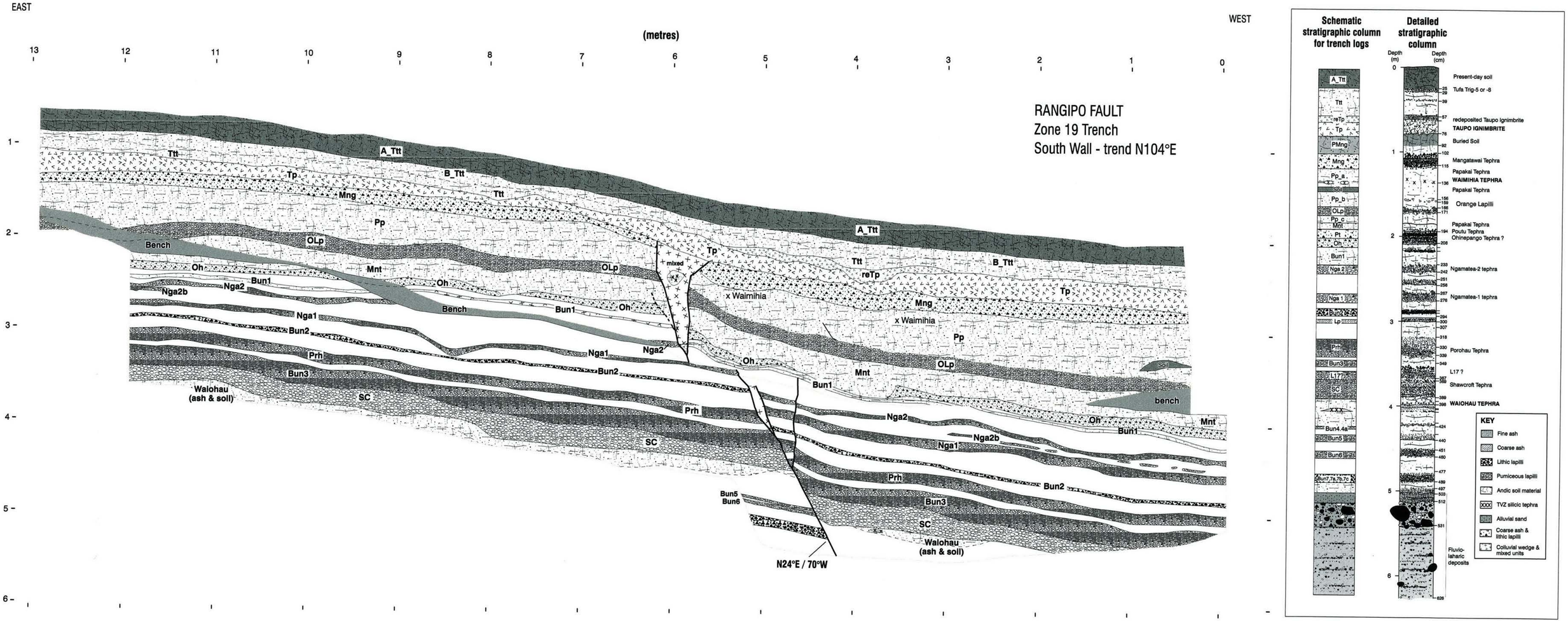

Figure. 3.14A) Zone 19 trench log, South wall. NZMS 260 (T20) 2743595, 6197155. Schematic stratigraphic column is modified Tank Track Trench log.

RANGIPO FAULT
Zone 19 Trench
North Wall - trend N104°E

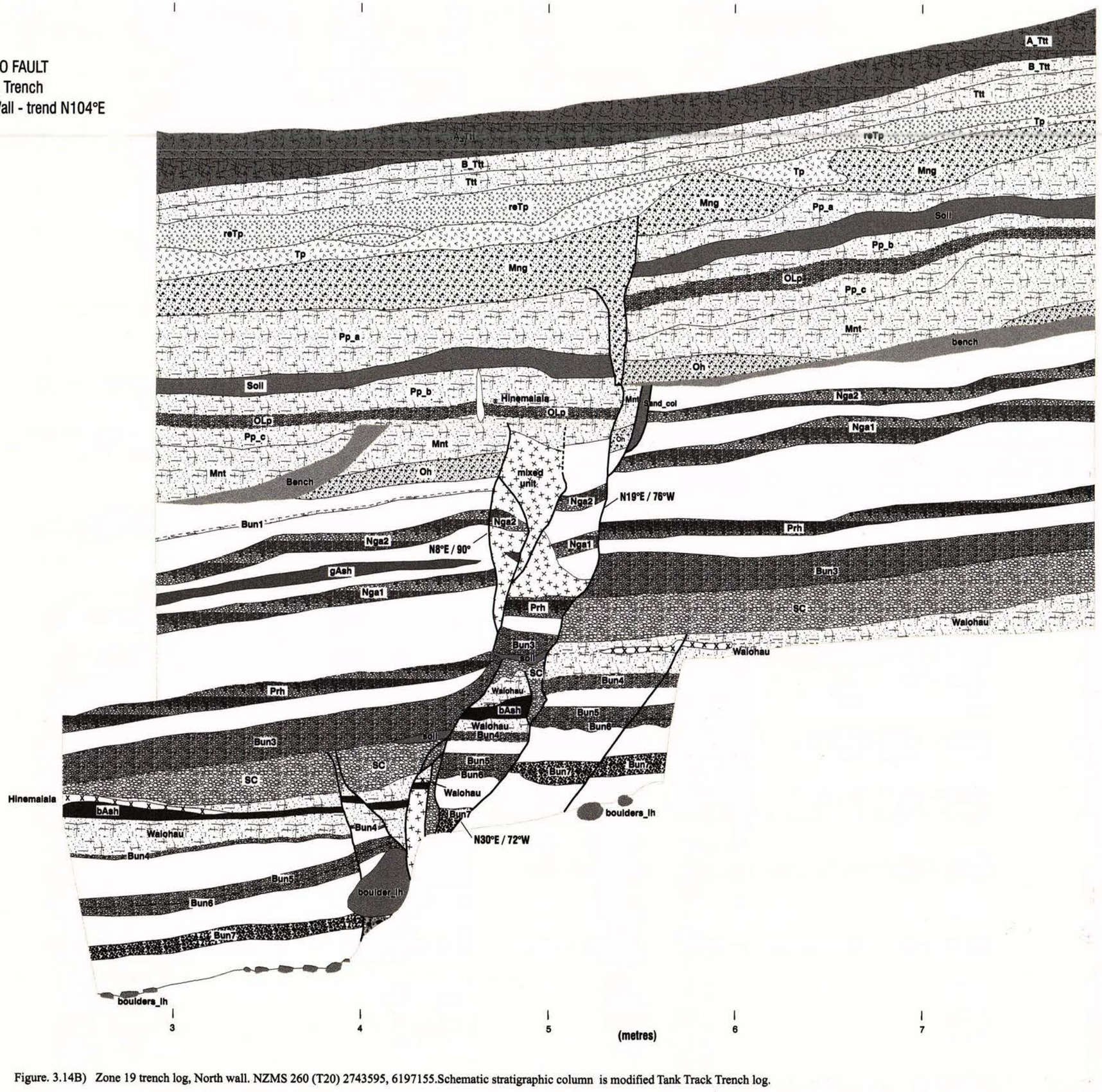

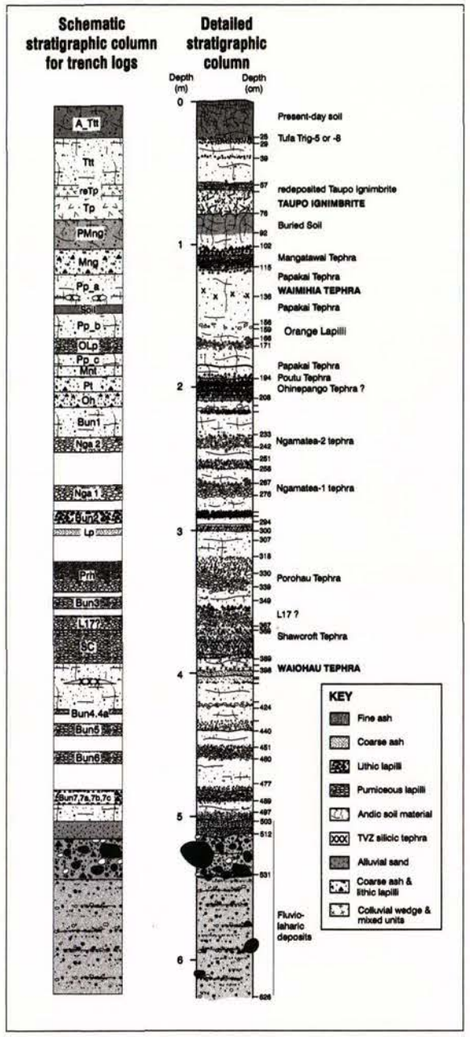

Figure. 3.14B) Zone 19 trench log, North wall. NZMS 260 (T20) 2743595, 6197155.Schematic stratigraphic column is modified Tank Track Trench log.

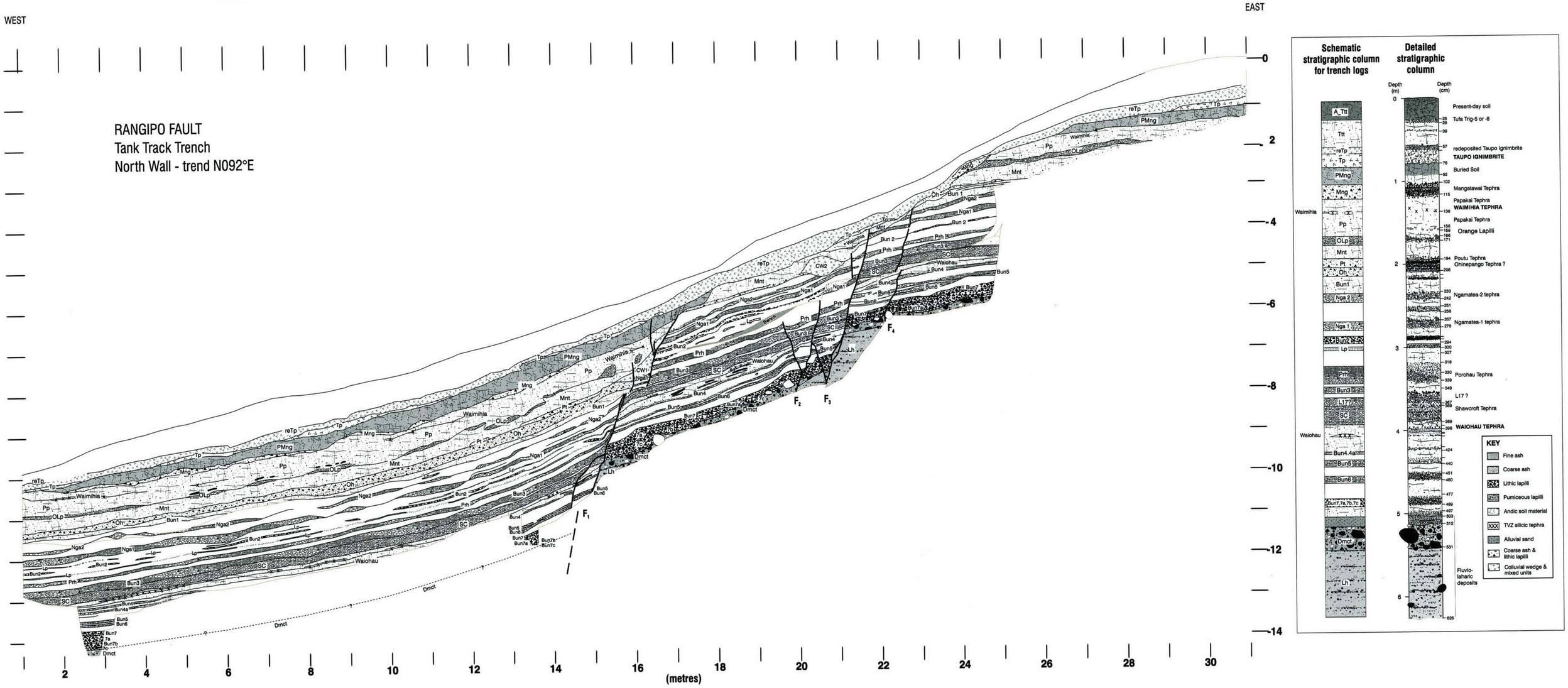

Figure 3.15A) Restoration of the top of the Taupo Tephra (base of reworked Taupo Tephra, ReTp), Tank Track Trench log.

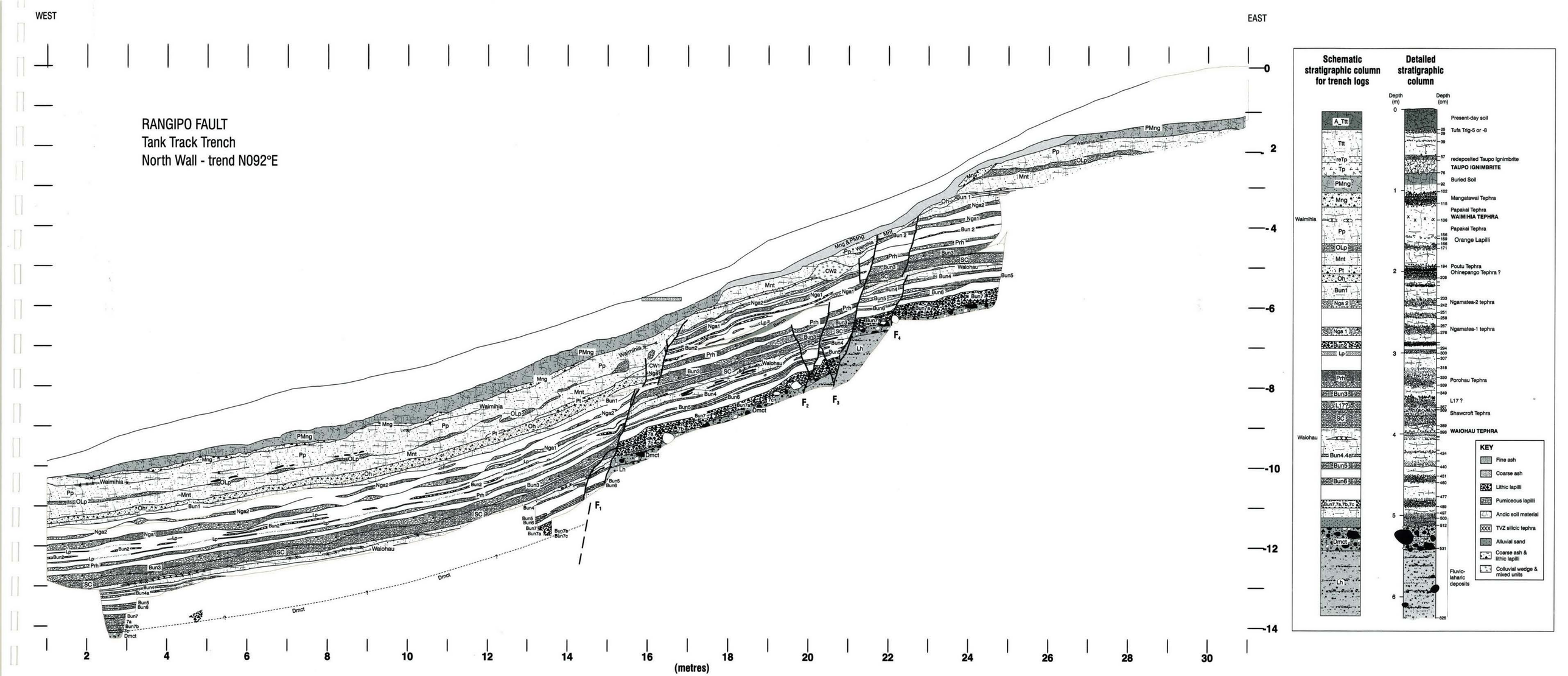

Figure 3.15B) Restoration of the top of the soil on Mangatewai Tephra, Tank Track Trench log.

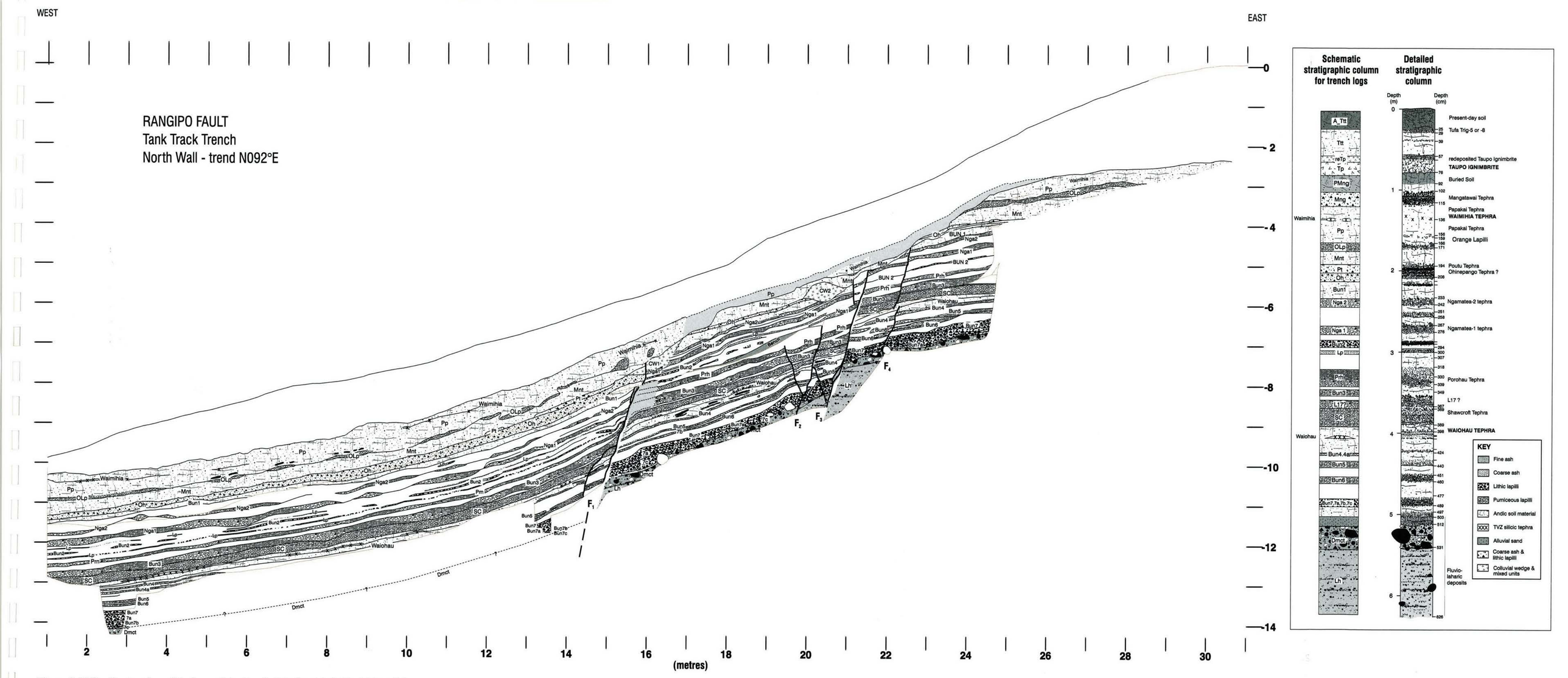

Figure 3.15C) Restoration of the base of the Papakai Tephra, Tank Track Trench log.

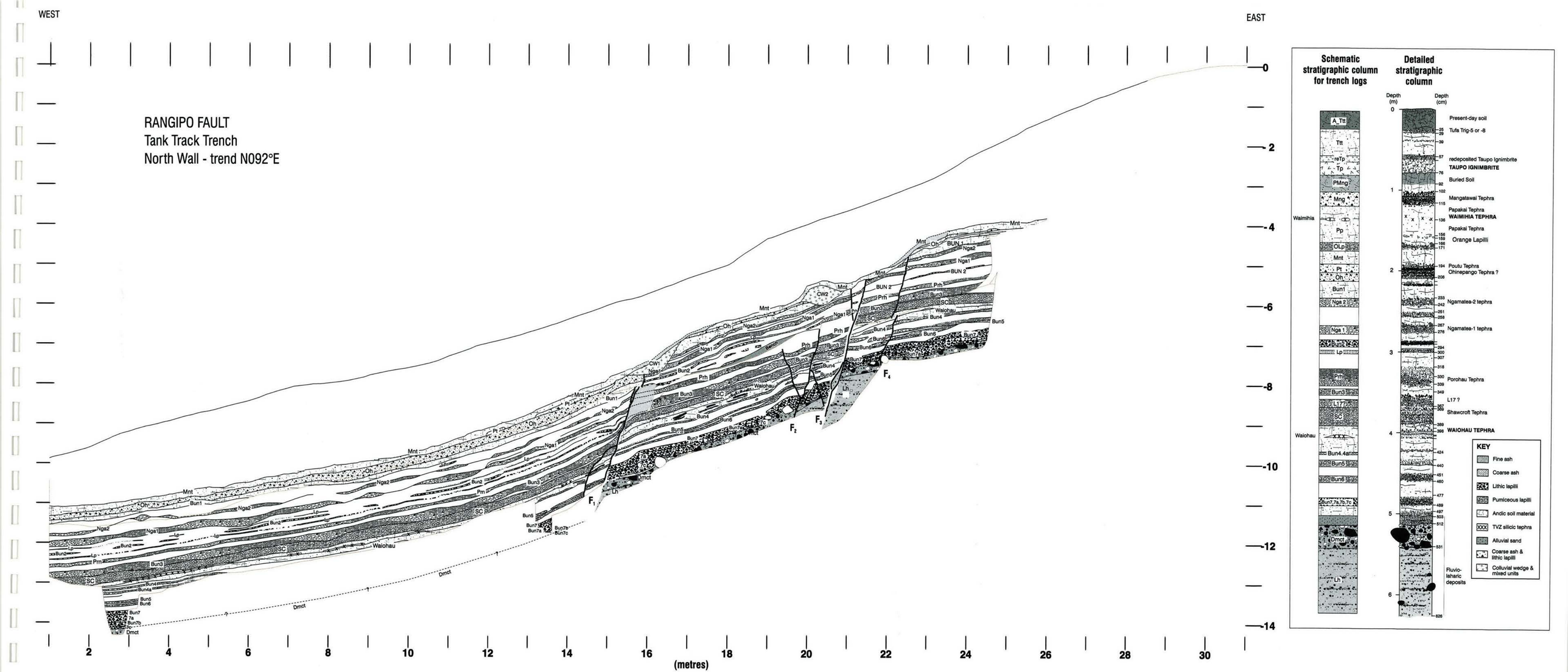

Figure 3.15D) Restoration of the base of Mnt, Tank Track Trench log.

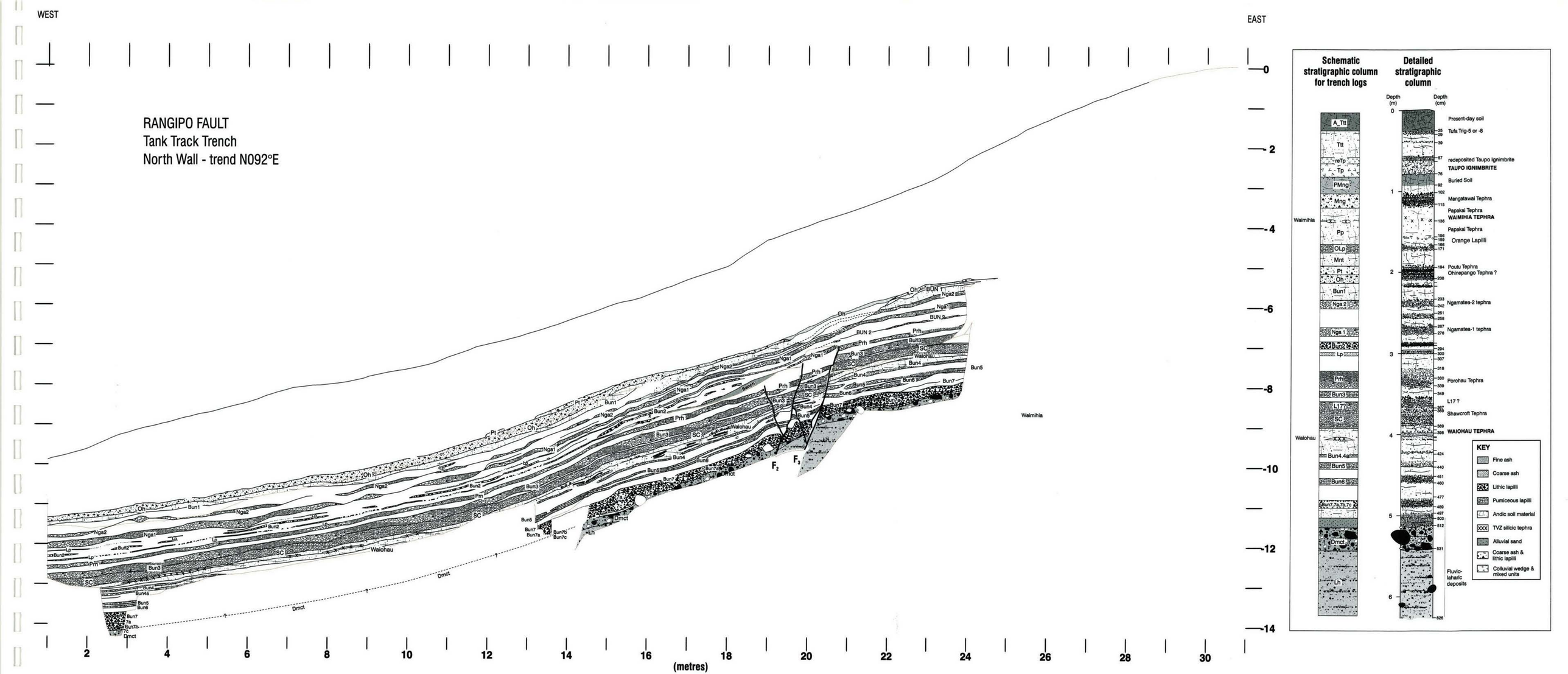

Figure 3.15E) Restoration of the base of the Ohinepango Tephra, Tank Track Trench log.

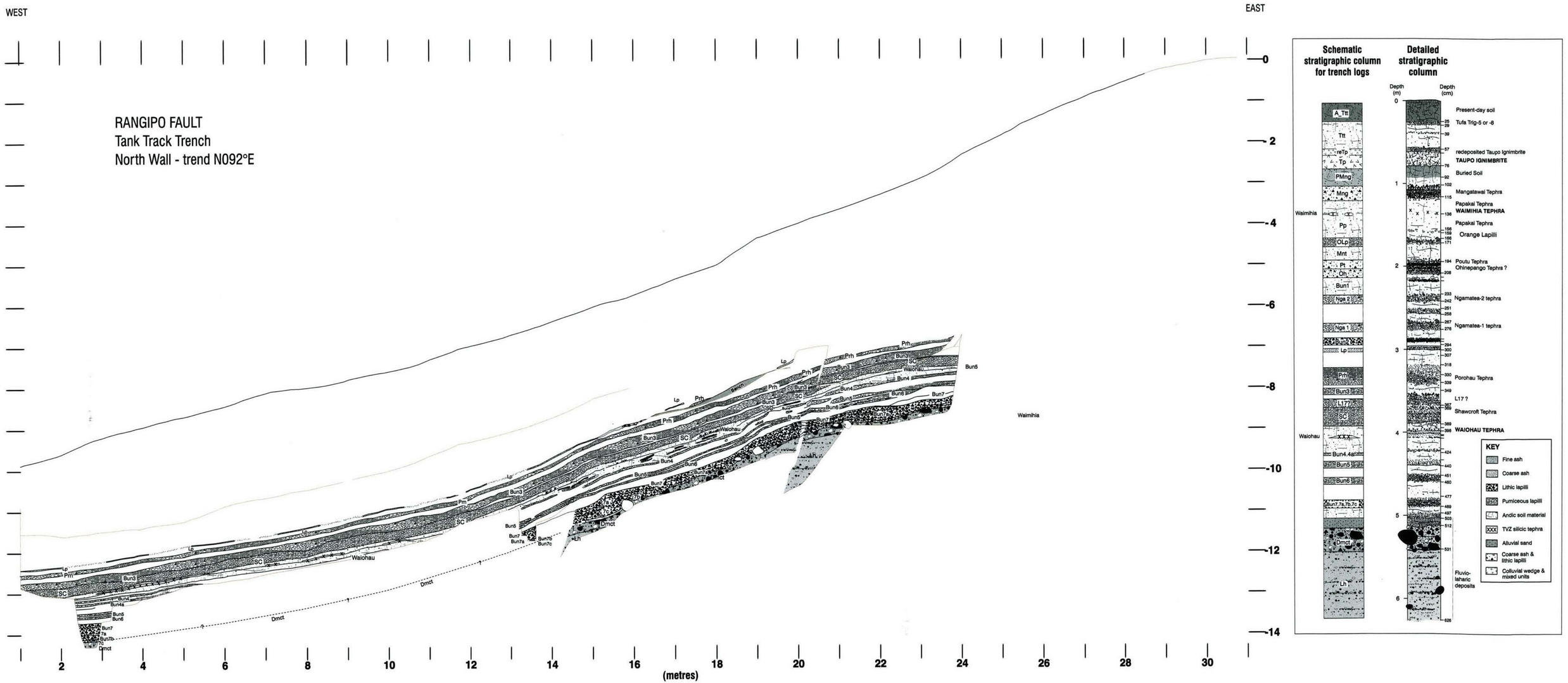

Figure 3.15F) Restoration of the base of the Poarehu Tephra, Tank Track Trench log.

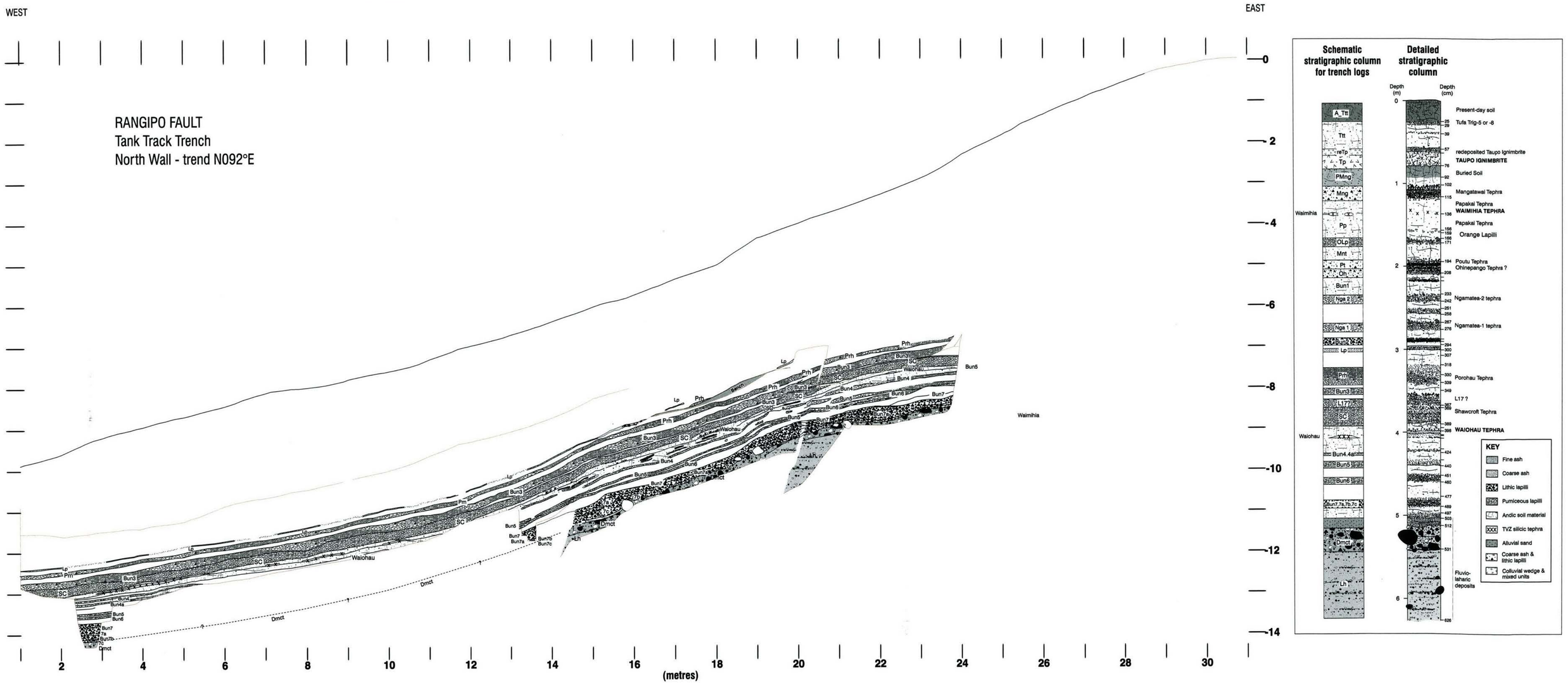

Figure 3.15F) Restoration of the base of the Poarehu Tephra, Tank Track Trench log.

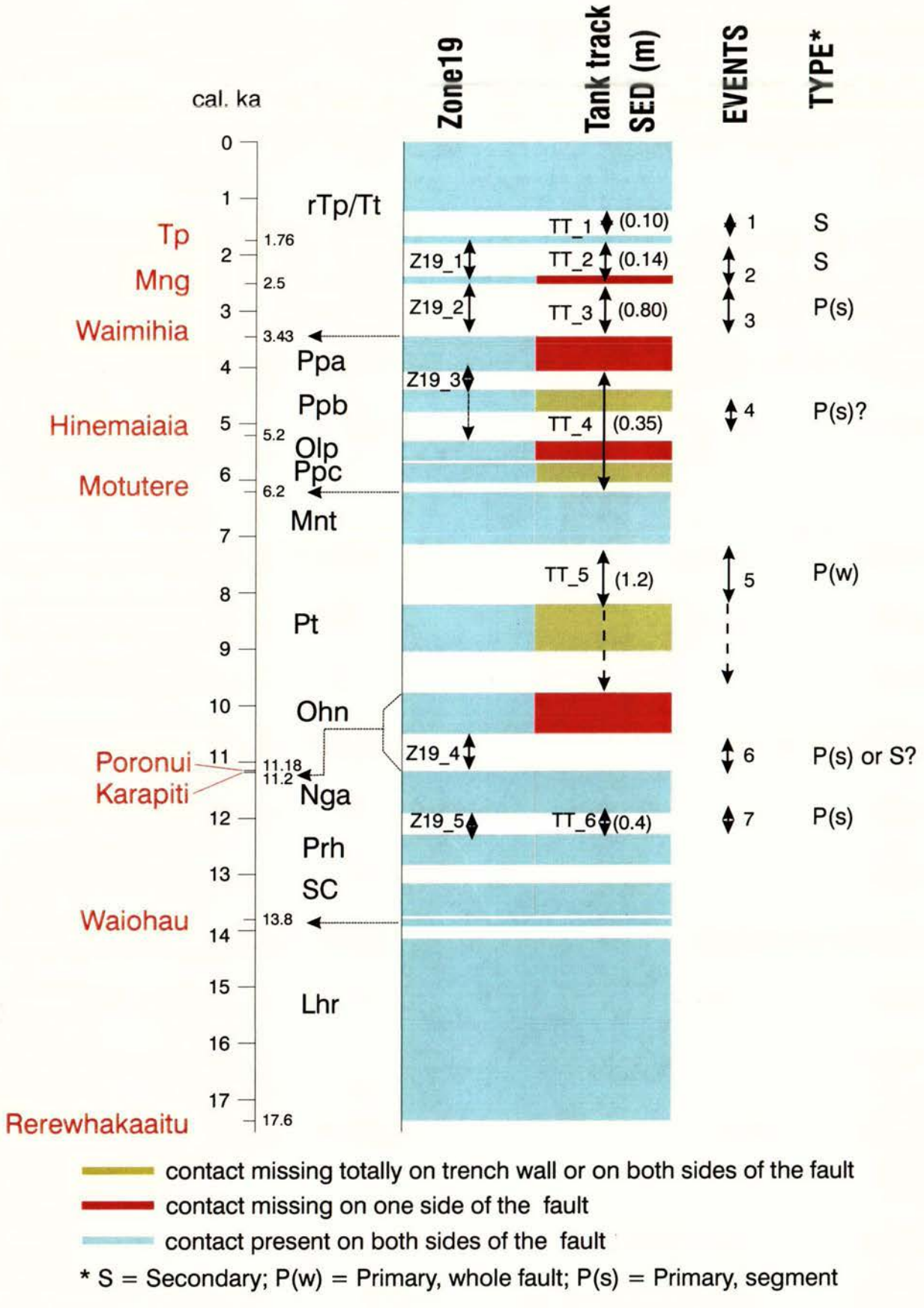

Figure 3.16: Faulting event history for the Zone 19 and Tank Track trenches. Colour shaded areas represent the age of the tephra marker beds, and the numbered arrows, the composite recorded faulting events. SED: single event displacement.

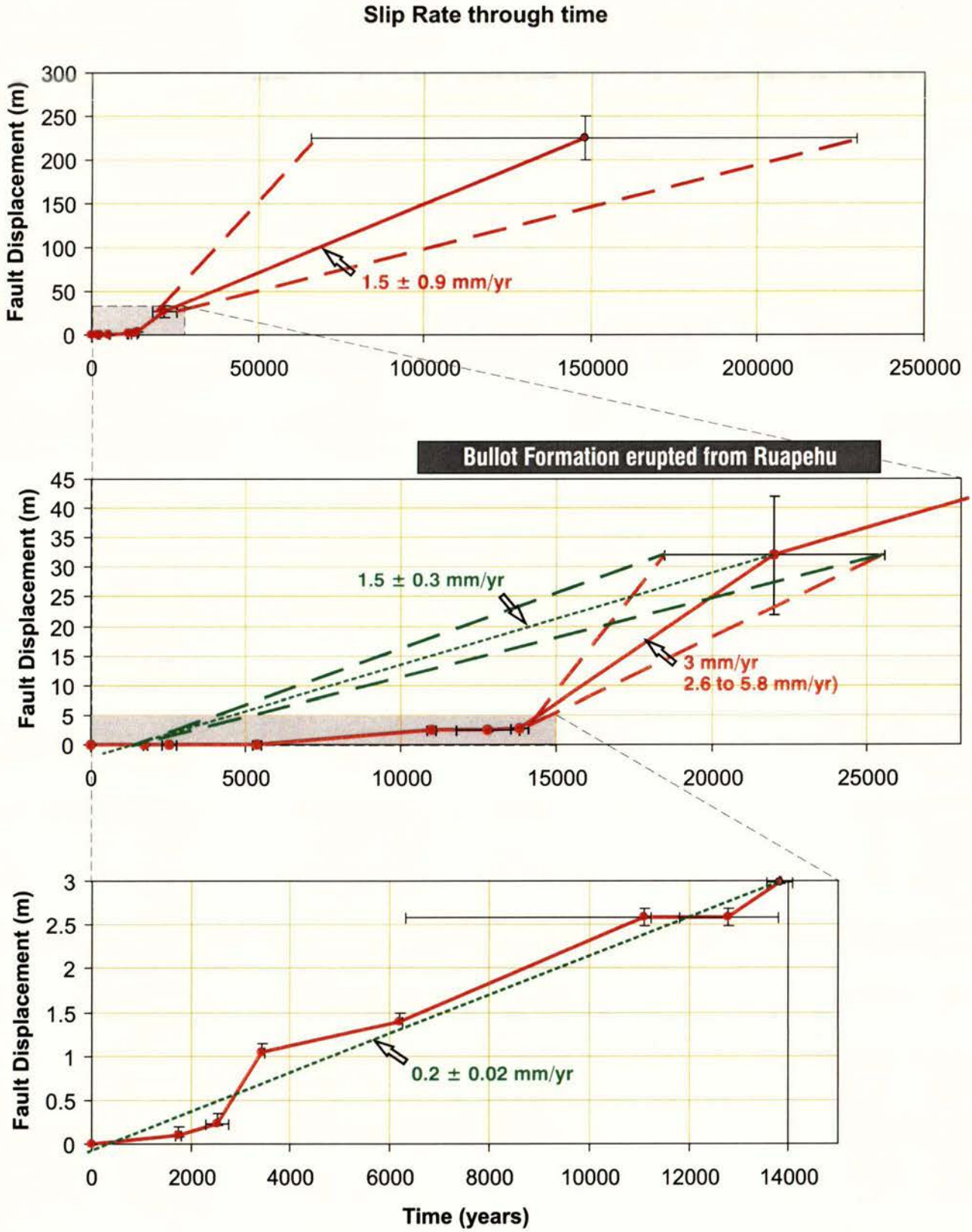

Figure 3.17: Rangipo Fault slip rate (gradient) variations with time. The lower graph was constructed from trench data and the upper two from scarp heights on surfaces of known age.

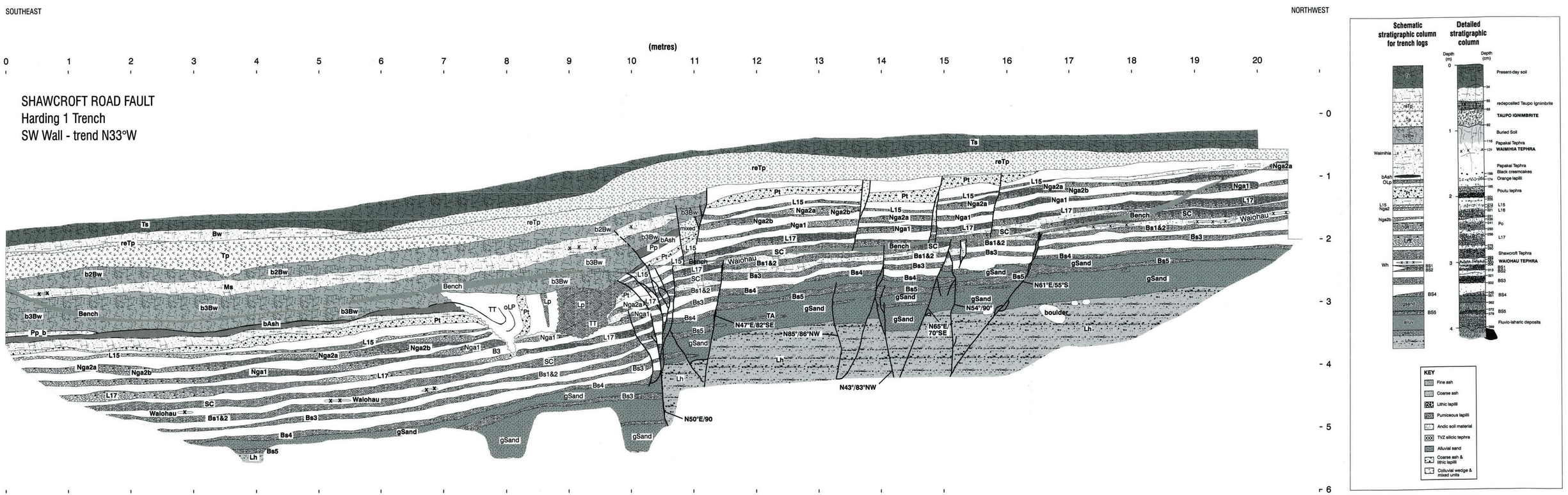

Figure 4.1A Harding 1 trench log, southwest wall. NZMS 260 T20/405930. Composite stratigraphic log was compiled at trench grid verticals 6 (0-0.9 m), 5 (0.9-1.7 m, NE wall), 5 (1.7-3.5 m, SW wall), and 10 (3.5-4 m).

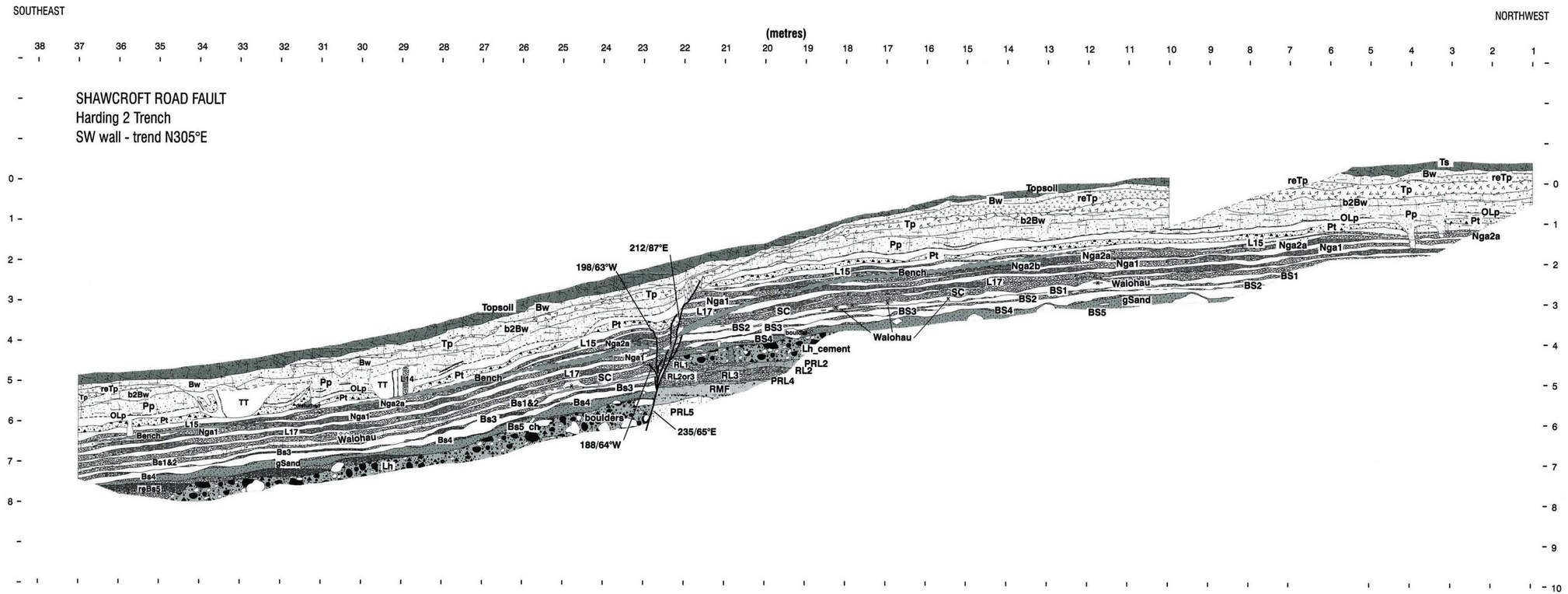

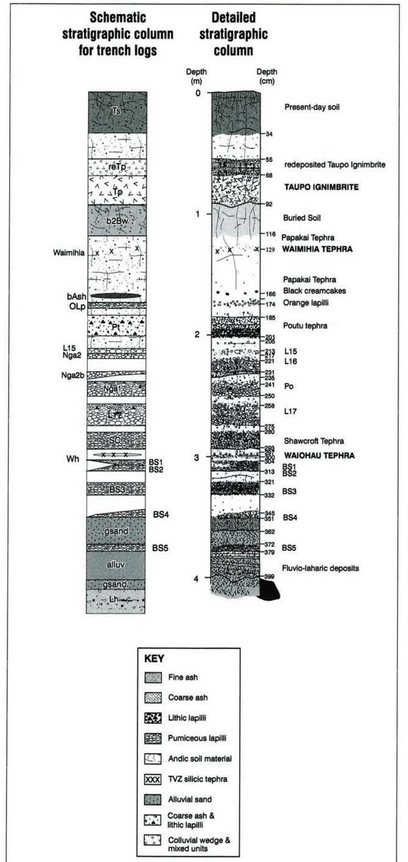

Figure 4.1B) Harding 2 trench log, southwest wall. NZMS 260 T20/409935. Composite stratigraphic log was compiled at trench grid verticals 5 (0-0.4 m), 6 (0.4-0.8 m), 7 (0.8-1.6 m), 12 (2.8-3.4 m), 20 (3-4.4 m), 21 (4-4.5 m), and 22 (4.5-5.3 m).

APPENDIX

Appendix . Major element glass compositions of key silicic tephra layers from Rangipo Fault trench sites compared with their tephra correlatives

Sample number	Trench Locality	SiO_2	Al_2O_3	TiO_2	FeO	MgO	CaO	Na_2O	K_2O	Cl	H_2O	*n*
Waimihia Tephra & correlatives												
	Site 3 - Tank Track	76.28	13.20	0.22	1.84	0.20	1.31	4.08	2.76	0.12	2.91	12
		(0.23)	(0.12)	(0.07)	(0.06)	(0.04)	(0.08)	(0.17)	(0.10)	(0.06)	(0.92)	
R4	Tufa Trig S2	76.82	12.79	0.18	1.72	0.17	1.27	3.96	2.99	0.11	0.88	11
	(Donoghue 1991)	(0.24)	(0.08)	(0.04)	(0.12)	(0.04)	(0.09)	(0.24)	(0.11)	(0.02)	(0.66)	
5b	L. Tutira	77.23	12.80	0.20	1.78	0.16	1.35	3.53	2.79	0.17	2.44	6
	(Eden et al. 1993)	(0.31)	(0.12)	(0.04)	(0.16)	(0.02)	(0.03)	(0.24)	(0.13)	(0.01)	(1.63)	
Waiohau Tephra & correlatives												
	Site 3 - Tank Track	78.19	12.40	0.14	1.02	0.15	0.91	3.68	3.29	0.14	3.75	12
		(0.28)	(0.17)	(0.09)	(0.08)	(0.03)	(0.09)	(0.16)	(0.12)	(0.13)	(1.22)	
	Site 2 - Zone 3 lower	78.28	12.38	0.17	0.99	0.13	0.87	3.75	3.31	0.13	3.64	11
		(0.37)	(0.15)	(0.04)	(0.07)	(0.03)	(0.08)	(0.14)	(0.14)	(0.07)	(1.16)	
	Site 4 – Zone 19	78.13	12.44	0.14	1.07	0.15	0.90	3.75	3.24	0.18	3.73	10
		(0.25)	(0.19)	(0.05)	(0.06)	(0.02)	(0.06)	(0.15)	(0.08)	(0.10)	(1.46)	
R12	Missile Ridge	78.60	12.15	0.14	0.94	0.12	0.92	3.87	3.20	0.13	1.86	11
	(Donoghue 1991)	(0.28)	(0.12)	(0.04)	(0.07)	(0.02)	(0.14)	(0.15)	(0.21)	(0.03)	(1.36)	
AT-194	Pukaki crater, Auckland	78.41	12.35	0.17	1.04	0.16	0.87	3.42	3.25	0.18	3.31	11
	(Sandiford et al. 2001)	(0.32)	(0.11)	(0.07)	(0.14)	(0.09)	(0.06)	(0.14)	(0.17)	(0.06)	(0.90)	
Wh	L. Rotomanuka, Waikato	78.61	12.35	0.13	0.92	0.14	0.89	3.60	3.26	0.10	4.99	10
	(Lowe 1988)	(0.30)	(0.13)	(0.03)	(0.08)	(0.01)	(0.04)	(0.28)	(0.10)	(0.03)	(3.00)	

All major element determinations were made on a JEOL JXA-733 electron microprobe housed at Victoria University of Wellington. Analyses were determined using a beam current of 8 nA, beam diameter of 20 υm and 3 x 10 sec peak counts (meaned). Values are in weight-percent oxide, recalculated to 100% on a fluid-free basis. H_2O by difference from 100%; Total iron expressed as FeO; n = number of analyses. Analyst: Alan Palmer, Massey University.

References:

Eden, D.N. Froggatt, P.C., Trustrum, N.A. Page, M.J. 1993: A multiple-source Holocene tephra sequence from lake Tutira, Hawkes Bay, New Zealand. *New Zealand Journal of Geology and Geophysics* 36: 233-242.

Lowe, D.J. 1998: Stratigraphy, age, composition and correlation of late Quaternary tephras interbedded with organic sediments in Waikato lakes, North Island, New Zealand. *New Zealand Journal of Geology and Geophysics* 31: 125-165.

Sandiford, A.; Alloway, B.V.; Shane, P. 2001: A 28,000–6,600 cal. yr record of local and distal volcanism preserved in a paleolake, Auckland, New Zealand. *New Zealand Journal of Geology and Geophysics* 44: 323-336.

Institute of Geological & Nuclear Sciences Limited

Gracefield Research Centre
69 Gracefield Road
PO Box 30 368
Lower Hutt
New Zealand
Phone +64-4-570 1444
Fax +64-4-570 4600

Rafter Research Centre
30 Gracefield Road
PO Box 31 312
Lower Hutt
New Zealand
Phone +64-4-570 4637
Fax +64-4-570 4657

Dunedin Research Centre
764 Cumberland Street
Private Bag 1930
Dunedin
New Zealand

Phone +64-3-477 4050
Fax +64-3-477 5232

Wairakei Research Centre
114 Karetoto Road, SH1
Wairakei
Private Bag 2000
Taupo
New Zealand
Phone +64-7-374 8211
Fax +64-7-374 8199

For more information visit the GNS website
http://www.gns.cri.nz

A Crown Research Institute

Cover photographs from GNS photo library